Synthesis and Evaluation of Photocatalytic Properties of BiOBr for Wastewater Treatment Applications

By

Ayla Ahmad

A thesis submitted to the Faculty of Graduate and Postdoctoral Studies in partial fulfillment of the requirements for the M.A.Sc. degree in Chemical Engineering

Department of Chemical and Biological Engineering

Faculty of Engineering

University of Ottawa

Abstract

Visible light-driven photocatalysis has shown considerable potential in the area of clean and renewable energy, as well as in wastewater treatment. This thesis describes the synthesis, characterization and applicability of a visible-light active photocatalyst, bismuth oxybromide (BiOBr). The photocatalytic activity of BiOBr was investigated through its preparation via hydrothermal and solvothermal synthesis routes under various conditions. Hydrothermal catalyst was prepared using non template based method while for solvothermal synthesis CTAB was used as a template. Parameters of temperature and time of thermal treatment were optimized for each synthesis method and overall tests for catalyst dosage and recyclability were performed. An overall optimal route leading to high photocatalytic performance was also proposed based on the obtained results. Studies were also conducted to examine the applicability of optimally synthesized BiOBr in drinking water applications by studying catalyst-mediated disinfection of *E. coli* and degradation of phenol. Favourable results were obtained, confirming the prospective application of BiOBr as a viable photocatalyst for disinfection. Furthermore, the potential of enhancing BiOBr to further improve its performance is described through synthesis of a novel $PdCl_2$/BiOBr based photocatalyst. Overall, the performance of BiOBr under various conditions in this study establishes its potential as a holistic photocatalyst and merits further development.

Résumé

Au fil des dernières années, la photocatalyse à lumière visible a généré de l'intérêt considérable dans les domaines d'énergie renouvelable et de traitement des eaux. La thèse ici présentée décrit la synthèse, la caractérisation et l'application d'un nouveau photocatalyseur, l'oxybromure de bismuth (BiOBr), au traitement des eaux usagées. Les études expérimentales décrites dans le deuxième chapitre concernent l'activité photocatalytique du BiOBr préparé par synthèse hydrothermique et solvothermique en variant les paramètres importants. Le catalyseur hydrothermique fut préparé sans échafaud, tandis que celui synthétisé par le procédé solvothermique utilisait le CTAB comme échafaud. La durée de la réaction et la température furent optimisés pour chaque méthode de synthèse, et des tests de dosage de catalyseur et de recyclabilité furent performés. Un procédé général basé sur les résultats obtenus et menant à une haute activité photocatalytique fut proposé. Le chapitre 3 explore l'utilité du BiOBr synthétisé dans des applications de traitement des eaux usagées en étudiant la désinfection photocatalytique d'*E. coli* et de la dégradation du phénol, un polluant organique, par irradiation à lumière visible. Les résultats obtenus confirment le potentiel du BiOBr comme photocatalyseur. Le dernier chapitre traite des méthodes pour améliorer la performance du photocatalyseur. Il fut déterminé que l'ajout de $PdCl_2$ à la surface du BiOBr améliore considérablement son activité photocatalytique. Les résultats de la recherche décrite dans ce document établissent le BiOBr comme un excellent candidat pour la photocatalyse à lumière visible, qui mérite plus de recherche lors d'études subséquentes.

Acknowledgements

Conducting my master's research at the University of Ottawa has been a tremendous learning and growing experience for me. At this point, I would like to extend my immense appreciation and deepest gratitude to the people without whom this great journey would not have been the same. Following are a few of these people who stood out for me for their role in my academic success and otherwise.

- Firstly I would like to mention my mentor and supervisor Dr. Jason Zhang for encouraging me to pursue my master's degree under his supervision and for constantly providing invaluable support and virtual advice for my current research as well as future career path. I would also like to acknowledge NSERC, OGS and University of Ottawa for scholarships.
- All professors at the Department of Chemical Engineering and Dr. Ronald Droste from Civil Engineering for their guidance and assistance whenever I needed it. I'd like to also thank the chair of our department, Dr. David Taylor, for his continued support and direction.
- My senior group members Joanne Gamage for her immeasurable help and expertise and Gabriel Potvin for his wisdom and assistance. My colleagues Alison Reiche, Patrick Plouffe, Dominic Pjontek and Neveen Alqasas for their great company, understanding and making work environment amusing and conducive.
- Louis Tremblay for his help with technical support and laboratory management. Susana Luiz for her extensive help with experiments.
- My friends who stood by me through thick and thin and kept my morale high.
- And last but by no means the least, my family, whose unconditional love and support sustained me. My parents' constant care, encouragement, inspiration, reassurance and faith became my driving force that helped me get through every situation no matter how challenging or daunting. My sister Aatika and brother Aeyon for being my closest friends and supporters.

Table of Contents

List of Figures

List of Tables

Nomenclature

AOP	Advanced oxidation process
CB	Conduction band
CFU	Colony forming unit
CTAB	Cetyltriethylammnonium bromide
e^-/h^+	Electron and hole pairs
EDS	Energy dispersive spectroscopy
EG	Ethylene glycol
pgm	Platinum group metal
RhB	Rhodamine B
ROS	Reactive oxygen species
SEM	Scanning electron microscopy
UV-vis	Ultraviolet visible
VB	Valence band
VLD	Visible-light driven
XPS	X-Ray photoelectron spectroscopy
XRD	X-Ray diffraction

Introduction

As industries and populations around the world grow, the demand for clean water sources is becoming more prevalent. Consequently, treating and reusing wastewater has become tremendously important. Current wastewater treatment technologies such as adsorption and coagulation merely concentrate the pollutants, enabling them to pass to a different phase and therefore cause secondary pollution. The most commonly used disinfection process, chlorination, is known to generate by-products that are mutagenic and carcinogenic to human health. Newer technologies, such as ozone and UV disinfection are expensive and energy intensive and hence their applications are limited. Therefore, research is on-going to develop more efficient and effective wastewater treatment technologies.

One of the methods that have recently been investigated in this regard is photocatalysis. Photocatalysis is an advanced oxidation process based on utilization of light energy for activation of a semiconductor which then brings about degradation of pollutants. In the process of photocatalysis, semiconductors need to absorb energy equal to or higher than their energy gap which brings about movement of electrons from lower to higher energy levels (VB to CB). This movement of electrons generates pairs, made of a negatively charged electron and a positively charged hole (e-/h+), which have the ability to oxidize donor molecules. This mechanism is demonstrated in Figure 1 below.

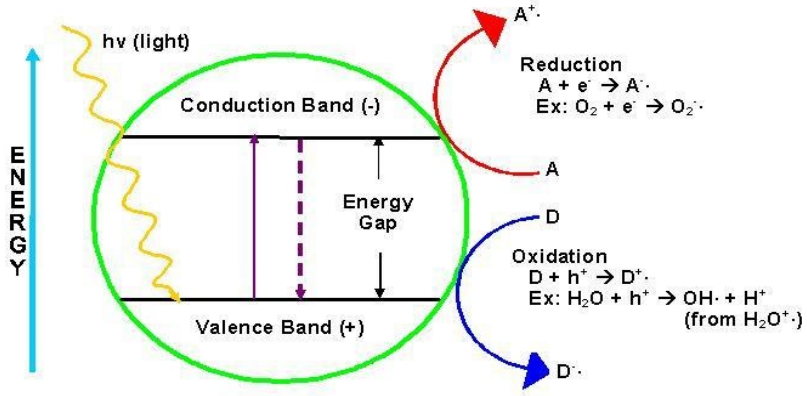

Figure 1 – Mechanism of Photocatalysis [i]

The most prevalent photocatalyst used in industry today is titanium dioxide (TiO_2). It offers the benefits of being inert, inexpensive, stable and requires little post-processing. However, due to its wide band gap of 3.2 eV, TiO_2 can only absorb light energy in the UV region. This makes it relatively unattractive for wastewater treatment since it cannot be activated by natural solar light. Therefore, the majority of research being conducted in the field of photocatalysis is focused on enhancing TiO_2 to improve its visible light absorption or development of novel visible light active photocatalysts.

Recently, bismuth oxyhalides (BiOX, X=Cl, Br, I) have been investigated for their photocatalytic properties with favourable results. Among them, bismuth oxybromide (BiOBr) showed the most promising results. Research on BiOBr photocatalysis is in its primary phase and there are a many challenges in applications of BiOBr as a photocatalyst. The focus of this study was to evaluate BiOBr as a visible light active photocatalyst and address some of these challenges in efforts to advance interest in its applications as a photocatalyst in water treatment. The main problems limiting the application of BiOBr are as follows

- Various methods of synthesis exist for the production of BiOBr and certain parameters play a role in its performance and their effects are not clearly understood.
- Thus far in research, applications of BiOBr have been limited to only a few pollutants and conditions and therefore its versatility as a photocatalyst is uncertain.
- Enhancement in its photocatalytic performance has been limited and must be investigated in order to establish prospective for further development.

This research project was designed based on the problem statements described above and the objectives of this study are threefold

1. Investigate the effects of synthesis methods and parameters on photocatalytic activity of BiOBr to maximize efficiency (Chapter 2).

2. Extend resulting optimal photocatalyst to various classes of pollutants and test its performance in different conditions (Chapter 3).
3. Test chemical variation of photocatalyst by using platinum group metal (pgm) salt $PdCl_2$ and evaluate its effect on performance of BiOBr (Chapter 4).

This research was divided into three distinct sections, each pertaining to one main objective with the overall goal being establishment of BiOBr as a viable visible light active photocatalyst for water treatment applications. This manuscript based thesis details the findings and implications of each section of research, presented as separate chapters as described above.

[1] Photocatalysis Mechanism" - http://dev.nsta.org/evwebs/1952/photocatalysis.htm (Used with permission)

Chapter 1 - BiOBr as a Photocatalyst for Wastewater Treatment: A Review

1.1 Introduction

Rapid industrial development, population growth and long-term droughts have led to an increased demand for clean water sources. More than 4 billion people around the globe do not have access to clean and sanitized water supply and millions have died due to severe waterborne diseases [1]. In the future, these figures are expected to grow due to discharge of more and more toxins and contaminants into the natural water cycle [2]. One of the ways to tackle this problem is to reuse treated municipal wastewater from agricultural and industrial activities. Since these wastewaters constitute a large portion of total water resources, their reuse can compensate for some of the water shortage.

Industrial wastewater generated from various manufacturing industries such as pharmaceutical, textile, pesticides and other organic chemical manufacturing industries contains different concentrations of suspended solids, organic textile dyes and harmful coliforms. As a result, these effluents are intensely colored and are polluted with high concentration of organic and other refractory compounds which cause toxicity and foul odours in water. Degradation of these non-biodegradable organic compounds is not possible by conventional biological treatment processes [3]. Currently available water treatment technologies such as adsorption and coagulation simply concentrate the pollutants, causing secondary pollution [4, 5] while disinfection processes such as chlorination of water generate by-products that are mutagenic and carcinogenic to human health [6]

In recent years, photocatalysis based on semiconductors (called photocatalysts) has emerged as a promising method for the treatment of wastewater due to efficiency in degrading a wide range of refractory organic pollutants into readily biodegradable compounds, reduction of toxic metals and inactivation of bacterial species [7]. The most prevalent photocatalyst is TiO_2 that can only be activated by ultraviolet light, which forms merely 3-5% of total solar radiation. Since visible light accounts for 43% of the solar spectrum, development of efficient visible-light-driven photocatalysts has become attractive. Among these, bismuth oxybromide (BiOBr) is of particular importance because it is relatively stable under visible light irradiation and offers efficient degradation of a variety of pollutants [8]. This paper provides a detailed review of BiOBr as a visible light activated photocatalyst.

1.2 Background of Semiconductor Photocatalysis

Photocatalysis is a combination of photochemistry and catalysis and is defined as the acceleration of a photoreaction (reaction using light) by the presence of a catalyst [9]. The catalyst may excite the photoreaction by interaction with the substrate in its ground state or excited state.

Over the past two decades, the interest in application of semiconductor photocatalysis has grown exponentially especially in the areas of water, air and wastewater treatment. Today, semiconductors are usually selected as photocatalysts, because semiconductors have a narrow gap between the valence and conduction bands. In order for photocatalysis to proceed, a semiconductor needs to absorb energy equal to or more

than its energy gap. This movement of electrons forms e-/h+ or negatively charged electron/positively charged hole pairs.

In order for a photocatalysis process to occur, two principle criteria must be met:

i) Absorption of solar irradiation by some chemical substance

ii) Effective separation of electron hole pairs with little energy loss before they lose their input energy through recombination

The presence of light is also an important prerequisite for photocatalysis. Usually "light" is taken to mean electromagnetic radiation in the visible, near-ultraviolet and near-infrared spectral range [9]. Although photocatalysis has been studied in detail with respect to a myriad of different light sources, it should be noted that UV radiation by lamps or ozone production is expensive. Therefore, research is now focusing more on those photocatalysts which can be driven by solar radiation, i.e. light with a wavelength longer than 300 nm, generally between 400-700 nm [10].

Fujishima and Honda reported the first photoinduced splitting of water on a TiO_2 electrode [11]. Ever since then, interest in this semiconductor, first in academia and then in industry, has grown exponentially. The high quantum yield and stability of TiO_2 are key reasons for the dominance of this semiconductor. In spite of these advantages, there are several limitations of TiO_2 photocatalysis. In general, its photocatalytic reaction rates are modest, and consequently it is not appropriate for high output processes such as the decontamination of heavily polluted industrial wastewaters [12, 13]. It allows for a high charge recombination rate of photogenerated electrons and holes. However, the most important drawback of TiO_2 photocatalysis is derived from

the mismatch between the TiO_2 band gap energy and sunlight spectra, which overlap only in the UVA (320- 400 nm) and UVB (290- 320 nm) ranges. As a consequence, TiO_2 based photocatalysis can only take advantage of UV light which forms less than 5% of the solar energy irradiated on the earth's surface, and its potential as a sustainable technology cannot entirely be fulfilled.

Due to these limitations, intensive efforts have been made to develop visible light-responsive photocatalysts, such as metal/non-metal doped TiO_2, inorganic bismuth compounds and ferrites. Although most of the photocatalysts show marked visible-light responsive activity, their stabilities, the relationship between structure and photocatalytic reactivity and the photocatalysis mechanisms remain uncertain. Therefore, synthesizing novel visible-light responsive photocatalysts and exploring their photocatalytic performance are of great interest and potential reward.

Recently, bismuth oxyhalides (BiOX, X= Cl, Br, I) have been investigated because of their unique properties and potential applications. Among these, the photocatalytic activity of BiOBr is particularly promising and as a result it has become a hotspot for many current photocatalysis research projects.

1.3 Structure of BiOBr

As a general rule, the photocatalytic activity of a semiconductor is closely related to the mobility of photogenerated charge carriers and the positions of conduction band (CB) and valence band (VB) in the photocatalyst [14]. In metal oxide photocatalysts, the VB is commonly composed of O 2p. However, the VB of materials containing Bi mostly consists of O 2p and Bi 6s hybrid orbitals and the CB consists of Bi 6p. It is reported

that a broad VB increases the mobility of the photogenerated carriers [15]. Bismuth-based photocatalysts exhibit this phenomenon because the Bi 6s orbital is largely dispersed, which is more beneficial to increasing the mobility of photogenerated carriers [14]. Moreover, it was reported that the Bi-O sites in Bi^{3+} doped TiO_2 acted as electron traps in the photocatalytic reaction [16]. Therefore, materials containing Bi are potentially highly active photocatalysts.

BiOBr is of particular importance among the bismuth oxyhalides compounds because it is visible-light responsive, quite stable under light irradiation and shows greater photocatalytic activity than the commercialized Degussa P25 (TiO_2 aerosol mixture comprising of Rutile and Anatase phases) under UV illumination [8, 17-18]. The unique electrical, optical and photocatalytic activity of BiOBr is due to its intrinsic crystalline layer and lamellar structure [8, 17]. The internal electric fields in layered materials are considered to favor charge separation, which can subsequently induce redox reactions on the semiconductor surface and contribute to enhance the photocatalytic activity of these materials [19- 21]. BiOBr is a layer-structured semiconductor that consists of tetragonal $[Bi_2O_2]$ positive slabs, which are interleaved by double slabs of bromide to form $[Bi_2O_2Br_2]$ layers along the c axis [22, 23]. The permanent static electric fields between $[Bi_2O_2]$ and $[Br_2]$ layers can work as accelerators for the separation of electron–hole pairs upon photoexcitation to favor a high photocatalytic efficiency of BiOBr [21].

1.4 Synthesis of BiOBr Structures

Although commercial suppliers can provide high quality single crystals of a variety of semiconductors, some experiments require a sample to be grown to certain specifications that are not commercially available. In such cases, crystal growth must be achieved in the laboratory. Crystal growth is an art form and many techniques and skills are employed in order to achieve high quality samples. Besides the crystal structure, the photocatalytic performance of a specific semiconductor is closely linked to its particle size and crystallinity and these parameters significantly depend on the synthesis routes [7, 8, 17, 18, 24]. There are various methods of synthesizing BiOBr and newer methods are being developed as research progresses. These methods result in different kinds of crystal structures, particles sizes and morphology. Research is on-going to discover a general suitable synthesis method that produces highly photocatalytic BiOBr and allows the fundamental understanding of the crystalline structure evolution and its influence on photocatalytic performance of BiOBr [20]. Several synthesis methods that are presently employed are briefly discussed in this section.

1.4.1 Hydrolysis Method

Hydrolysis is a relatively simple method that can be used to synthesize BiOBr photocatalyst crystals. In this method, the reagent Bi_2O_3 is dissolved in excessively concentrated halogen acid, HBr, to obtain a $BiBr_3$-HBr aqueous system. The pH value is then adjusted in the range 2-3 [25] using a weak base and this results in appearance

of photocatalyst precipitates at the bottom. The precipitates are then purified by filtration and washed with distilled water several times and upon drying, yellowish BiOBr powder can be obtained.

The reactions that occur are shown in Equations (1) and (2) as follows

$$Bi_2O_3 + 6HBr \rightarrow 2BiBr_3 + 3H_2O \qquad (1)$$

$$BiBr_3 + H_2O \rightarrow BiOBr\downarrow + 2HBr \qquad (2)$$

The hydrolysis method produces homogenous sheet shaped nano-plates of BiOBr. Hydrolysis requires only drying at low temperature instead of roasting and can therefore be operated with lower cost and shorter times compared to other traditional methods [25]. Although hydrolysis is a widely used method for synthesis of bismuth oxyhalides due to a higher degree of simplicity and high purity product, there are some inherent drawbacks. The product obtained through hydrolysis is poorly crystalline and the synthesis process is uncontrollable [26].

1.4.2 Hydrothermal Method

Hydrothermal synthesis is an environment-friendly and cost-effective synthesis method for a variety of nano-materials [27, 28]. In hydrothermal synthesis for BiOBr, solutions containing Bi are heated in autoclaves to produce more pronounced crystal structures. Typically, a small amount of $Bi(NO_3)_3 \cdot 5H_2O$ is dissolved in acetic acid (HAc), and the resulting solution is added to de-ionized water and potassium bromide (KBr) under vigorous stirring [20]. Upon the mixing of solutions, yellow precipitates immediately appear which then turn light yellow as dissolution is completed. After constant stirring

at room temperature, the suspension is transferred into a Teflon-lined stainless steel autoclave and heated at a designated heating temperature for a designated time. The crystallite size and growth direction of the BiOBr samples strongly depends on both the synthesis temperature and the duration of heating process [20]. The resulting precipitate is then filtrated and washed thoroughly with distilled water to remove any possible ionic species in the product. Ultimately, fine powder of BiOBr is obtained.

Due to its versatility and ability to control particle size, shape and crystallinity by adjusting the hydrothermal treatment parameters, hydrothermal synthesis has been extensively used to prepare bismuth oxyhalides. Hydrothermal synthesis generally takes place in alkaline aqueous solutions at high temperature [29, 30]. However, the basic environment of the alkaline aqueous solutions leads to varied composition and morphology of bismuth oxyhalides at elevated synthesis temperatures [29, 30]. Jiang's group has also reportedly performed hydrothermal synthesis under acidic conditions with favourable results [20]. Photocatalytic activity reported by hydrothermal methods, however, is still lower than that reported by template or emulsion assisted methods.

1.4.3 Solvothermal Method

Recently, hierarchical structured BiOBr microspheres have emerged as popular and have been successfully prepared via various synthesis routes. In solvothermal methods, special solvents and/or templates are employed to achieve hierarchal structures. Conventional template-directed synthesis is an effective approach, in which hard or soft templates or surfactants are utilized to tailor the growth process. A common surfactant used for synthesis of BiOBr is cetyltriethylammnonium bromide (CTAB) which may

also act as a bromide source [19]. Several different solvothermal techniques and protocols have been developed in order to synthesize BiOBr three dimensional microspheres. Zhang and coworkers [17] established a general one-pot solvothermal route to prepare hierarchical BiOX (X = Cl, Br, I) microspheres by employing ethylene glycol as the solvent. Tang's group [8] demonstrated the ethylene glycol-assisted solvothermal synthesis of three-dimensional (3-D) microspherical BiOBr architectures assembled by nanosheets.

In recent years, microwave heating has been widely applied in material synthesis with several advantages: (1) shorter reaction time; (2) more uniform product dimensions and composition; and (3) ease in tuning compositions of the products [19]. Preparation of BiOBr hierarchical microspheres based on the self-assembly of mesocrystal nanosheets through a microwave-assisted solvothermal route has also been investigated. Chen's group [19] reported the successful synthesis of BiOBr hierarchical microspheres constructed by mesocrystal nanosheets through a facile and rapid microwave-assisted solvothermal route. 3D hierarchically nanostructured BiOBr microspheres and microflowers have successfully been synthesized by the solvothermal method [31].

Among present synthesis methods, the solvothermal method appears to be the most promising as the resulting products demonstrate very high photocatalytic activity. While solvothermal synthesis has been reported as a good strategy to prepare assembled BiOBr nano-crystal, the organic solvent involved is potentially harmful to the environment [17]. Moreover, template-directed routes are usually subject to tedious procedures and impurities may possibly be introduced [32]. These routes also lead to

distinctive crystalline structures, which as a result show significant differences in their performance [31].

1.4.4 Microemulsion Method

Due to the complications present in template assisted solvothermal methods, template-free routes to the inorganic materials with hollow interiors are also favourable [32]. As a substitute route to templates, emulsion and miniemulsion systems have been employed to produce hollow structures (particularly spheres). Huang's group [32] have reported a facile one-pot approach to the uniform BiOBr hollow microspheres. Successful synthesis of well-defined flowerlike BiOBr hierarchical nanostructures by a facile and fast microwave irradiation method has also been reported [31].

Reverse micro-emulsion synthesis has been adopted to prepare nanosized BiOBr, but most of the syntheses require large quantities of surfactants to generate micelles, thereby increasing the complexity. The entire process thus becomes complicated, time-consuming, and costly and may not produce model crystalline phases [24].

1.4.5 Ionothermal Method

A variation can be made to the solvothermal method by using an ionic liquid, thereby introducing an improved and unique synthesis method commonly known as the ionothermal method. Ionic liquids (ILs) are non-volatile and non-flammable organic salts with low melting points [33]. The main benefits of using ILs as solvents or additives in inorganic synthesis are their greater capability for solvation and

stabilization of metal cations. As a result, ILs are often used as capping agents or surfactants [33].

The use of ILs as unique soft materials capable of promoting the nucleation and in-situ growth of 3D hierarchical bismuth oxybromide mesocrystals without using any surfactants has recently been reported [33]. These structures had a very high adaptability to water treatment. BiOBr uniform flower-like hollow microsphere and porous nanosphere structures have also been successfully synthesized through a one-pot EG-assisted solvothermal process in the presence of reactable IL 1-hexadecyl-3-methylimidazolium bromide ([C16mim]Br) [34]. It was also determined that the IL [C16mim]Br not only acted as solvent and template but also as the Br source for the fabrication of BiOBr hierarchical architectures [33]. Ionothermal synthesis of BiOBr is, however, a relatively new field and the use of ILs to effectively produce this photocatalyst still requires further exploration. Moreover, ILs are currently only produced on laboratory scale and establishment of their large scale production is important prior to their utilization in extensive BiOBr synthesis.

1.5 Parameters of Synthesis

As mentioned in the previous section, there are numerous different methods and techniques which can be employed to synthesize BiOBr. Moreover, each of these techniques can be performed with a different set of conditions which would result in diversely structured photocatalysts with different photocatalytic activities. Optimization of an ideal synthesis route along with its respective parameters is an area of research that requires more attention and exertion. Limited work, however, has been done in

this field and following are the main parameters that may be altered in order to achieve different structures.

1.5.1 Temperature

The temperature at which synthesis is performed can alter the characteristics of the product significantly. In hydrothermal synthesis, temperature plays a key role and increasing the temperature of hydrothermal treatment results in preferred oriental growth in the anisotropic direction along the face of the BiOBr crystals [19]. Temperature must also be carefully controlled in the solvothermal, ionothermal and microemulsion methods in order to achieve desired results [8, 17, 31, 33].

1.5.2 Time

The duration of thermal treatment is another parameter that affects the structure of resulting BiOBr crystals. The prolongation of hydrothermal treatment leads to an increase in the intensity of Bragg peaks of BiOBr and the peaks become narrower, which are attributed to an increase of average particle size [19]. Time is also an important factor in solvothermal synthesis whereby prolonging the treatment may result in higher photocatalytic activities in some cases. Ionothermal and microemulsion methods have not extensively explored parameter of time.

1.5.3 pH Value

The pH of solutions used to synthesize the crystals may also play an important role in the quality of product and its crystal structure. In hydrolysis synthesis, the precipitates of BiOBr appear only upon lowering the pH to an acidic range [25]. The structure of

hydrothermally synthesized crystals in basic environments is very different from those synthesized in the acidic environment [20]. The basic environment of alkaline aqueous solutions leads to varied composition and morphology of bismuth oxyhalides while acidic environment offers better control of crystal structure [20]. Adjustments of pH conditions have not been reported using solvothermal methods thus far.

1.6 Variations of BiOBr

Although BiOBr offers high photocatalytic activity, efforts have been made to enhance its properties by introducing different chemical variations. This section summarizes some of these variations introduced to BiOBr.

1.6.1 Doping

Often it is advantageous to be able to manipulate the equilibrium optoelectronic properties of a semiconductor. This can be achieved by introducing impurities into the crystal structure of the semiconductor [9]. This foreign element, known as a dopant is added to alter equilibrium concentration of electrons or holes and the new location of these levels determines changes in the electrical and optical properties of the solid.

In recent years, the interest in noble metal decorated photocatalytic materials has grown since noble metal (Ag, Au, Pt, etc.) nanoparticles exhibit strong absorption of light in the UV−vis region resulting from their surface plasmon resonance (SPR) property and they may also act as electron receptors [35-37]. When anchoring noble metal nanoparticles on the light-excited semiconductors, they can effectively enhance photocatalytic activity via the improvement of photoabsorption and interfacial charge

transfer [38-41]. In addition, doping may enhance the photocatalyst's degradation ability due to the improvement of the charge separation.

Few works have been reported in this regard to improve activity of BiOBr. Ag/Ti doped BiOBr as well as Ti-doped BiOBr photocatalysts have been prepared by Jiang and coworkers [42, 43]. Ti-doped BiOBr offered better activity than non-doped BiOBr, while all the Ag/Ti samples exhibit remarkable enhancement in photocatalytic activity in comparison with that of the Ti-doped BiOBr microspheres due to the improvement of photoabsorption and the charge separation [42]. Ag doping has been performed on BiOBr and it was found that silver metal nanoparticles have a unique role in promoting the photocatalytic performance of BiOBr catalyst in the degradation of different dyes [44].

1.6.2 Heterojunction

Another method used to improve the photocatalytic activity of a semiconductor is by heterojunction. A heterojunction is the interface that occurs between two layers or regions of dissimilar crystalline semiconductors that have unequal band gaps. Heterojunction is an effective and simple strategy to improve the photocatalytic activity of a photocatalyst, and the fabrication of heterostructured photocatalysts BiOX/BiOY (X, Y = Cl, Br, I) with matching band potentials has turned out to be another new approach for enhancement of pure BiOX [45, 46]. Compared with impurity doping method, the formation of a heterojunction between two semiconductors with different band gaps is more flexible for broadening the visible light absorption and less sensitive

to the component homogeneity [47]. However, only a few works have been reported on BiOBr heterostructures.

Heterostructures of BiOBr with BiOI have been synthesized and it was found that BiOI/BiOBr exhibited higher photocatalytic activities on the degradation of MO than pure BiOI and BiOBr under visible light irradiation due to the formation of BiOI–BiOBr heterojunction which could suppress the recombination of photogenerated electron–hole pairs efficiently [48] Synthesis of AgBr–BiOBr heterojunctions has also been reported in literature [49]. The loading of Ag significantly affects the performance of AgBr-BiOBr heterostructure. However, these heterostructures are prone to deactivation in the photocatalytic reactions since the AgBr is vulnerable and transformed to Ag_2O under light irradiation. The as-formed Ag_2O reduces the intimate interface of AgBr–BiOBr catalysts light excitation, and serves as a recombination center of photogenerated charge carriers, resulting in the deactivation of the catalysts [49]. A highly effective visible-light-driven photocatalyst based on the formation of a heterojunction interface between BiOBr and BHO was prepared by Khalil's group [47]. This novel yBiOBr-(1−y)BHO heterostructure exhibited a superior photocatalytic performance in comparison with the pure phases of BiOBr and BHO.

In addition to production of heterostructures with other semiconductors, BiOBr composites have also been investigated. Zhang and coworkers [50] recently explored a novel composite consisting of BiOBr along with graphene. Graphene is an allotrope of carbon and it was composited with BiOBr via a hydrothermal process. The resulting composite had significantly higher photocatalytic activity than pure BiOBr. This shows

that by varying the crystal structure and adding different materials to BiOBr, its photocatalytic properties can be enhanced to achieve even better results.

1.7 Applications and Pollutants

BiOBr is a flexible and widely applicable photocatalyst and may be used for a number of environmental applications like wastewater treatment, air pollution control and splitting of water into hydrogen and oxygen. The majority of works published, however, focus on the utilization of BiOBr for water treatment processes. BiOBr is capable of degrading a plethora of different pollutants and this section briefly discusses the pollutants that can successfully be degraded by BiOBr.

1.7.1 Dyes

The textile manufacturing and finishing industries utilize great quantities of dyes, 50% of which are discharged directly into the wastewater. Synthetic dyes contain many complex structures, most of which are macromolecules that are difficult for microorganisms to decompose [51]. These dyes render a colour to the water, impact light penetration, and reduce the solubility of gases (dissolved oxygen in particular) upon their release in water. Some dyes are also toxic in nature, which further impacts ecology in the water [51]. Dyes are important model pollutants for wastewater photocatalysis since they are a threat to water ecology and aesthetics. Moreover, their presence and concentration changes within water are relatively easy to monitor.

BiOBr has been applied for the degradation of a number of dyes. One of the most commonly used model pollutants for BiOBr photocatalysis is Rhodamine B (RhB) [19,

52-56] which is an organic dye. BiOBr photocatalytic degradation has also been widely applied to methyl orange (MO) [8, 19, 18, 20, 57-59]. The results have demonstrated that MO can be effectively reduced to non-toxic products by visible light photocatalysis using BiOBr. Other dyes that have been explored for visible light degradation by BiOBr include methylene blue (MB) [33] and Azure B [3]. BiOBr has relatively high photocatalytic activity for degradation of all the dye mentioned above. This shows that BiOBr can be effectively used for removal of excess dyes from wastewaters.

The photodegradation process is generally carried out in a slurry reactor where a small amount of photocatalyst is added to a certain concentration of the dye. The solution is irradiated with visible light from a pseudo-solar source. A sample is taken at small time intervals and the concentration of dye at each interval is determined by using a UV-spectrophotometer. Therefore, the degradation of dye can be obtained as a function of time and photocatalytic activity can be easily monitored.

1.7.2 Organics and Aromatics

In addition to textile dyes, olfactory organics are another major problem for wastewater treatment processes. Therefore, the application of BiOBr for degradation of organics in water has been investigated, however to a smaller extent.

4-Nonylphenol (4-NP), 4-t-octylphenol (4-t-OP), sodium pentachlorophenate (PCP-Na) and bisphenol A (BPA) are typical phenolic endocrine disruptive chemicals (EDCs), which have received great concerns worldwide due to their disruptive effects [60]. Chang and coworkers [60] investigated the degradation of these four kinds of EDCs by bismuth based photocatalysts. The results demonstrated very weak degradation for all

four compounds by the BiOBr. Xiao's group however, demonstrated that BiOBr can successfully degrade phenol in water [61]. Chen et al. [19] also demonstrated that BiOBr photocatalyst can degrade phenol in water under UV irradiation with an efficiency of 99% over a period 80 minutes.

In addition to phenol, BiOBr photocatalysis has also been applied to toluene, a common pollutant that is very difficult to degrade [61]. The demonstrated results are favourable for BiOBr showing a two times higher activity than the commercially dominant TiO_2 photocatalyst (Degussa P25) [62]. BiOBr can also successfully degrade tetrabromobisphenol A [63], which is also an endocrine disruptor.

Polybrominated diphenyl ethers (PBDEs) have recently aroused global concern due to their increasing levels in the environment and biota, and potential adverse effects on wildlife and humans. Photolytic and biotic degradation of PBDEs has been reported previously; however, most studies have been focused on PBDE environmental transformation, and information on the potential method for eliminating PBDE contamination in the environment was limited [64-67]. BiOBr can successfully degrade PBDEs and this system is currently being patented [68].

Benzotriazole is a toxic heterocyclic aromatic compound which has become a pervasive contaminant in the aquatic environment. Xu's group [69] studied the degradation of benzotriazole by BiOBr photocatalyst under simulated solar irradiation. It was demonstrated that about 90% of benzotriazole can be degraded after 3 hours of irradiation which compares to 50% by P25 TiO_2 under the same conditions [69].

The process of degradation is similar to the one that is used for dyes described in the previous subsection. However, the concentration of organics cannot always be detected by UV spectrophotometer and therefore methods like HPLC are used.

1.7.3 Disinfection

Chemical oxidizing, e.g. chlorine, hydrogen peroxide, ozone etc., have long been used to treat microbial pollution of waters. However, these compounds are not completely efficient in deactivating some resistant microorganisms and furthermore result in the production of harmful by-products. Therefore, it is necessary to utilize more advanced and efficient methods to disinfect wastewaters. As of late, photocatalysis has been investigated as an alternative treatment for wastewater disinfection. TiO_2 in particular has extensively been applied to disinfection systems. Therefore, for a catalyst to be considered effective for its wastewater treatment potential, it must demonstrate some disinfection capabilities. Consequently, BiOBr photocatalysis has also been applied to systems containing microorganisms to observe its effects on disinfection.

Micrococcus lylae, a gram positive bacterium, has been used as a model bacterium to test the disinfection characteristics of BiOBr [33]. It was determined that BiOBr can kill *Micrococcus lylae* in water under fluorescent light irradiation [33]. The fluorescent light photocatalytic disinfection is safe and cost effective as compared to disinfection using UV and chlorine since the latter ones use hazardous irradiation and produce disinfection by-products in the process [33]. This presents a strong potential for BiOBr to be used in disinfection processes.

In addition to microorganisms, toxins produced by these microorganisms pose a great threat. Cyanotoxins are toxins produced in cyanobacteria and have caused illness worldwide in both humans and animals [70]. Some of the most common cyanotoxins found in potable water are microcystins (MCs), which have been identified as strongly hepatotoxic and are known to promote formation of tumors. Recently, it was interestingly discovered that BiOBr can catalyze the degradation of microcystin-LR (MC-LR) in water at neutral pH under visible light [70]. This is a very useful finding since MCs undergo insufficient oxidation by chlorination and BiOBr degradation can prove to be a promising alternative.

1.7.4 Heavy Metal Ions

In addition to microorganisms, organics and organic dyes, BiOBr systems have also been applied to bring about heavy metal reduction in wastewater.

Chromium (VI) is a hazardous pollutant, and its efficient removal from the environment is of great importance [33]. Zhang and coworkers [33] found that BiOBr nanostructures can remove Cr (VI) with a minimum removal rate of 90% within 6 hours. In another study, it was demonstrated that BiOBr flowerlike structures possessed a large BET surface area and exhibited excellent removal capacity and fast adsorption rate for Cr (VI) in a wide pH range, which demonstrated that it could be used as an ideal material for the removal of Cr (VI) ions from water [71]. This opens up a lot of possibilities for application of BiOBr photocatalysis systems.

1.7.5 Air Pollution

Air pollution control is yet another field where photocatalysis has proved to be very useful and effective. TiO_2 has already been commercialized and is in use by a lot of Asian countries for the purpose of keeping the air cleaner. Therefore, a good photocatalyst must be applicable to air pollution treatment. Research on application of BiOBr for air pollution control has been limited. However, the works that have been done show positive results.

Nitrogen monoxide (NO) is one of the most common gaseous pollutants [72]. Although traditional techniques such as physical adsorption, biofiltration, and thermal catalysis methods can remove NO from industrial emission, they are not economically feasible for the removal of NO at parts per billion (ppb) levels in indoor air. In one study, bismuth oxybromide (BiOBr) nanoplate microspheres were used to remove NO in indoor air under visible light irradiation [73]. Interestingly, BiOBr microspheres demonstrated excellent photocatalytic NO removal ability under visible light irradiation. More remarkably, the BiOBr microspheres were stable and could keep long-term activity after multiple photocatalytic removal runs [73]. Another study reported that BiOBr and graphene nanocomposites display superior performance in photocatalytic removal of gaseous nitrogen monoxide (NO) to pure BiOBr under visible light irradiation [72]. This shows that BiOBr can also be used for air pollution systems.

1.8 Conclusion

This review summarizes the main research areas and progress made in the photocatalysis of BiOBr. Although the discovery of this photocatalyst is relatively recent and the works done in this area are limited, a review of literature in this area demonstrates that BiOBr could be an excellent prospective commercial photocatalyst. Its applications in treatment of wastewater by degrading organics, organic dyes, heavy metal ions, microorganisms and applications in air pollution make it a very good alternative for commercially available TiO_2. Moreover, it is visible light active which introduces the possibility of utilizing much of the solar radiation, and hence is an attractive cost cutting agent in the field of photocatalysis.

There are, however, areas that need to be further researched and impinged on before BiOBr could be developed as a commercially available and widely used photocatalyst. The main issue that should be undertaken is that BiOBr is a photocatalyst whose structure is highly dependent on its synthesis method and the various parameters associated with the method. This makes it difficult to choose one particular method over another while utilizing this photocatalyst. Further research is being conducted on improving the photoactivity and determining optimal synthesis routes for BiOBr. Chemical variations and disinfection studies relating to BiOBr are also few and need further investigation. Overall, the future of BiOBr as a photocatalyst appears to be bright with many possibilities and promises.

References

[1] Malato, S., Fernandez-Ibanez, P., Maldonado, M.I., Blanco, J., Gernjak, W., 2009. Decontamination and disinfection of water by solar photocatalysis: recent overview and trends. Catal. Today 147, 1-59

[2] Wintgens, T., Salehi, F., Hochstrat, R., Melin, T., 2008. Emerging contaminants and treatment options in water recycling for indirect potable use. Water Sci. Technol. 57, 99-107

[3] Sharma, D., Bansal, A., Ameta, R., Sharma, H.S., 2011. Photocatalytic degradation of Azure B using Bismuth oxide semiconducting powder. Int. J. ChemTech. Res. 3, 1008-1014

[4] Tanaka, K., Padermpole, K., Hisanaga, T., 2000. Photocatalytic degradation of azo dyes. Water Res. 34, 327–333

[5] Padmanabhan, P.V.A., Sreekumar, K.P., Thiyagarajan, T.K., Satpute, R.U., Bhanumurthy, K., Sengupta, P., Dey, G.K., Warrier, K.G.K., 2006. Nano-crystalline titanium dioxide formed by reactive plasma synthesis. Vacuum 80, 11-12

[6] Lu, J., Zhang, T., Ma, J., Chen, Z., 2009. Evaluation of disinfection by-products formation during chlorination and chloramination of dissolved natural organic matter fractions isolated from a filtered river water. J. Hazard. Mater. 162, 140-145

[7] Chong, M.N., Jin, B., Chow, C.W.K., Saint, C., 2010. Recent developments in photocatalytic water treatment technology: A review. Water Res. 44, 2997-3027

[8] Zhang, J., Shi, F.J., Lin, J., Chen, D.F., Gao, J.M., Huang, Z.X., Ding, X.X., Tang, C.C., 2008. Self- Assembled 3-D architectures of BiOBr as a visible-light-driven photocatalyst. Chem. Mater. 20, 2937–2941

[9] Serpone, N., Pelizzetti, E., 1989. Photocatalysis fundamentals and applications. John Wiley and Sons, 3-175

[10] Galvez, J.B., Ibanez, P.F., Rodriguez, S.M., 2007. Solar Photocatalytic Detoxification and Disinfection of Water: Recent Overview. J. Sol. Energy Eng. 129, 4-15

[11] Fujishima, A., Honda, K., 1972. Electrochemical Photolysis of Water at a Semiconductor Electrode. Nature, 238, 37-38

[12] Herrmann, J.M., 1999. Heterogeneous photocatalysis: fundamentals and applications to the removal of various types of aqueous pollutants Catal. Today, 53, 115-129.

[13] Hoffmann, M. R., Martin, S. T., Choi, S. T., Bahnemann, S. T., 1995. Environmental applications of Semiconductor Photocatalysis. Chem. Rev., 95, 69–96.

[14] An, H., Du Y., Wang T., Wang C., Hao W., Zhang J., 2007. Photocatalytic Properties of BiOX (X= Cl, Br, and I). Rare Met., 27, 243-251.

[15] He, C., and Gu M., 2006. Photocatalytic activity of bismuth germinate $Bi_{12}GeO_{20}$ powders. Scripta Mater., 54, 1221-1229.

[16] Rengaraj S., Li X.Z., Tanner P.A., Pan Z.F., and Pang G.K.H., Photocatalytic degradation of methylparathion: An endocrine disruptor by Bi3+-doped TiO2, J. Mol. Catal. A, 2006, 247, 36.

[17] Zhang, X., Ai, Z., Jia, F., Zhang, L., 2008. Generalized One-Pot Synthesis, Characterization, and Photocatalytic Activity of Hierarchical BiOX (X = Cl, Br, I) Nanoplate Microspheres. J. Phys. Chem. C 112, 747–753.

[18] Shang, M., Wang, W., Zhang, L., 2009. Preparation of BiOBr lamellar structure with high photocatalytic activity by CTAB as Br source and template. J. Hazard. Mater. 167, 803–809.

[19] L. Zhang, X. F. Cao, X. T. Chen, Z. L. Xue, J., 2011. BiOBr hierarchical microspheres: Microwave-assisted solvothermal synthesis, strong adsorption and excellent photocatalytic properties. J. Colloid Interf. Sci. 354, 630 –636.

[20] Z. Jiang, F. Yang, G. Yang, L. Kong, M. O. Jones, T. Xiao, P. P. Edwards, 2010. The hydrothermal synthesis of BiOBr flakes for visible-light-responsive photocatalytic degradation of methyl orange. J. Photochem. Photobiol. A, 212, 8 –13

[21] Liu, Y., Son, W.J., Lu, J., Huang, B., Dai, Y., Whangho, M.H., 2011. Composition Dependence of the Photocatalytic Activities of $BiOCl_{1-x}Br_x$ Solid Solutions under Visible Light. Chem. Eur. J., 17, 9342 – 9349.

[22] K. Y. Jung, S. B. Park, S.-K. Ihm, 2004. Local structure and photocatalytic activity of B_2O_3–SiO_2/TiO_2 ternary mixed oxides prepared by sol–gel method. Appl. Catal. B, 51, 239 –245.

[23] S. Y. Chai, Y. J. Kim, M. H. Jung, A. K. Chakraborty D. Jung, W. I. Lee, 2009. Heterojunctioned BiOCl/Bi_2O_3, a new visible light photocatalyst. Catal. Commun. 262, 144 – 149

[24] Henle, J., Simon, P., Frenzel, A., Scholz, S., Kaskel, S., 2009. Nanosized BiOX (X = Cl, Br, I) Particles Synthesized in Reverse Microemulsions. Chem. Mater. 19 (2007) 366–373

[25] Shi, Z. Q., Wang, Y., Fan, C.M., Wang, Y.F., Ding, G.Y., 2011. Preparation and photocatalytic activity of BiOCl catalyst. Trans. Nonferrous Met. Soc. China 21, 2254-2259.

[26] Wang, W., Huang, F., Lin, X., Yang, J., 2008. Visible-light-responsive photocatalysts xBiOBr–(1−x)BiOI, Catal. Commun. 9, 8–12

[27] Rabenau, A., 1985. The Role of Hydrothermal Synthesis in Preparative Chemistry. Angew. Chem. Int. Ed. 24, 1026–1040.

[28] H. Kodama, S. Horiuchi, A. Watanabe, 1988. The hydrothermal synthesis of bismuth oxide chlorides. J. Solid State Chem. 75, 279–284.

[29] H. Deng, J. Wang, Q. Peng, X. Wang, Y. Li, 2005. Controlled Hydrothermal Synthesis of Bismuth Oxyhalide Nanobelts and Nanotubes. Chem. Eur. J. 11, 6519–6524.

[30] J. Wang, Y. Li, 2003. Synthesis of single-crystalline nanobelts of ternary bismuth oxide bromide with different compositions. Chem. Commun. 18, 2320–2321.

[31] Y. Chen, M. Wen, Q. Wu, 2011. Stepwise blossoming of BiOBr nanoplate-assembled microflowers and their visible-light photocatalytic activities. Cryst. Eng. Comm., 13, 3035–3039

[32] Cheng, H., Huang, B., Wang, Z., Qin, X., 2011. One-Pot Miniemulsion-Mediated Route to BiOBr Hollow Microspheres with Highly Efficient Photocatalytic Activity. Chem. Eur. J., 17, 8039 – 8043

[33] Zhang, D., Wena, M., Jianga, B., Li, G., Yub, J., 2012. Ionothermal synthesis of hierarchical BiOBr microspheres for water treatment. J. Hazard. Mater., 210, 104-111

[34] Xia, J., Yin, S., Li, H., Xu, H., Xu, L., Xu, Y., 2011. Improved visible light photocatalytic activity of sphere-like BiOBr hollow and porous structures synthesized *via* a reactable ionic liquid. Dalton Trans., 40, 5249–5258.

[35] Seh, Z. W., Liu, S., Low, M., Zhang, S., Liu, Z., Mlayah, A., Han, M., 2012. Janus Au-TiO2 Photocatalysts with Strong Localization of Plasmonic Near-Fields for Efficient Visible-Light Hydrogen Generation. Adv. Mater., 24, 2310−2314.

[36] Wang, P., Huang, B., Qin, X., Zhang, X., Dai, Y., Wei, J., Whangbo, M., 2008. Ag/AgCl: A Highly Efficient and Stable Photocatalyst Active under Visible Light. Angew. Chem., Int. Ed. 47, 7931−7933.

[37] Ma, R., Sasaki, T., Bando, Y. J. Am., 2004. Layer-by-Layer Assembled Multilayer Films of Titanate Nanotubes, Ag- or Au-Loaded Nanotubes, and Nanotubes/Nanosheets with Polycations. Chem. Soc., 126, 10382−10388.

[38] Cheng, H., Huang, B., Wang, P., Wang, Z., Lou, Z., Wang, J., Qin, X., Zhang, X., Dai, Y., Synthesis of Highly Efficient Ag/AgCl Plasmonic Photocatalysts with Various Structures. Chem. Commun., 47, 7054−7056.

[39] Liu, J., Sun, Y., Li, Z., 2012. Ag loaded flower-like BaTiO3 nanotube arrays: Fabrication and enhanced photocatalytic property. Cryst. Eng. Comm., 14, 1473−1478.

[40] Xi, G., Ye, J., Ma, Q., Su, N., Bai, H., Wang, C. J., 2012. In Situ Growth of Metal Particles on 3D Urchin-like WO3 Nanostructures. Am. Chem. Soc., 134, 6508−6511.

[41] Matsubara, K.; Tatsuma, T., 2007. Morphological changes and multicolor photochromism of Ag nanoparticles deposited on single-crystalline TiO2 surfaces. Adv. Mater., 19, 2802−2806.

[42] Jiang, G., Wang, R., Wang, X., Xi, X., Hu, R., Zhou, Y., Wang, S., Wang, T., Chen, W., 2012. Novel Highly Active Visible-Light-Induced Photocatalysts Based on BiOBr with Ti Doping and Ag Decorating. Appl. Mater. Interfaces, 4, 4440−4444.

[43] Wang, R., Jiang, G., Wang, X., Hu, R., Xi, X., Bao, S., Zhou, Y., Tong, T., Wang, S., Wang, T., Chen, W., 2011. Efficient visible-light-induced photocatalytic activity over the novel Ti-doped BiOBr microspheres. Powder Technology, 228, 258–263.

[44] Yu, C., Fan, C., Meng, X., Yang, K., Cao, F., Li, X., 2011. A novel Ag/BiOBr nanoplate catalyst with high photocatalytic activity in the decomposition of dyes. Reac. Kinet. Mech. Cat., 103, 141–151

[45] T.B. Li, G. Chen, C. Zhou, Z.Y. Shen, R.C. Jin, J.X. Sun, New photocatalyst BiOCl/BiOI
composites with highly enhanced visible light photocatalytic performances,
Dalton Trans. 40 (2011) 6751–6758.

[46] J. Cao, B.Y. Xu, B.D. Luo, H.L. Lin, S.F. Chen, Novel BiOI/BiOBr heterojunction photocatalysts with enhanced visible light photocatalytic properties, Catal.
Commun. 13 (2011) 63–68.

[47] Khalil, S.S., Uvarov, V., Fronton, S., Popov, I., Sasson, Y., 2012. A Novel Heterojunction BiOBr/Bismuth Oxyhydrate Photocatalyst with Highly Enhanced Visible Light Photocatalytic Properties. J. Phys. Chem., 116, 11004−11012

[48] Cao, J., Xu, B., Lin, H., Luo, B., Chen, S., 2011. Chemical etching preparation of BiOI/BiOBr heterostructures with enhanced photocatalytic properties for organic dye removal. Chem. Eng. J. 185, 91– 99.

[49] Kong, L., Jiang, Z., Lai, H.H., Nicholls, R.J., Xiao, T., Jones, M.O., Edwards, P.P., 2012. Unusual reactivity of visible-light-responsive AgBr–BiOBr heterojunction photocatalysts. J. Catal., 293, 116–125

[50] Zhang, X., Chang, X., Gondal, M.A., Zhang, B., Liu, Y., Ji, G., 2012. Synthesis and photocatalytic activity of graphene/BiOBr composites under visible light. Appl. Surf. Sci. 258, 7826– 7832.

[51] Lin W.C., Yang, W.D., Jheng, S.Y, 2012. Photocatalytic degradation of dyes in water using porous nanocrystalline titanium dioxide. J. Taiwan. Inst. Chem. Eng., 43, 269–274.

[52] X.F. Chang, G. Yu, J. Huang, Z. Li, S.F. Zhu, P.F. Yu, C. Cheng, S.B. Deng, G.B. Ji, 2010. Enhancement of photocatalytic activity over NaBiO3/BiOCl composite prepared by an in situ formation strategy. Catal. Today, 153, 193–199.

[53] L. Zhang, W.Z. Wang, L. Zhou, M. Shang, S.M. Sun, 2009. Fe3O4 coupled BiOCl: A highly efficient magnetic photocatalyst. Appl. Catal. B: Environ., 90, 458–462.

[54] S.J. Wu, C. Wang, Y.F. Cui, T.M. Wang, B.B. Huang, X.Y. Zhang, X.Y. Qin, P. Brault, 2010. Synthesis and photocatalytic properties of BiOCl nanowire arrays. Mater. Lett. 64, 115–118.

[55] C.H. Wang, C.L. Shao, Y.C. Liu, L.N. Zhang, 2008. Photocatalytic properties BiOCl Bii2o3 nanofibers prepared by electrospinning. Scripta Mater. 59 (2008) 332–335.

[56] M.A. Gondal, X.F. Chang, M.A. Ali, Z.H. Yamani, Q. Zhou, G.B. Ji, 2011. Adsorption and degradation performance of Rhodamine B over BiOBr under monochromatic 532 nm pulsed laser exposure. Appl. Catal. A: Gen. 397, 192–200.

[57] J.M. Song, C.J. Mao, H.L. Niu, Y.H. Shen, S.Y. Zhang, 2010. 'Hierarchical structured bismuth oxychlorides: self-assembly from nanoplates to nanoflowers via a solvothermal route and their photocatalytic properties. Cryst. Eng. Commun. 12, 3875–3881.

[58] Y.Q. Lei, G.H. Wang, S.Y. Song, W.Q. Fan, H.J. Zhang, 2009. 'Synthesis, characterization and assembly of BiOCl nanostructure and their photocatalytic properties. Cryst. Eng. Commun. 11, 1857–1862.

[59] F. Chen, H.Q. Liu, S. Bagwasi, X.X. Shen, J.L. Zhang, 2010. Photocatalytic study of BiOCl for degradation of organic pollutants under UV irradiation. J. Photochem. Photobiol. A
215, 76–80

[60] Chang, X., Huang, J., Cheng, C., Sui, Q., Sha, W., Ji, G., Deng, S., Yu G., 2010. BiOX (X = Cl, Br, I) photocatalysts prepared using NaBiO3 as the Bi source: Characterization and catalytic performance. Catal. Commun., 11, 460–464

[61] Xiao, P., Zhu, L., Zhu, Y., Qian, Y., 2012. Room- Temperature Synthesis of BiOBr Sub-Microflowers and Their Photocatalytic Properties. J. Nanosci. Nanotechnol., 12, 2008-2013

[62] Feng, Y., Li, L., Li, J., Wang, J., 2011.Synthesis of mesoporous BiOBr 3D microspheres and their photodecomposition for toluene. J. Hazar. Mater., 192, 538–544

[63] Xu, J., Meng, W., Zhang, Y., Li., L., 2011. Photocatalytic degradation of tetrabromobisphenol A by mesoporous BiOBr. Appl. Catal. B: Environ., 107, 355– 362

[64] Nose K, Hashimoto S, Takahashi S, Noma Y, Sakai SI. 2007. Degradation pathways of decabromodiphenyl ether during hydrothermal treatment. Chemosphere, 68, 120-125.

[65] Sun CY, Zhao D, Chen CC, Ma WH, Zhao JC. 2009. TiO2-Mediated Photocatalytic
Debromination of Decabromodiphenyl Ether: Kinetics and Intermediates. Environ Sci Technol 43, 157-162.

[66] Li A, Tai C, Zhao ZS, Wang YW, Zhang QH, Jiang GB, Hu JT. 2007. Debromination of decabrominated diphenyl ether by resin-bound iron nanoparticles. Environ Sci Technol 41, 6841-6846

[67] Zhou J, Jiang WY, Ding J, Zhang XD, Gao SX. 2007. Effect of Tween 80 and β-cyclodextrin on degradation of decabromodiphenyl ether (BDE-209) by whiterot fungi. Chemosphere 70, 172-177.

[68] Xue Li, Jun Huang, Shu B. Deng, Gang Yu, Jing Qi, Xiao F. Chang, 2010. Photocatalytic Decomposition of Decabromodiphenyl Ether (BDE-209) over BiOBr Driven by Visible Light: Kinetics and Intermediates. Paper presented at *Sixth International Symposium on Flame Retardants,* BFR 2013 San Francisco, CA

[69] Xu, J., Li, L., Guo, C., Zhang, Y., Wang, S., 2013. Removal of benzotriazole from solution by BiOBr photocatalysis under simulated solar irradiation. Chem. Eng. J., 221, 230-237

[70] Yanfen, F., Yingping, H., Jing, Y., Pan,W., Genwe C., 2011. Unique Ability of BiOBr To Decarboxylate D-Glu and D-MeAsp in the Photocatalytic Degradation of Microcystin-LR in Water. Environ. Sci. Technol., 45, 1593–1600

[71] Li, G., Qin, F., Yang, H., Lu, Z., Sun, H., Chen, R., 2012. Facile Microwave Synthesis of 3D Flowerlike BiOBr Nanostructures and Their Excellent Cr (VI) Removal Capacity. Eur. J. Inorg. Chem., 25, 2508–2513

[72] Ai, Z., Ho, W., Lee, S., 2011. Efficient Visible Light Photocatalytic Removal of NO with
BiOBr-Graphene Nanocomposites. J. Phys. Chem. C, 115, 25330–25337

[73] Ai, Z., Ho, W., Lee, S., Zhang, L., 2009. Efficient Photocatalytic Removal of NO in Indoor Air with Hierarchical Bismuth Oxybromide Nanoplate Microspheres under Visible Light. Environ. Sci. Technol., 43, 4143–415

Chapter 2 - Optimization of Visible Light Activated BiOBr Photocatalyst for Wastewater Treatment Applications

2.1 Introduction

Rapid industrial development, population growth and long-term droughts have led to an increased demand for clean water sources. More than 4 billion people around the globe do not have access to clean and sanitized water supply and millions have died due to severe waterborne diseases (Malato et al., 2009). Treating and reusing industrial wastewater has thus become of utmost importance.

Industrial wastewaters generated from various manufacturing industries such as pharmaceutical, textile, pesticides and other organic chemicals manufacturing industries contain different concentrations of organic textile dyes. As a result, these effluents are intensely colored and are polluted with high concentration of organic and other refractory compounds which cause toxicity and foul odours in water. Degradation of these non-biodegradable organic compounds is not possible by conventional biological treatment processes (Sharma et al. 2011). Currently available water treatment technologies such as adsorption and coagulation simply concentrate the pollutants enabling them to be passed to a different phase and therefore cause secondary pollution (Tanaka et al., 2000, Padmanabhan et al., 2006). The most commonly used disinfection process is chlorination of water. However, this process generates by-products that are known to be hazardous to human health (Lu et al., 2009). Lately, there has been a lot of research in application of the advanced oxidation processes (AOP's) for removal of these organic compounds in

wastewater. Photocatalytic degradation was found to be the most promising and efficient process among AOPs in controlling the environmental pollution and wastewater treatment due to its demonstrated efficiency in degrading a wide range of refractory organic and other pollutants into readily biodegradable compounds (Sharma et al., 2011). Photocatalysis uses light energy to activate the photocatalyst, generally a semiconductor, which modifies the rate of a chemical reaction without being involved itself.

Among the possible semiconductors, TiO_2, or titanium dioxide, is most extensively used. However, it can only be activated by ultraviolet light (wavelength < 400 nm), which forms about 5% of the solar spectrum. Considering that visible light accounts for 43% of the solar spectrum, the development of efficient visible-light-driven photocatalysts is becoming attractive and much effort has been devoted to this research as solar photocatalysis technology is inexpensive, environmentally friendly, and universally applicable (Zhang et al., 2012).

Bismuth oxyhalide compounds (BiOX, X= Cl, Br, I) have recently been found to be potential photocatalysts under UV or visible-light illumination (Wang et al., 2008). Among the bismuth oxyhalides, BiOBr is of particular importance because it is visible-light responsive, relatively stable under light irradiation and offers efficient degradation of a variety of pollutants (Zhang et al., 2008).

One of the main challenges of applying BiOBr as a viable photocatalyst is that there are various methods of synthesis for this catalyst and many parameters exist which play a role in the performance of this catalyst. Therefore, it is necessary to discover a general suitable synthesis method and advance fundamental understanding of the crystalline structure

evolution and its influence on photocatalytic performance of BiOBr. The focus of this research is to determine optimum synthesis parameters and crystalline structure to maximize efficiency. The two synthesis methods selected for comparison are hydrothermal and solvothermal synthesis routes since they have emerged as the most promising synthesis methods for production of BiOBr (Zhang et al., 2011, Rabenau, 1985, Deng et al., 2005). The parameters at which catalyst preparation are optimized are temperature and time of thermal treatment as effects of these two parameters on catalyst performance are most pronounced. Such a comparison and optimization has not been conducted so far to the best of our knowledge.

2.2 Materials and Methods

2.2.1 Synthesis

All reagents were purchased from Sigma-Aldrich in their pure form. BiOBr samples were first synthesized using a template free hydrothermal synthesis process. 1 g $Bi(NO_3)_3 \cdot 5H_2O$ was dissolved in 3 mL acetic acid (HAc), and was dissolved in 30 mL distilled de-ionized water containing 0.24 g KBr under magnetic stirring. Upon mixing of the two solutions, yellow precipitates of BiOBr were immediately observed. After stirring for 20 min at room temperature, the suspension was transferred into a Teflon-lined stainless steel autoclave and heated at a designated heating temperature for a designated amount of time. The resulting precipitate was filtered, washed thoroughly with distilled water to remove any possible ionic species in the product, and then dried at 60 ºC to obtain BiOBr as a dried powder. To investigate effects of synthesis parameters on the photocatalyst performance, the samples were synthesized with different treatment durations and temperatures. To reveal effects of

time, samples were heated at 120ºC for durations of 3, 6, and 12 h. For temperature analysis, samples were heated 120 ºC, 150 ºC and 180 ºC, for duration of 6 h.

BiOBr was also prepared by a simple solvothermal method with $Bi(NO_3)_3 \cdot 5H_2O$ as the Bi source. Cetyltriethylammnonium bromide (CTAB), a common surfactant used for synthesis of BiOBr which acts a template as well as a bromide source was used in this method. Initially, 0.55 g of CTAB was dissolved in 40 mL of ethylene glycol (EG) solution, and 0.73 g of $Bi(NO_3)_3 \cdot 5H_2O$ was added. The resulting solution was stirred magnetically for 20 min at room temperature, and the mixture was transferred to a Teflon lined stainless steel autoclave and heated at in an oven at a certain temperature for a selected amount of time. After cooling to room temperature, the resulting precipitate was filtrated, washed with distilled water and ethanol several times, to remove ionic and organic species and then dried at 60 ºC overnight. In the study, the effects of time and temperature of treatment on catalyst performance were evaluated as well. The heating was carried out at 120 ºC, 150 ºC and 180 ºC for 3h to investigate temperature effect and effects of time were investigated by heating at 180 ºC for durations of 3h, 6h and 12h.

2.2.2 Characterization

The crystal structures and purity of samples were characterized by X-ray powder diffraction (XRD) with a Cu-Kα radiation diffractometer recorded with 2θ scope ranging from 10-80º. Scanning electron microscopy (SEM) was used to take images of the prepared BiOBr samples employing the accelerating voltage of 5 or 20 kV. UV-vis diffusion reflectance spectrum of the samples was analyzed with a UV-vis spectrophotometer (Thermo Evolution 300) equipped with an accessory to analyze powder samples.

2.2.3 Photocatalytic Activity

The photocatalytic activity of each of the prepared samples was evaluated by degradation of a pollutant in water. Rhodamine B (RhB), a common textile dye, was used as the model pollutant. The activity of the photocatalyst synthesized at each different condition was tested by analyzing decomposition of RhB under visible light irradiation in a slurry mode batch reactor. 250 mL of 10 ppm RhB solution was added to the reactor and an amount of 1 g/L BiOBr was added to it. The slurry was magnetically stirred in dark for 40 minutes in order to ensure establishment of adsorption-desorption equilibrium. A 300 Watt tungsten halide lamp was used to mimic sunlight and a cut-off filter was used to filter out any radiation below 410 nm ensuring the photocatalysis was carried out strictly under visible light irradiation. A 2.5 mL sample was taken from the reactor at small time intervals and photocatalyst was separated from the solution by centrifugation. The optical density of the supernatant was then analyzed by UV-vis spectrophotometer and the concentration of dye at each time interval was determined by using standard calibration curve of the dye. Dark and light controls were tested to rule out the effects of adsorption and dye photolysis, respectively.

2.3 Results and Discussion

2.3.1 XRD Analysis

The purity and crystallinity of the obtained BiOBr samples were examined using powder XRD measurements. Figure 1 shows the XRD patterns of hydrothermally synthesized BiOBr before and after photocatalytic treatment. All the detectable peaks in the pattern were assigned to pure BiOBr (JCPDS card no. 78-0348) and no impurity peaks were

detected, showing high purity of the product. The peaks are narrow and intense which implies good crystallinity of BiOBr samples. The intensities of the diffraction peaks with (0 0 1) series are much stronger than others which shows that the samples are anisotropic and grew along the (0 0 3) plane which is in accordance with the crystal structure of BiOBr (Shang et al., 2009). The XRD results also show that BiOBr is stable under visible light as the XRD pattern of the sample shows little change after photocatalytic activity.

The BiOBr samples formed through solvothermal synthesis were also analyzed by XRD and the results are shown in Figure 2. Samples display high of purity as established by lack of impurity peaks. The narrow broadening of peaks implies well crystallized material. The wide peaks also suggest that the crystalline size of samples is small (Zhang et al., 2011). The most intense peak occurs at the (1 1 0) position which implies growth in that direction. Also, the solvothermal BiOBr is very stable and the crystals show little change after photocatalytic activity.

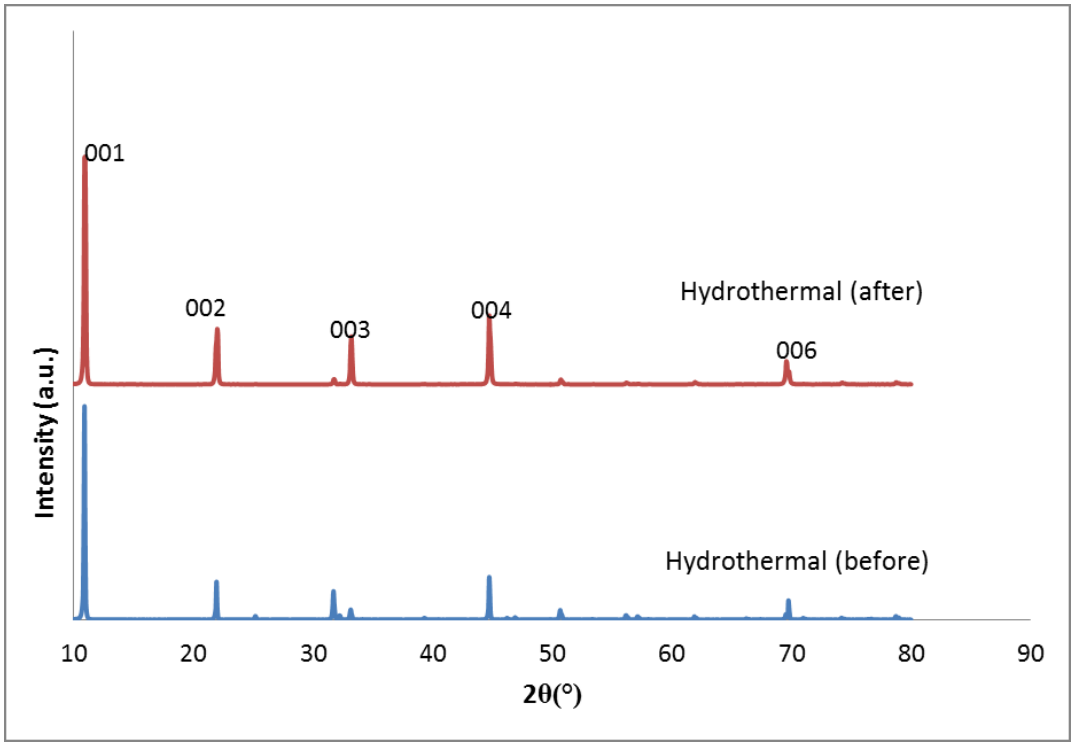

Figure 1- XRD patterns of hydrothermally synthesized BiOBr before and after photocatalytic treatment.

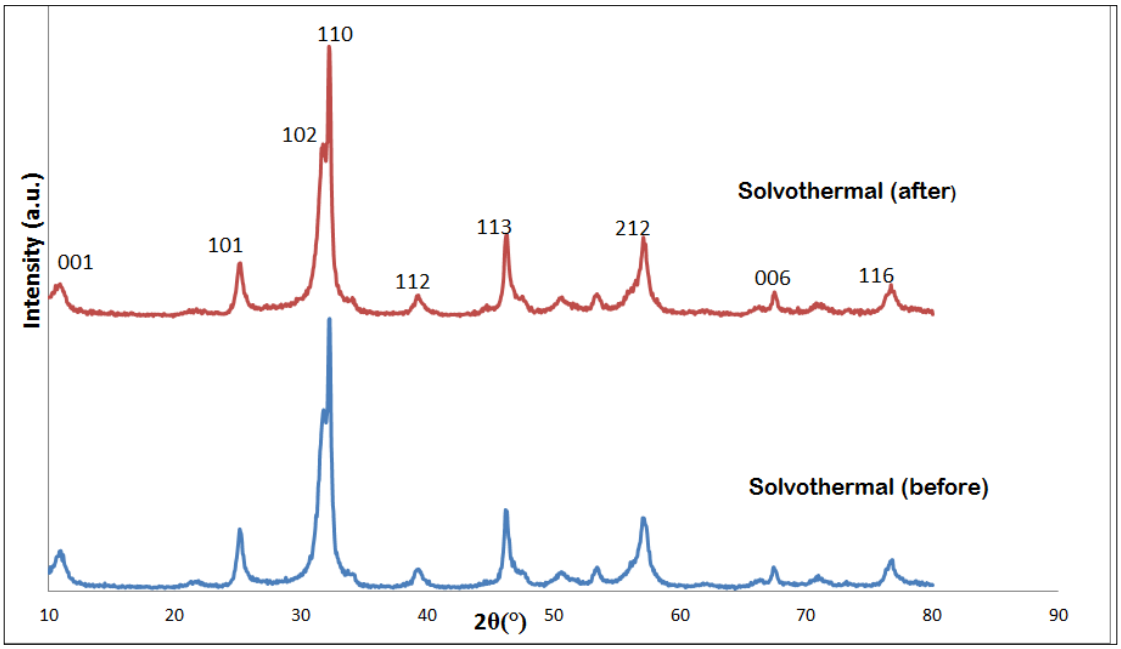

Figure 2- XRD patterns of Solvothermally Synthesized BiOBr before and after Photocatalytic Treatment

BiOBr forms a layered structure that consists of tetragonal $[Bi_2O_2]$ positive slabs, which are interleaved by double slabs of bromide to form $[Bi_2O_2Br_2]$ layers along the c axis (Jung et al., 2004, Chai et al., 2009). The permanent static electric fields between $[Bi_2O_2]$ and $[Br_2]$ layers can work as accelerators for the separations of electron–hole pairs upon photoexcitation to favor a high photocatalytic efficiency of BiOBr (Liu et al., 2011).

2.3.2 SEM Analysis

The morphology of BiOBr catalyst was characterized by scanning electron microscopy (SEM). It can be noted that the hydrothermally produced BiOBr crystals form nanoplates while those produced solvothermally appear as microspheres (Figures 3 and 4, respectively). The hydrothermal flakes/plates have an average thickness of 11.3 μm with a wider size distribution. The surface of nanoplates is smooth.

The microspheres (Figure 4) are somewhat uniform in size with an average diameter of 4.7 µm. The layered structure of bismuth based oxyhalides and EG solvent may have played a key role in the formation of 3-D microspheres. It is known that EG interacts with metal ions to produce alkoxides which causes the separation of nucleation and growth (Zhang et al., 2008). This could possibly assist in the formation of 3-D microspheres; however, the reason for this morphology is not entirely known (Zhang et al., 2008). The exterior surface of microspheres is not smooth but consists of threadlike fibers. This increases the ability of catalyst to separate and conduct photogenerated hole-electron pair efficiently (Shang et al., 2009). The 3-D spherical structure also provides a higher surface area to the catalyst, suggesting that the performance of these structures may be better than that of the plates.

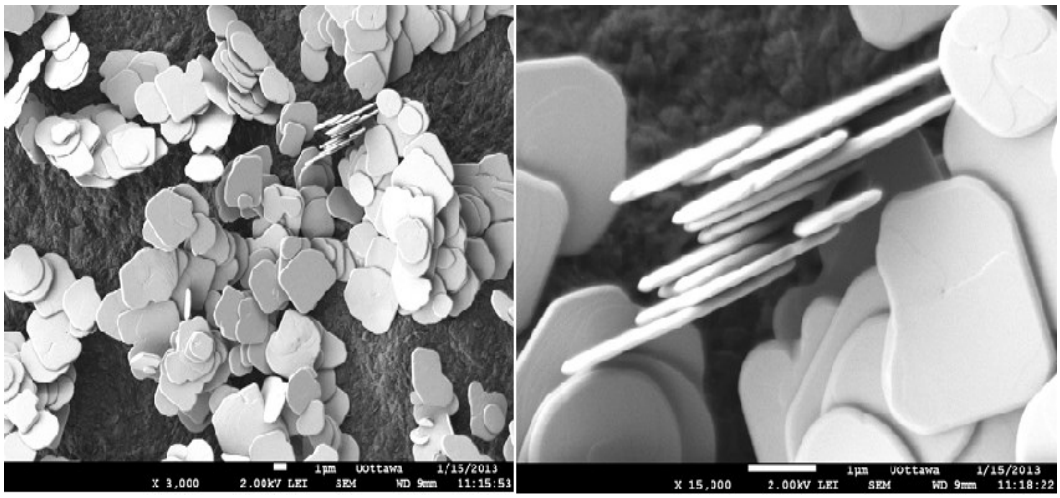

Figure 3- SEM images of hydrothermally synthesized BiOBr plates (t = 6 h, T = 120 °C)

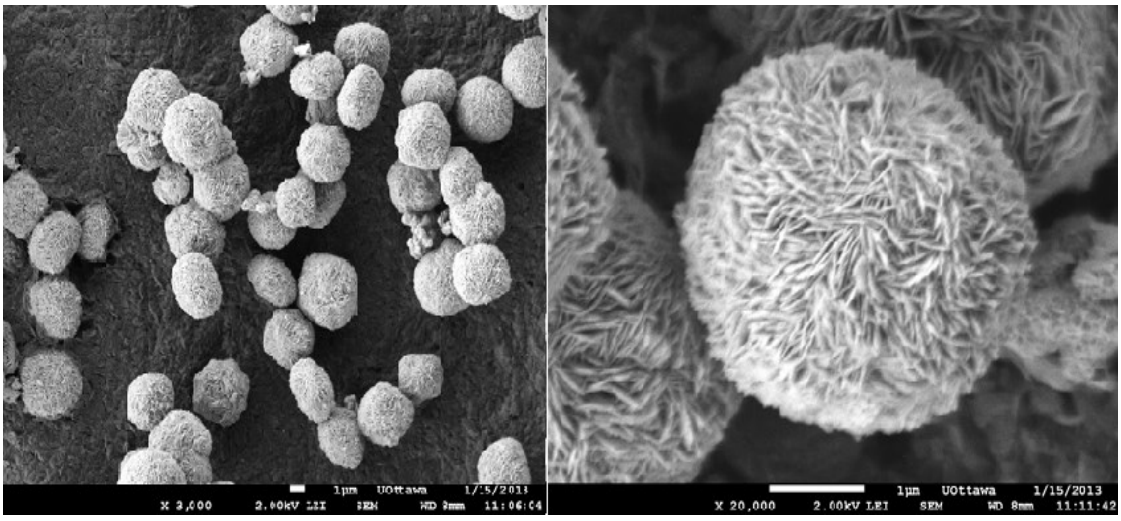

Figure 4- SEM images of solvothermally synthesized BiOBr microspheres

(t = 3 h, T = 180 °C)

2.3.3 UV-vis Diffuse Reflectance Spectra

The optical properties of BiOBr were investigated using UV-vis spectroscopy. The diffuse reflectance spectra of BiOBr hydrothermal and solvothermal samples are shown in Figure 5. Both samples indicate an increase in photoabsorption below 475 nm which is in accordance with literature (Shang et al., 2009) and suggests that these photocatalysts would be active under visible light. The band gap transition for both samples is comparable. The band gaps of samples were obtained via Tauc plots and it was found to be 2.82 eV for hydrothermally synthesized photocatalyst while that for solvothermal sample was 2.9 eV.

2.3.4 Photocatalytic activity

The photocatalytic performance for BiOBr in this paper is presented as residual concentration C/C_0, where C is the concentration at a given time and C_0 is the initial concentration, as a function of time.

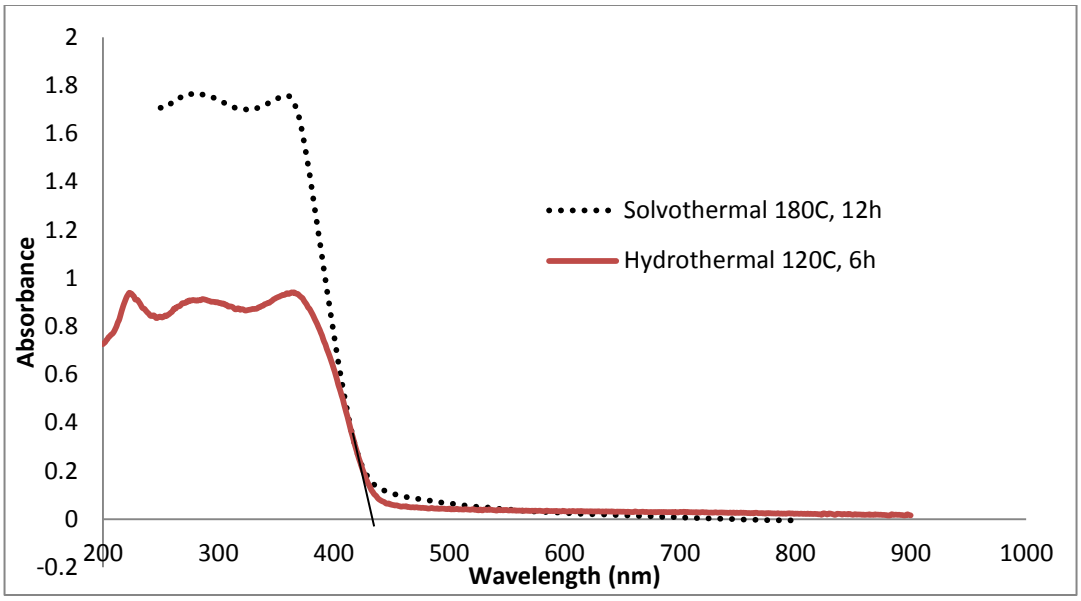

Figure 5- UV Diffuse Spectra of Solvothermal and Hydrothermal BiOBr samples

2.3.4.1 Time Studies

The influence of time of thermal treatment on photocatalytic performance of hydrothermal and solvothermal BiOBr is shown in Figures 6 (A) and (B), respectively. For hydrothermal synthesis, photocatalytic performance is maximized at 6 h whereas treatment for 3 h shows the least activity. This is due to the fact that as the time of treatment is increased, the flakes undergo better crystallite growth. However, prolonging the treatment also causes an increase in particle size which would lead to smaller surface area and thus lower activity. Due to these competing mechanisms, an optimum exists which is 6 h in this case.

For solvothermal synthesis, as the time of treatment is increased, the photocatalytic performance decreased. This is due to the decrease of microsphere diameter and loss of its surface fibers as the thermal treatment is prolonged. Rough fibers on the microsphere surface warrant a larger surface area to volume ratio, which is decreased as these fibers deteriorate over time. Therefore, the photocatalyst performs better at shorter treatment times.

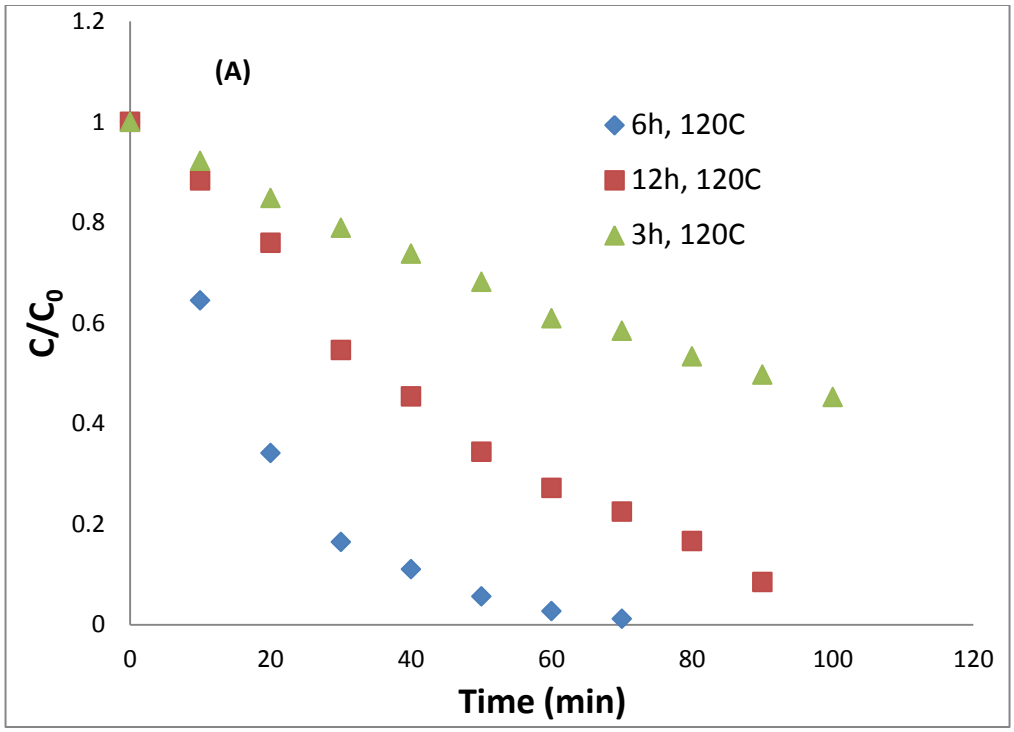

Figure 6 (A) – Effect of time of thermal treatment on photocatalytic activity on hydrothermally synthesized BiOBr

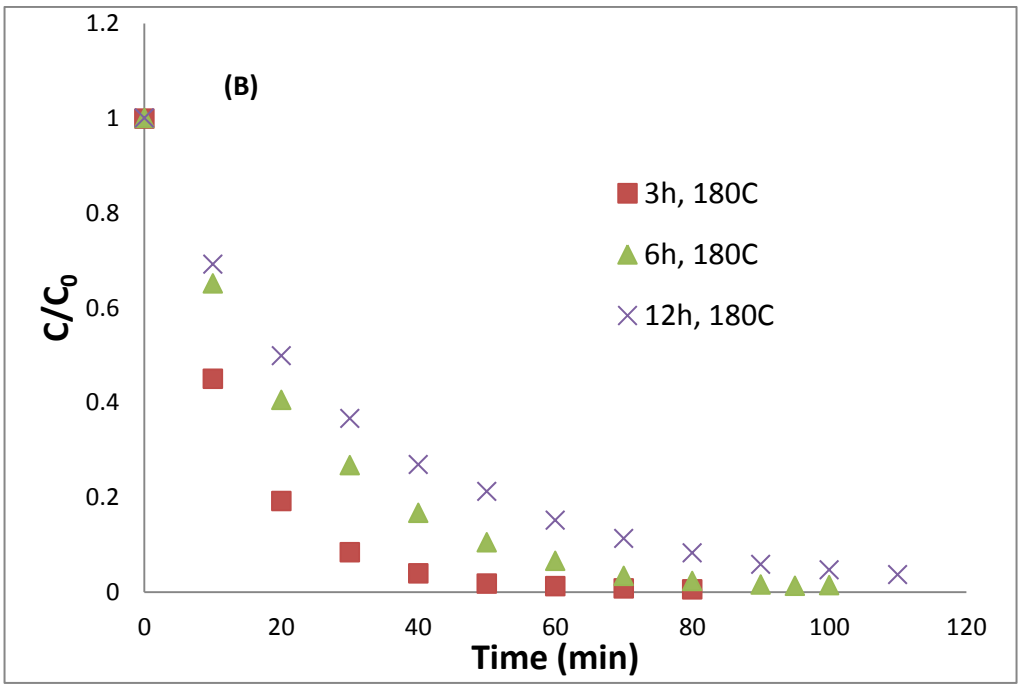

Figure 6 (B) – Effect of time of thermal treatment on photocatalytic activity on solvothermally synthesized BiOBr

2.3.4.2 Temperature Studies

The effect of temperature of thermal treatment on the photocatalytic activity of BiOBr is demonstrated in Figures 7 (A and B). Hydrothermal BiOBr samples show a decrease in activity as the temperature is increased. The XRD results show that for hydrothermal synthesis, increasing the treatment temperature results in preferential growth along the (0 0 1) direction. SEM results also show an increase in plate diameter as the temperature increases. As a result, it is likely that the photocatalytic activity decreases with the increase in temperature due to larger flakes (Figure 7-A). This result is in accordance with those reported in literature (Jiang et al., 2010). Therefore, the optimum thermal treatment conditions for hydrothermal synthesis found in this study are 120ºC for 6 h.

The results for temperature effect on the solvothermal samples show a different trend. In this case, as the temperature is increased, the performance of catalyst improves (Figure 7-B). This is due to the fact that as the temperature of treatment is increased, solvothermally synthesized microspheres decrease in size which increases the available surface area available for dye molecules. Also, the flaking in the surface of the spheres increases which also promotes the separation of electrons and holes due to presence of channels. Therefore, the performance of BiOBr is highest at the upper limit temperature of 180ºC when synthesized solvothermally. It is not advised to increase the temperature much beyond 180ºC in order to avoid boiling of EG.

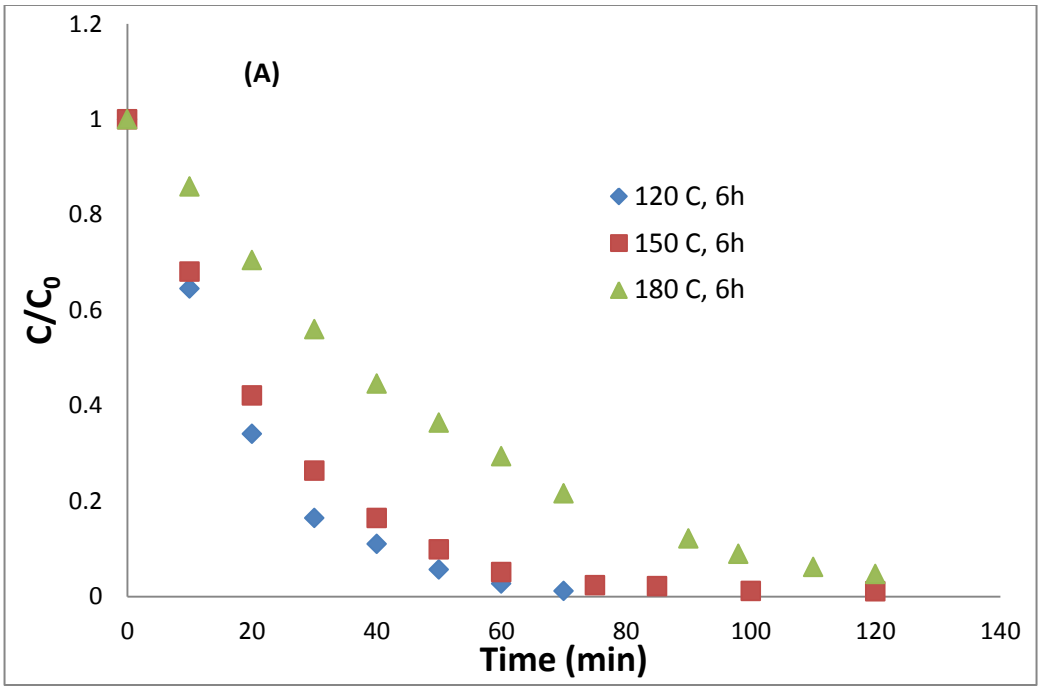

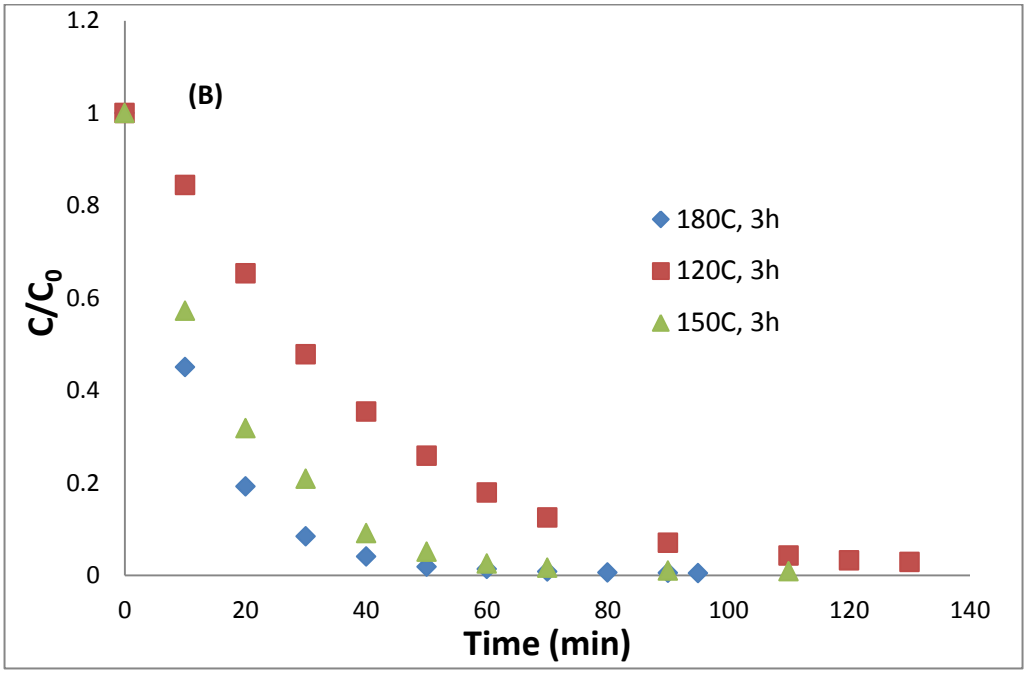

Figure 7- Effect of Temperature of thermal treatment on photocatalytic activity (A) Hydrothermally Synthesized BiOBr (B) Solvothermally Synthesized BiOBr

2.3.4.3 Synthesis Studies

Samples prepared by the solvothermal synthesis method display better photocatalytic activity than those prepared by the hydrothermal method as can be observed by the rate constants for photocatalytic degradation of RhB (Table 1). The highest rate of degradation of RhB occurred for the BiOBr sample that was prepared solvothermally with thermal treatment at 180 ºC for 3h. The superior performance by solvothermal samples is due to their micro-spherical morphology which consists of nanoscale building blocks. The 3-D spherical structure with rough fibers on the surface, increase the surface area to volume ratio of the catalyst. These hierarchal structures also have higher adsorption capacity which allows more efficient transport for the reactant molecules to active sites. Moreover, formation of these template aided structures prevents aggregation of particles which is a common problem with hydrothermal structures. This facilitates degradation of pollutant molecules due to higher exposed area and better separation of electrons and holes. Therefore, solvothermal synthesis method shows more efficient results than that obtained by hydrothermal synthesis.

Table 1- Rate Constants for Photocatalytic Activity of Different BiOBr Samples

Synthesis Method: Hydrothermal			
Temperature (ºC)	Time (h)	Rate constant k (min^{-1})	R^2
120	6	0.0599	0.9910
150	6	0.0434	0.9633
180	6	0.0239	0.9807
120	3	0.0079	0.9983
120	12	0.0231	0.9542
Synthesis Method: Solvothermal			
Temperature (ºC)	Time (h)	Rate constant k (min^{-1})	R^2
120	3	0.0283	0.9946
180	3	0.0712	0.9667
180	6	0.0452	0.9944
180	12	0.0309	0.9971

2.3.5 Catalyst Loading

The catalyst loading for the photocatalytic degradation process is an important parameter as it determines the amount of catalyst expended per cycle and therefore the optimum loading must be determined. The effect of initial catalyst loading for the optimized solvothermal photocatalyst is demonstrated in Figure 8 whereby the catalyst dosage was varied from 0.25 g/L to 1.5 g/L for the same pollutant concentration. It can be noted that as catalyst dosage is increased from 0.25 g/L, the activity also increases up to a catalyst dosage of 1 g/L. The rate constant for degradation of RhB at this value is 0.105 min^{-1} (Figure 9). Beyond a concentration of 1 g/L, a decrease is noted in the activity and for a dosage of 1.5 g/L, the rate constant decreased to 0.053 min^{-1} which is roughly half of that for 1 g/L. This result is expected since as the amount of catalyst is increased, the number of available active sites also increases, which increases the amount of hydroxyl radicals produced, thus enhancing the photocatalytic activity (Chiou et al., 2007, Suwanchawalit et al., 2008). However, increasing the catalyst loading excessively negatively affects the photocatalytic activity due to a higher extent of light scattering which negatively impacts light penetration (Behnajady et al., 2011, Wong et al., 2003, Suri et al., 1993). As a result, the photoactivity is reduced and a dosage of 1g/L is deemed as the optimized dosage. However, it must be noted that since the difference in performance for 0.5 g/L and 1 g/L is small, from an economic point of view, the catalyst dosage of 0.5 g/L may be given preference in practical applications as less catalyst would be expended and less energy would be required for regeneration.

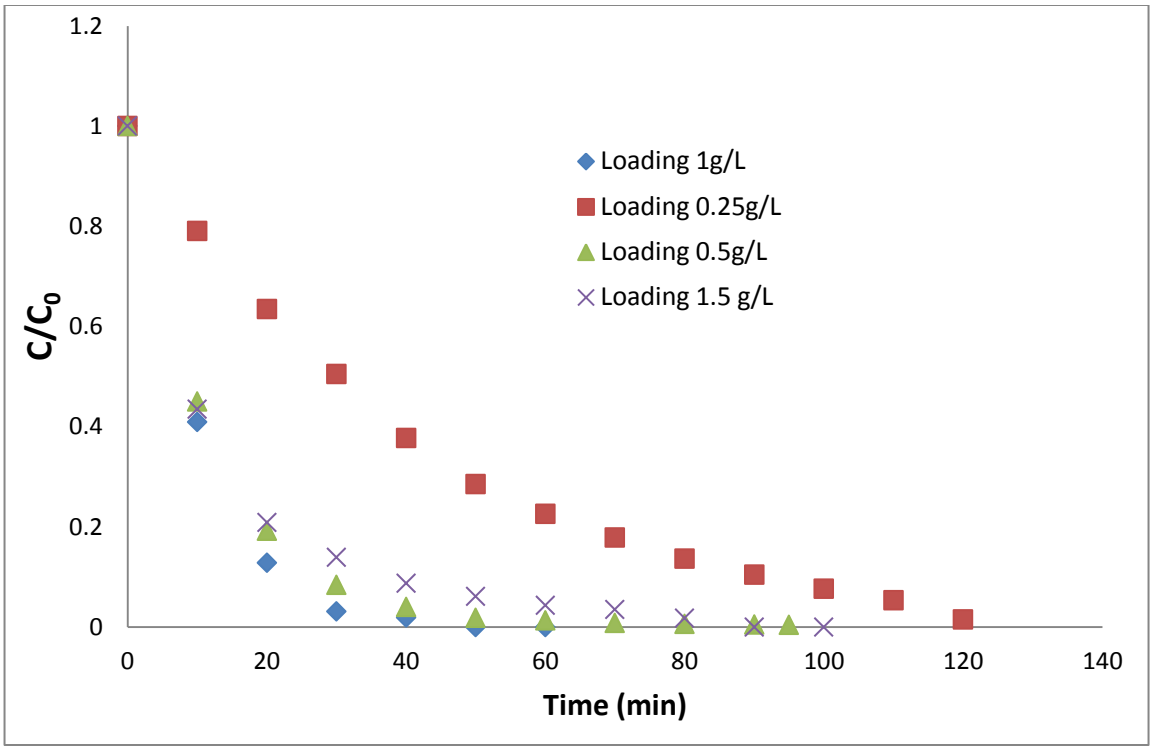

Figure 8- Effect of catalyst loading on photocatalytic activity of optimized solvothermal BiOBr

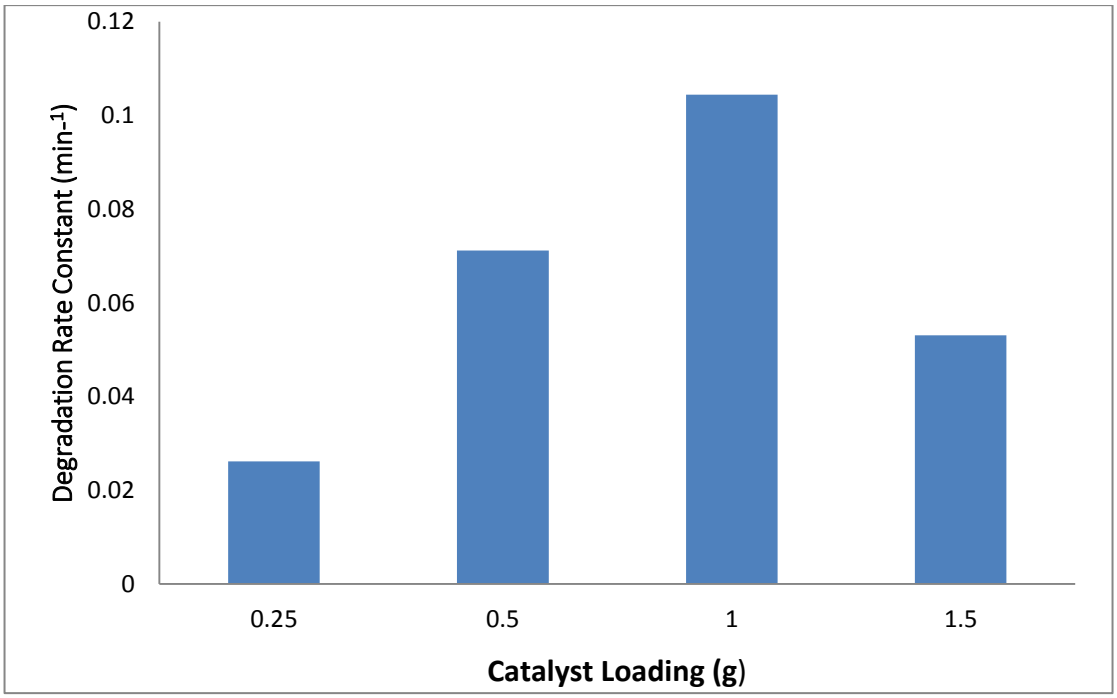

Figure 9- Degradation rate constant for various catalyst loadings

2.3.6 Recyclability Tests

Recyclability tests were performed in similar manner to the photocatalytic activity tests except for this case, catalyst was recovered at the end of the run. The catalyst was filtered, washed and then dried to regenerate it in powder form and subsequent runs were then carried out with this catalyst sample. The results are demonstrated in Figure 10, where only the solvothermally synthesized catalyst (180 ºC, 3h) results are shown but similar results were obtained for both solvothermal and hydrothermal samples. XRD data as well as SEM results support this finding that the catalyst remains intact with negligible change in photocatalytic activity. This demonstrates that the BiOBr catalyst is stable and may be reused over many runs, which is an important prerequisite for any photocatalyst.

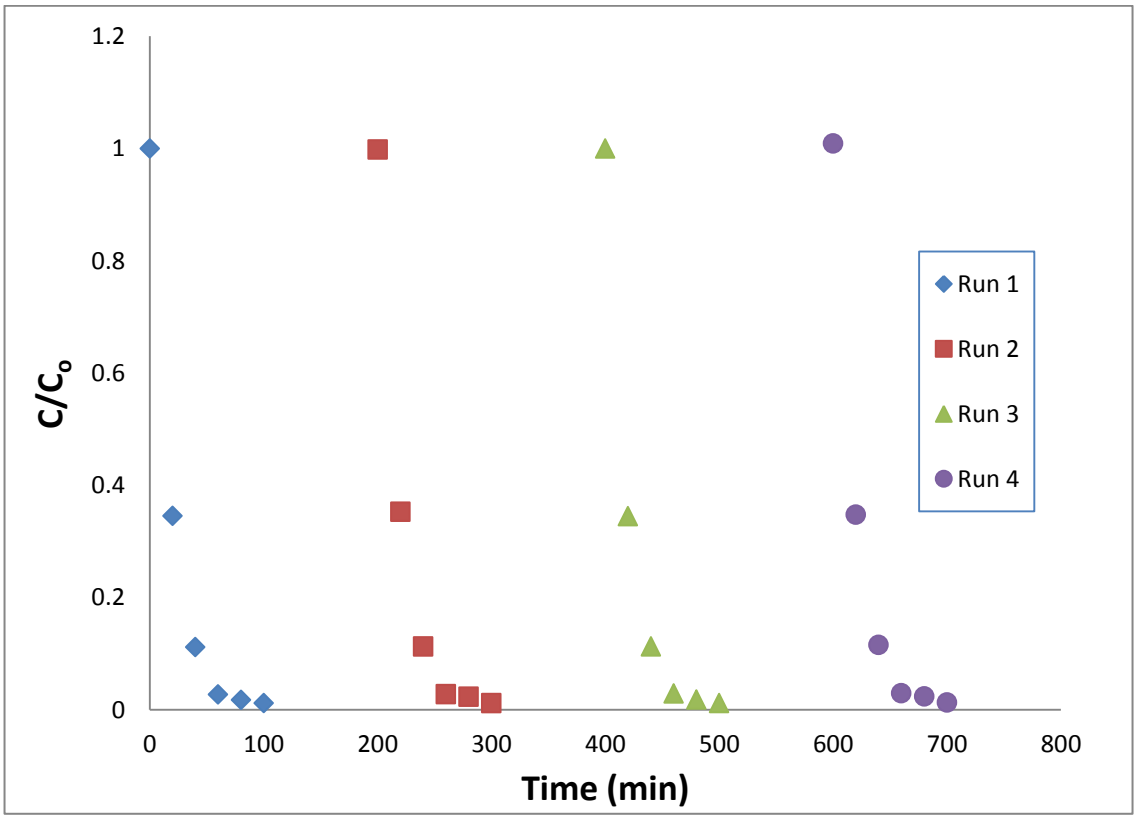

Figure 10- Recyclability tests for BiOBr catalyst (Solvothermal, 180°C, 3h)

2.4 Conclusion

BiOBr catalyst was successfully synthesized by solvothermal and hydrothermal methods under a series of different conditions. Through the degradation of RhB, it was demonstrated that the time and temperature of thermal treatment play a key role in the performance of photocatalyst. Moreover, the synthesis method is also important as it affects the morphology and structure of crystals. It was found that the solvothermal method is superior to the hydrothermal method due to formation of 3-D microspheres in the former rather than nanoplates which are formed through the latter method. Recyclability tests demonstrate that BiOBr is stable and reusable. Overall, BiOBr has been demonstrated to be a promising photocatalyst upon optimization for applications in wastewater treatment.

Author Information:
Ayla Ahmad – University of Ottawa
Zisheng Zhang* – University of Ottawa
*Corresponding author

References

Behnajady, M., Alizade, B., Modirshahla, N., 2011. Synthesis of Mg-Doped TiO2 Nanoparticles under Different Conditions and its Photocatalytic Activity. Photochemistry and Photobiology 87, 1308-1314

Chai, S.Y., Kim, Y.J., Jung, M.H., Chakraborty A.K., Jung, D., Lee, W.I., 2009. Heterojunctioned BiOCl/Bi_2O_3, a new visible light photocatalyst. Catal. Commun. 262, 144–149

Chiou, C. H., Juang, R. S., 2007. Photocatalytic degradation of phenol in aqueous solutions by Pr-doped TiO2 nanoparticles. J. Hazard. Mater. 149, 1–7

Chong, M.N., Jin, B., Chow, C.W.K., Saint, C., 2010. Recent developments in photocatalytic water treatment technology: A review. Water Res. 44, 2997-3027

Deng, H., Wang, J., Peng, Q., X. Wang, X., Y. Li, Y., 2005. Controlled Hydrothermal Synthesis of Bismuth Oxyhalide Nanobelts and Nanotubes. Chem. Eur. J. 11, 6519–6524

Jiang, Z., Yang, F., Yang, G., Kong, L., Jones, M.O., Xiao, T., Edwards, P.P., 2010. The hydrothermal synthesis of BiOBr flakes for visible-light-responsive photocatalytic degradation of methyl orange. J. Photochem. Photobiol. A, 212, 8 –13

Jung, K.Y., Park, S.B., Ihm, S.K., 2004. Local structure and photocatalytic activity of B_2O_3–SiO_2/TiO_2 ternary mixed oxides prepared by sol–gel method. Appl. Catal. B, 51, 239 –245

Liu, Y., Son, W.J., Lu, J., Huang, B., Dai, Y., Whangho, M.H., 2011. Composition Dependence of the Photocatalytic Activities of $BiOCl_{1-x}Br_x$ Solid Solutions under Visible Light. Chem. Eur. J., 17, 9342 – 9349

Lu, J., Zhang, T., Ma, J., Chen, Z., 2009. Evaluation of disinfection by-products formation during chlorination and chloramination of dissolved natural organic matter fractions isolated from a filtered river water. J. Hazard. Mater. 162, 140-145

Malato, S., Ibanez, P.F., Maldonado, M.I., Blanco, J., Gernjak, W., 2009. Decontamination and disinfection of water by solar photocatalysis: recent overview and trends. Catal. Today 147, 1-59

Padmanabhan, P.V.A., Sreekumar, K.P., Thiyagarajan, T.K., Satpute, R.U., Bhanumurthy, K., Sengupta, P., Dey, G.K., Warrier, K.G.K., 2006. Nano-crystalline titanium dioxide formed by reactive plasma synthesis. Vacuum 80, 11-12

Rabenau, A., 1985. The Role of Hydrothermal Synthesis in Preparative Chemistry. Angew. Chem. Int. Ed. 24, 1026–1040

Shang, M., Wang, W., Zhang, L., 2009. Preparation of BiOBr lamellar structure with high photocatalytic activity by CTAB as Br source and template. J. Hazard. Mater. 167, 803–809

Sharma, D., Bansal, A., Ameta, R., Sharma, H.S., 2011. Photocatalytic degradation of Azure B using Bismuth oxide semiconducting powder. Int. J. ChemTech. Res. 3, 1008-1014

Suri, R. S., Liu, J., Hand, D. W., Crittenden, J. C., Perram, D. L., Mullins, M. E., 1993. Heterogeneous photocatalytic oxidation of hazardous organic contaminants in water. Water Environ. Res. 65, 665-673

Suwanchawalit C., Wongnawa, S., 2008. Influence of calcination on the microstructures and photocatalytic activity of potassium oxalate-doped TiO2 powders. Appl. Catal., A. 338, 87–99

Tanaka, K., Padermpole, K., Hisanaga, T., 2000. Photocatalytic degradation of azo dyes. Water Res. 34, 327–333

Wang, W., Huang, F., Lin, X., Yang, J., 2008. Visible-light-responsive photocatalysts xBiOBr–(1−x)BiOI, Catal. Commun. 9, 8–12

Wintgens, T., Salehi, F., Hochstrat, R., Melin, T., 2008. Emerging contaminants and treatment options in water recycling for indirect potable use. Water Sci. Technol. 57, 99-107

Wong, C. C., Chu, W., 2003. The direct photolysis and photocatalytic degradation of alachlor at different TiO2 and UV sources. Chemosphere 50, 981–987

Zhang, J., Shi, F.J., Lin, L., Chen, D.F., Gao, J.M., Huang, Z.X., Ding, X.X., Tang, C.C., 2008. Self-Assembled 3-D architectures of BiOBr as a visible-light-driven photocatalyst, Chem. Mater. 20, 2937–2941

Zhang, L., Cao, X.F., Chen, X.T., Xue, Z.L., 2011. BiOBr hierarchical microspheres: Microwave-assisted solvothermal synthesis, strong adsorption and excellent photocatalytic properties. J. Colloid Interf. Sci. 354, 630 –636

Zhang, D., Wena, M., Jianga, B., Li, G., Yub, J., 2012. Ionothermal synthesis of hierarchical BiOBr microspheres for water treatment. J. Hazard. Mater., 210, 104-111

Chapter 3 – Application of Solvothermally Synthesized BiOBr to Disinfection and Degradation of Organics

3.1 Introduction

A growing number of water sources are not only polluted with hazardous organic and inorganic chemicals, but also with pathogenic microorganisms and this has evolved as a growing problem around the world (Schoenen, 2002; Fry, et al., 2008; Hou, et al., 2012). An estimated 1.1 billion people lack access to clean drinking water, putting them at an increased risk of contracting waterborne illnesses (Ede, et al., 2012; Zhu, et al., 2012). In order to combat presence of disease causing microorganisms, chemical oxidation technologies such as chlorination and ozonation have been applied to drinking water (Gibbons & Laha, 1999; Goslan, et al., 2009). However, despite the use of these technologies with considerable efficacy, several issues related to these processes have become apparent (Ede, et al., 2012). The chlorination of organic compounds in water can lead to the formation of harmful and undesirable by-products, such as trihalomethanes and chlorophenols, which are known to be mutagenic (Jolley, et al., 1990; Dunlop, et al., 2002). Chemical oxidation processes, particularly ozonation, require expensive chemicals and equipment for onsite disinfection (Dalrymple, et al., 2010). They can also lead to secondary pollution (Dunlop, et al., 2002). Moreover, chemical disinfectants can also cause problems such as foul odors and taste in drinking water sources (Gray, 1994). However, the biggest problem with these existent potable water disinfection methods is the emergence of waterborne pathogens, such as *Cyptosporidium*, which are resistant to chemical disinfection (Dunlop, et al., 2002; Szewzyk, et al., 2000; Betancourt & Rose, 2004). While direct UV radiation alone is capable of sustained disinfection, the hazards of intensive and direct use

of UV radiation limit its application solely for medical and technical purposes (Zhang, et al., 2010). All of the abovementioned concerns have led researchers to investigate alternative technologies for disinfection of water intended for human consumption that can efficiently inactivate microorganisms without the production of toxic by-products (Zhu, et al., 2012; Lazarova, et al., 1999).

Ever since Matsunaga and coworkers reported the bactericidal effect of TiO_2 photocatalyst under UV irradiation for the first time in 1985 (Matsunaga, et al., 1985), photocatalytic disinfection has been extensively carried out for disinfection and inactivation of microorganisms in water (Li & Qu, 2009; Kim & Kwak, 2008). Advanced oxidation processes (AOPs) including photocatalysis potentially offer good alternative disinfection of drinking water, particularly in developing countries where solar irradiation may be employed for the disinfection process (Ede, et al., 2012). Reactive radicals produced in photocatalytic processes can degrade a wide range of chemical compounds and inactivate harmful microorganisms in potable water (Kim & Kwak, 2008). However, current photocatalytic processes which are TiO_2 driven are limited due to its poor quantum efficiency and wide band gap which allows it to only absorb in the UV light region (Hou, et al., 2012). Since UV light forms only 5% of the entire solar energy, the utilization of solar radiation for such photocatalytic processes is not possible (Zhang, et al., 2003). Several methods have been employed in order to make TiO_2 compatible with solar light by shifting its optical response towards the visible light region. Methods include doping TiO_2 with transition metals or non-metals and dye sensitization have been applied in studies with considerable improvement of visible light absorption of TiO_2 (Ide, et al., 2010; Xiao & Ouyang, 2010). Despite reported improvements in absorption, enhanced TiO_2

photocatalysts present several limitations such as toxicity and self-photodegradation of organic dye, instability of metal doped titania and low absorption efficiency of non-metal-doped titania in the visible light region (Chen & Mao, 2007; Zhu, et al., 2012). Moreover, only a few of the developed photocatalysts are applicable to disinfection under visible light (Zhang, et al., 2010). As a result, research is still on-going to discover a photocatalyst with narrow band gap that can be activated by visible light and can effectively bring about inactivation of microorganisms and degradation of other pollutants.

In recent times, bismuth oxyhalides, BiOX (X = Cl, Br, I), have been extensively applied in research due to their unique optical properties and favourable potential industrial applications (Henle, et al., 2007; Zhang, et al., 2008 a; Xia, et al., 2010). Among the bismuth oxyhalides, BiOBr is of particular prominence due to its strong visible-light activation, good stability under light irradiation and demonstration of efficient degradation of a variety of pollutants under various conditions (Zhang, et al., 2008 a). The electrical, optical and photocatalytic properties of BiOBr are due to its intrinsic crystalline layer and lamellar structure which make it distinctive as a photocatalyst (Zhang, et al., 2008 b). It has been reported that BiOBr shows greater photocatalytic activity than the commercialized Degussa P25 (TiO_2 aerosol mixture comprised of rutile and anatase phases) under visible light illumination (Shang, et al., 2009; Zhang, et al., 2008 b). Practical applications of BiOBr are limited due to lack of optimized synthesis methods and photocatalytic conditions. Our research group has previously investigated and reported an optimal synthesis route for producing highly efficient visible-light active BiOBr crystals via a solvothermal method using CTAB (Chapter 2). Under the reported conditions, BiOBr appears to be a promising visible-light active photocatalyst for wastewater treatment. In

order for BiOBr to be practically relevant, it must also demonstrate applicability to potable water purification by degradation of a wider range of pollutants as well as disinfection properties.

The drinking water treatment industry employs procedures based on use of surrogate bacteriological indicators in order to evaluate the efficiency of the disinfection process (Dunlop, et al., 2002). A commonly used indicator of drinking water treatment efficiency is *Escherichia coli* (*E. coli*), a gram negative bacterium (Baker & Herson, 1999; Karunakaran, et al., 2010). The main reason for its extensive use is that it is generally relatively safe to use in common disinfection experiments; also if *E. coli* is not detected in treated water, it is regarded as free from faecal contamination which is a common type of contamination to be tackled (Baker & Herson, 1999; Dunlop, et al., 2002). Photocatalytic inactivation studies using *E. coli* as a model bacterial pollutant and BiOBr as photocatalyst under visible light have not previously been reported to the best of our knowledge. Herein we synthesized BiOBr using a simple solvothermal route and subsequently investigated the photocatalytic disinfection of *E. coli* in visible light irradiation. Even though the rates of disinfection and inactivation time were calculated, these cannot usually be quantitatively compared to other studies since the operational parameters and reactor configurations differ in different laboratories. However, this study can be used to assess the potential of photocatalytic disinfection by a BiOBr photocatalyst.

An important operational parameter that can affect rate of degradation is pH (Daneshvar, et al., 2003). According to authorities, careful attention must be paid to pH control at all stages of water treatment to ensure satisfactory water clarification and disinfection (Fawell, et al., 2003). And since pH of various water supplies may vary compared to deionized water

which is used in most laboratory research studies, the effect of pH on performance of BiOBr photocatalyst was also evaluated. Moreover, in order to test applicability of BiOBr to organic pollutants, phenol degradation by the photocatalyst was also performed as part of this study. Phenols present a great disadvantage for use of chlorine to disinfect water since chlorination of phenols during the disinfection process produces chlorophenols which are very harmful by-products (Wang, et al., 2013). Consequently, successful photocatalytic degradation of phenol by BiOBr could establish promising applicability in drinking and wastewater treatment.

3.2 Experimental

3.2.1 Materials

Cetyltriethylammnonium bromide (CTAB) (purity >99%) was obtained from Sigma Aldrich and was used as obtained. Laboratory grade bismuth nitrate pentahydrate ($Bi(NO_3)_3 \cdot 5H_2O$), ethylene glycol (EG), Rhodamine B (RhB) and ethanol were obtained from Fisher Scientific and were used without any further purification or alteration. Crystallized phenol (purity >99%) from Fisher Scientific was used for phenol studies. HCl and NaOH solutions were used for pH adjustment and were both obtained from Fisher Scientific and used without any further purification. Distilled deionized (DD) water, obtained by using a Milli-Q water purification system by Millipore, was utilized throughout the experiment in order to wean out interference from other ions. Wild-type *Escherichia coli* K-12 (TG1 strain) was used as the model bacterium for the all bacterial inactivation studies. This strain was selected since it is known to be non-pathogenic and is a common model used in laboratory experiments.

3.2.2 Preparation of BiOBr

BiOBr was synthesized via an optimized solvothermal route using $Bi(NO_3)_3 \cdot 5H_2O$ as the Bi source. A common surfactant, cetyltriethylammnonium bromide (CTAB), was used in the synthesis route and it acted as a template as well as a bromide source for the final product. Initially, a calculated amount of CTAB was dissolved in 40 mL of ethylene glycol (EG) solution. Upon complete dissolution of CTAB in EG, an amount of $Bi(NO_3)_3 \cdot 5H_2O$ was added such that the ratio between CTAB and $Bi(NO_3)_3 \cdot 5H_2O$ was maintained as 1:1. The resulting solution was stirred magnetically for 20 minutes at room temperature, and the mixture was transferred to a Teflon-lined stainless steel autoclave and heated at in an oven at a temperature of 180ºC for 3 hours. Note that these parameters were obtained through optimization performed in our earlier studies. After cooling down to room temperature, the resulting precipitate was filtrated, washed with distilled water and ethanol several times, to remove ionic and organic species and then dried at 60ºC overnight.

3.2.3 Photocatalytic Disinfection Test

For disinfection studies, the number of viable bacterial cells was determined in terms of the colonies formed and diluted folds since these give insight into the cultivability of bacteria. The starting bacterial culture was prepared by growing *E. coli* K-12 (TG1) aerobically overnight in Luria-Bertani nutrient solution (Difco LB broth, Miller; containing 10 g/L tryptone, 5 g/L yeast extract, and 10 g/L NaCl) at 37^{o}C with constant shaking at 250 rpm until the stationary phase was reached. The initial concentration from the overnight culture was determined by a serial dilution using 0.9% sterilized saline and then plating 25 µL of the bacterial solution on LB agar plates. The initial bacterial suspension was prepared by diluting the initial culture such that the bacterial concentration in starting solution would be

10^6 CFU/mL. It was prepared by taking diluted solution and centrifuging it at 14 800 rpm for 5 minutes. The bacterial pellet obtained from centrifugation was re-suspended in 0.9% sterilized saline. This centrifugation and washing procedure was repeated three times to remove all growth media. 1 mL of the bacterial sample was finally added to 49 mL of the saline in order to obtain 50 mL of initial starting solution with a bacterial concentration of 10^6 CFU/mL.

The temporal course of bacterial inactivation was studied by adding the abovementioned 50 mL starting solution to a 100 mL Pyrex beaker and adding 1 g/L BiOBr photocatalyst to it. The sample was then exposed to visible light irradiation provided by a 300 Watt ELH tungsten halide bulb (Ushio) equipped with a UV filter (Kenko Zeta, λ>410 nm) in order for the photocatalysis induced disinfection to occur. The mixture was magnetically stirred at 160 rpm at all times to keep the photocatalyst-bacteria slurry in suspension. During the disinfection process, the temperature was rigorously maintained at 20 ±2 ^{o}C using a water bath in order to dissuade changes in bacterial population due to temperature changes. Samples were collected at planned periods and were serially diluted in saline and then spread onto LB agar plates using aliquot volumes ranging from 25-100 µL. Aliquots from each sample were spread on three separate LB agar plates for each dilution, and incubated at 37^{o}C for 18 hours. The bacteria were quantified using standard plate count method (for viable and cultivable bacteria) whereby counts in the range of 30-300 colony forming units (CFU) per plate were considered statistically significant and were used to calculate the viable cell concentration. All bacterial inactivation trials were performed in triplicate due to high degree of uncertainty in biological experiments. In order to prevent contamination

from outside sources, sterilization and containment measures were taken and all containers and tools used in the study were sterilized for 20 minutes at 121^{o}C prior to use.

3.2.4 Photocatalytic Degradation of Phenol

In order to test the degradation of phenol by BiOBr, 250 mL of 20 ppm phenol solution was added to the slurry based batch-reactor. 1 g/L of BiOBr was added to the solution and the slurry was magnetically stirred in dark for 40 minutes in order to ensure establishment of adsorption-desorption equilibrium. A 300 Watt ELH tungsten halide bulb (Ushio) was used to mimic sunlight and a cut-off filter was used to filter out any radiation below 410 nm ensuring the photocatalysis was carried out strictly under visible light irradiation. A 2.5 mL sample was taken from the reactor at certain time intervals and photocatalyst was separated from the solution by centrifugation. The optical density of the filtrate was analyzed by UV-vis spectrophotometer and the concentration of phenol at each time interval was determined by using the characterization curve of phenol.

3.2.5 Evaluating the Effects of pH

For evaluation of effects of pH, photocatalytic degradation experiments were carried out in a manner similar to the phenol experiments however instead of phenol, the model pollutant used was a common textile dye Rhodamine B (RhB). 250 mL of 10 ppm RhB solution was taken in a beaker and depending on whether the desired pH was acidic or alkaline, the solution pH was adjusted by using drop-wise addition of 0.5 M HCl or 0.5 M NaOH solution respectively. The solution pH was determined by using AB-15 Accumet pH meter manufactured by Fisher Scientific. 1 g/L BiOBr was then added to the solution and

formation of adsorption equilibrium in dark was allowed for 40 minutes. The solution was then exposed to irradiation and the degradation of dye as a function of time was monitored.

3.3 Results and Discussion

3.3.1 Photocatalytic Disinfection Test

Based on the vast photocatalytic properties of BiOBr, it can be hypothesized that in addition to degradation of chemical pollutants, BiOBr photocatalyst can be applied to the inactivation of pathogens. As discussed earlier, *E. coli* was selected as the model microorganism to evaluate the bactericidal activity of BiOBr. The bacterial disinfection was performed under visible light since it is safer and more cost effective relative to UV irradiation which is hazardous and expensive (Shannon, et al., 2008).

The results obtained from photocatalytic disinfection of *E.coli* using BiOBr as photocatalyst are demonstrated in Figure 1. The fractions of surviving bacteria were calculated as a ratio N_t/N_0, where N_t represents the bacterial concentration at the particular inactivation time and N_0 is the initial concentration (t = 0). It can be noted from the results that 95% of bacteria were inactivated within the fisrt 60 minutes in the presence of BiOBr under visible light irradiation. On the other hand, the dark control representing inactivation of bacteria by BiOBr in absence of any irradiation, and hence without photocatalysis, demonstrates insignificant inactivation. The ratio of bacteria inactivated in dark is less than 20% even after 2 hours which is contrasted to over 98% of bacteria inactivated by BiOBr photocatalysis. The small ratio of inactivation in dark by BiOBr can be attriuted to adsorption of bacteria by surface of the photocatalyst. The bacterial photolysis was performed by not adding any photocatalyst to the starting solution before exposing it to visible light irradiation. This run is representative of bacterial cell death in the absence of

any adsorptive, antibacterial, or photocatalytic phenomena. It can be deduced from the results that inactivation of bacteria by the visible light source was found to be negligible.

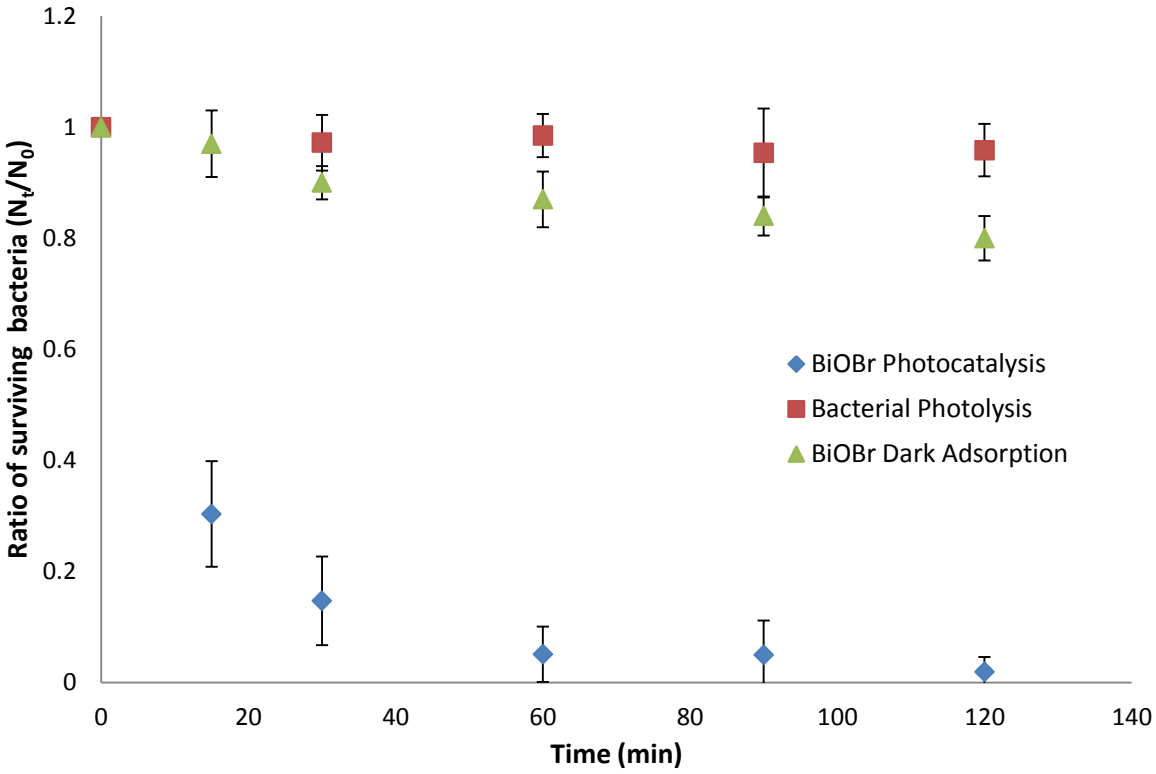

Figure 1 – Inactivation curve of *E. coli* using BiOBr as photocatalyst

On the basis of obtained results, it can be deduced that the death of bacterial cells in the presence of BiOBr was due to photocatalytic process when BiOBr was exposed to visible light irradiation. The oxygen species, such as hydroxyl radicals, formed during BiOBr photocatalysis are understood to interact with the *E. coli* bacteria to bring about cell destruction (Leung, et al., 2008; Yu, et al., 2005). The main features of live *E.coli* are well defined cell membranes and internal presence of proteins, enzymes and DNA (Hou, et al., 2012). Cell membranes in gram negative bacteria are characterized by an outer membrane containing lipopolysaccharides and an inner peptide layer (Hou, et al., 2012). The outer membrane plays the role of protecting the cell by providing a selective barrier preventing

toxic molecules from entering the cell and maintaining interacellular fluids (Hu, et al., 2007; Vaara, 1992). The oxygen species produced in BiOBr photocatalytic systems cause oxidation of functional groups in the cell membrane which disrupts membrane permeability leading to leakage of intracellular substances, destruction of microbial structure and eventually the inactivation of *E. coli* cells (Zhang, et al., 2010; Hou, et al., 2012; Maness, et al., 1999).

Reactive oxygen species are produced in most visible light induced photocatalytic processes, however, the activity demonstrated by BiOBr is relatively higher. The high photocatalytic bactericidal activity of solvothermally produced BiOBr may be due to the strong adsorption capability induced by its micrsopherical sturcture, which allows it to adhere to the cell membrane better. It has been demonstrated in earlier reports (Zhang, et al., 2012) that microspheres exhibit much higher light absorption intensity than other sheet structures of BiOBr. Therefore, the hierarchical microspherical structures caused light to multi-reflect between the BiOBr layers, allowing more light to be absorbed by BiOBr photocatalyst to generate electron-hole pairs for the photocatalytized oxidation of *E. coli* (Zhang, et al., 2012). BiOBr microspheres also offer a lower recombination rate for photogenerated electron-hole pairs and higher quantum efficiency which are all factors that contribute to its higher performance in photocatalyst-induced disinfection (Yu, et al., 2002).

3.3.2 Degradation of Phenol

Phenol and its compounds are common pollutants of aquatic systems and due to their harmful effects, they must effectively be treated. The chlorination of natural waters for disinfection produces chlorophenols and therefore chlorination is ineffective for phenol

removal (Akbal & Onar, 2003). Activated carbon adsorption is an acceptable method of removing phenols from aqueous phase. However, this process produces spent carbon as a waste leading to secondary pollution (Akbal & Onar, 2003). Therefore, mineralization technologies for phenol removal are needed to alleviate these problems. In order to test applicability of BiOBr based photocatalysis to phenol and related compounds, phenol degradation was studied under visible and UV irradiation. Since phenol is a colourless organic pollutant, its degradation was also studied to further confirm the occurrence of a surface photocatalytic process, which is not always recognized when using dyes, since they can undergo photosensitization under visible light irradiation (Wu, et al., 1998). This helps ascertain that the degradation of pollutant by BiOBr is due to direct or indirect photocatalysis (Zhang, et al., 2011).

The results from phenol degradation studies are presented in Figure 2. It can be noted that under the given conditions, phenol could be degraded to some extent by BiOBr under visible light and to a much greater extent under UV illumination with final degradation after 4 hours of irradiation being 30% and 87%, respectively. It should be noted that phenolic degradation under visible light has not been extensively reported with only one current study while degradation under UV irradiation has been relatively more widely reported (Zhang, et al., 2011; Xiao, et al., 2012; Li, et al., 2011).

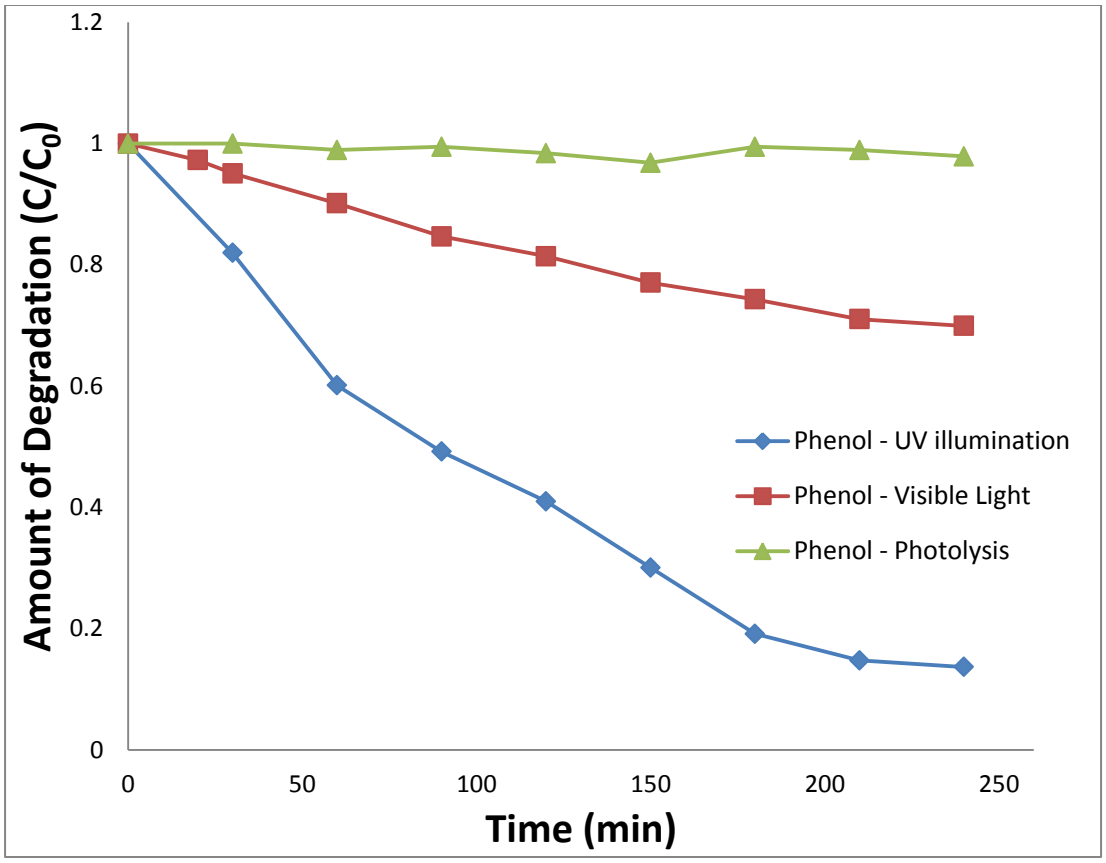

Figure 2 – Degradation of Phenol by BiOBr in UV and Visible Light Irradiation

It can be established that the activity of BiOBr in phenol solution is much lower than that in RhB solution. This is due to structural differences of phenol due to benzene rings making it more complex to degrade (Xiao, et al., 2012). The low visible light activity of BiOBr in phenol degradation can be explained by the band structure of BiOBr. Wang's group calculated the band structure of BiOBr using plane-wave density function theory (DFT) in order to investigate intrinsic reasons for lower visible light performance of BiOBr (Wang, et al., 2013). It was found that since the conduction band of BiOBr was additionally positive, molecular oxygen cannot trap photogenerated electrons to produce reactive oxygen radicals $\bullet O_2^-$ (Cao, et al., 2011; Shenawi-Khalil, et al., 2011). The generation of $\bullet O_2^-$ radicals is an important process during photocatalysis since they inhibit the recombination of

photoinduced charge carriers. Oxygen radicals would be especially beneficial in degradation of phenol and related compounds by favoring the breaking of benzene ring of phenol derivatives (Wei, et al., 2009). Therefore, the lower performance of BiOBr in phenol degradation can be attributed to undesirable positions of conduction bands which hinder its performance for phenol under visible light despite its merits of suitable band gap for visible light photocatalysis, layered structure and indirect semiconducting ability (Wang, et al., 2013). Despite the relatively low activity, it should be noted that the rate constant for phenol degradation reported in this study is 0.51 h^{-1} which compares to a reported value of 0.0183 h^{-1} in literature (Li, et al., 2011), showing that the performance by BiOBr photocatalyst synthesized by the proposed method is much higher. The greater activity under UV irradiation is explained by higher excitation energy of UV light compared to that of visible light, which positively affects transition of electrons from valence to conduction band of BiOBr and thus increases its photocatalytic activity (Shamsun, et al., 2006).

3.3.3 Effect of pH

The pH value of the solution is an important factor influencing the degradation of some pollutants in the photocatalytic process and can also be a critical operational variable (Dalrymple, et al., 2010; Gupta & Tanaka, 1995; Daneshvar, et al., 2003). Altering the initial pH can vary electrostatic interaction between the reactant and BiOBr surface and also shift the potential of redox reaction affecting the adsorption and reactivity of organic solutes (Jiang, et al., 2003; Zhao, et al., 2011). This parameter is also important since the pH of water may differ based on the source it is received from and it must be determined whether the particular pH is operational or an adjustment is required prior to treatment. The effect of

pH on photodegradation performance of solvothermally synthesized BiOBr was therefore evaluated.

Influence of pH on the degradation of RhB by BiOBr was investigated by adjusting pH to the desired value using dilute (0.5 M) HCl acidic or NaOH basic solutions. It should be noted that the pH value must be adjusted prior to the degradation reaction. The initial pH of 10 ppm RhB without any adjustment was found to be 4.8 in the deionized water solution. The effect of pH on degradation of RhB is presented in Figure 3 as follows. It can be noted from the figure that at very low and high pH values, the degradation of RhB deteriorates significantly. When the pH is decreased below the natural pH of RhB solution (pH = 4.8), the rate of degradation is lower. However, as the pH is increased, the degradation rate increases, reaching a maximum at around pH = 8. Beyond this pH, however, the activity decreases drastically and at a pH of 12, barely any degradation of RhB is observed.

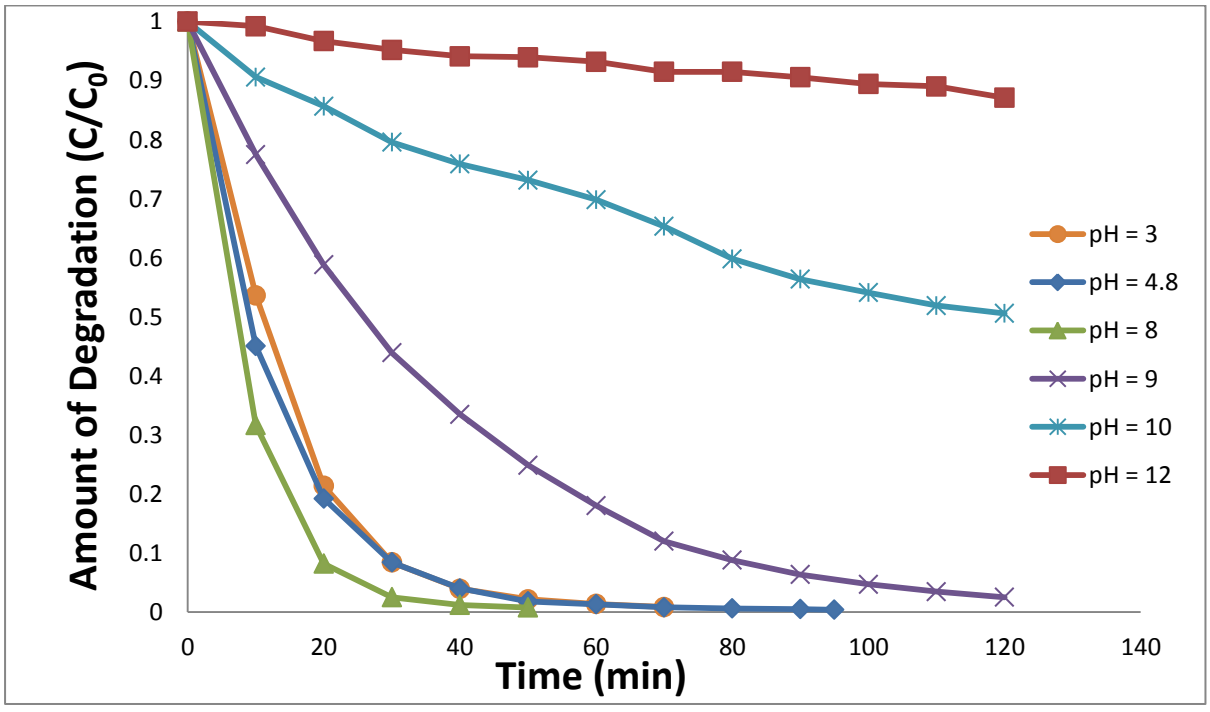

Figure 3 - Effect of pH on Degradation of RhB by BiOBr photocatalyst under Visible light

The results obtained in this study demonstrate that the initial pH value of RhB aqueous solution has significant effects on the adsorption and photocatalytic degradation by BiOBr photocatalyst under visible light. The results can be explained by the recognized effects of pH on surface charge of catalyst and pollutants, adsorption of contaminants on surface of the photocatalyst, and hydroxyl concentration, which ultimately affect the degradation efficiency (Ling-Li, et al., 2010). The pKa value for the aromatic carboxyl group (-COOH) present on RhB molecule, shown in Figure 4, is 4.0 (Li, et al., 2010). When the solution pH is lower than 4.0, RhB ion assumes a positive state charge and of the pH is increased over 4.0, the ion takes on a negative charge. Since the isoelectric point of BiOBr lies in the acidic range (Ling-Li, et al., 2010), both the catalyst and pollutant are negatively charged at the lower pH. As a result, the adsorption of RhB on the BiOBr surface is lower and this leads to lower degradation at lower pH values. An increase in degradation with increasing pH can be explained by the fact that in alkaline media, a higher level of hydroxide ions (OH-) induced the generation of hydroxyl free radicals (HO•). The formation of hydroxyl free radicals occurs from photooxidation of OH- by holes forming on the surface of the BiOBr photocatalyst (Chu, et al., 2007). Since hydroxyl free radicals are the primary oxidizing species in degradation of RhB, the rate of degradation is increased as the pH of the solution is increased. However, as the pH is increased beyond the ideal point, the effect of negative charging of BiOBr dominates and consequently inhibits RhB degradation. This is because the pollutant and BiOBr molecules at higher pH repel, lowering the adsorption of RhB on the surface of photocatalyst, which is known to lead to poor photochemical degradation (Chang, et al., 2010 a).

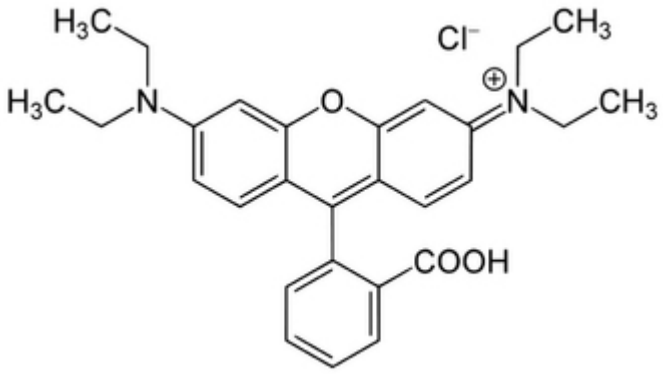

Figure 4 – Molecular structure of RhB

Therefore, an optimum pH exists for high photocatalytic activity of BiOBr which in this case is found to be around 8. This is in agreement with the value obtained by Zhao's group for BiOBr synthesized via the hydrolysis method, suggesting effect of pH is independent of synthesis route (Zhao, et al., 2011). It was also established that pH values that are too high or too low are not favourable for BiOBr to decompose the RhB molecule which is also in agreement with literature (Chang, et al., 2010 a) and theory as stated.

3.4 Conclusion

BiOBr crystals had previously been optimally synthesized using a CTAB mediated solvothermal synthesis route. In this study, bactericidal activity of thus synthesized BiOBr under visible light irradiation was studied using *E. coli* as model microorganism. It was shown that over 95% of bacteria could be inactivated in 60 min while almost the entire population was inactivated by the end of the 2 hour study. This demonstrates the strong potential of BiOBr in photocatalysis-induced disinfection systems. The effect of pH on activity of BiOBr was also evaluated and it was deduced that a pH value that is too high or

too low is detrimental to the photocatalytic performance of BiOBr. A moderately alkaline pH of 8 was found to be optimal for high activity. Phenol degradation studies also revealed that BiOBr can degrade organic pollutants in water, although activity in visible light irradiation for phenol was lower. Overall, it was demonstrated that solvothermally synthesized BiOBr photocatalyst seems promising for applications in wastewater and drinking water treatments since it can degrade a range of pollutants in varying conditions and has disinfection properties in visible light.

Author Information:
Ayla Ahmad – University of Ottawa
Zisheng Zhang* – University of Ottawa
*Corresponding author

References

Akbal, F., & Onar, A. N. (2003). Photocatalytic Degradation of Phenol . Environ. Monit. Assess. , 83, 295-302.

Baker, K. H., & Herson, D. S. (1999). Detection and occurrence of indicator organisms and pathogens. Water Environ. Res., 71, 530-551.

Betancourt, W. Q., & Rose, J. B. (2004). Drinking water treatment processes for removal of Cryptosporidium and Giardia. Vet.Parasitol. , 126, 219–234.

Cao, J., Xu, B. Y., Luo, B. D., Lin, H. L., & Chen, S. F. (2011). Novel BiOI/BiOBr heterojunction photocatalysts with enhanced visible light photocatalytic properties. Catal. Commun. , 13, 63-68.

Cao, J., Xu, B., Lin, H., Luo, B., & Chen, S. (2011). Chemical etching preparation of BiOI/BiOBr heterostructures with enhanced photocatalytic properties for organic dye removal. Chem. Eng. J., 185, 91-99.

Chang, X., Gondal, M. A., Al-Saadi, A. A., Ali, M. A., Shen, H., Zhou, Q., Ji, G. (2010 a). Photodegradation of Rhodamine B over unexcited semiconductor compounds of BiOCl and BiOBr. J. Colloid. Interface Sci., 377, 291-298.

Chen, X., & Mao, S. S. (2007). Titanium dioxide nanomaterials: synthesis, properties, modifications, and applications. Chem. Rev., 107, 2891–2959.

Chu, W., Choy, W. K., & So, T. Y. (2007). The effect of solution pH and peroxide in the TiO2-induced photocatalysis of chlorinated aniline. J. Hazard. Mater., 141, 86-91.

Dalrymple, O. K., Stefanakos, E., Trotz, M. A., & Goswami, D. Y. (2010). A review of the mechanisms and modeling of photocatalytic disinfection. Appl. Catal. B: Environ., 98, 27-38.

Daneshvar, N., Salari, D., & Khataee, A. R. (2003). Photocatalytic degradation of azo dye res 12 in water: investigation of the effect of operational parameters. J. Photochem. Photobiol. A, 157, 111-116.

Dunlop, P. S., Byrne, J. A., Manga, N., & Eggins, B. R. (2002). The photocatalytic removal of bacterial pollutants from drinking wate. J. Photochem. Photobiol. A, 148, 355-363.

Ede, S., Hafner, L., Dunlop, P., Byrne, J., & Will, G. (2012). Photocatalytic Disinfection of Bacterial Pollutants Using Suspended and Immobilized TiO2 Powders. Photochem. Photobiol., 212, 728-735.

Fawell, J. K., Lund, U., & Mintz, B. (2003). pH in drinking water. Geneva: World Health Organization.

Fry, L. M., Mihelcic, J. R., & Watkins, D. W. (2008). Water and nonwater-related challenges of achieving global sanitation coverage . Environ. Sci. Technol. , 42, 4298-4304.

Gibbons, J., & Laha, S. (1999). Water purification systems: a comparative analysis based on the occurrence of disinfection by-products. Environ. Pollut. , 106, 425-428.

Goslan, E. H., Krasner, S. W., Bower, M., Rocks, S. A., Holmes, P., Levy, L. S., & Parsons, S. A. (2009). A comparison of disinfection by-products found in chlorinated and chloraminated drinking waters in Scotland. Water Res., 43, 4698-4706.

Gray, N. F. (1994). Drinking Water Quality, Problems and Solutions (2nd ed.). Chichester, UK: John Wilet and Sons.

Gupta, H., & Tanaka, S. (1995). Photocatalytic mineralisation of perchloroethylene using titanium dioxide. Water Sci. Technol., 31, 47-54.

Henle, J., Simon, P., Frenzel, A., Scholz, S., & Kaskel, S. (2007). Nanosized BiOX (X = Cl, Br, I) particles synthesized in reverse microemulsions. Chem. Mater., 19, 366-373.

Hou, Y., Li, X., Zhao, Q., Chen, G., & Raston, C. L. (2012). Role of Hydroxyl Radicals and Mechanism of Escherichia coli Inactivation on Ag/AgBr/TiO2 Nanotube Array Electrode under Visible Light Irradiation. Environ. Sci. Technol., 46, 4042-4050.

Hu, C., Guo, J., Qu, J. H., & Hu, X. X. (2007). Photocatalytic degradation of pathogenic bacteria with AgI/TiO2 under visible light irradiation. Langmuir, 23, 4982−4987.

Ide, Y., Matsuoka, M., & Ogawa, M. (2010). Efficient visible-light-induced photocatalytic activity on gold-nanoparticle-supported layered titanate. J. Am. Chem. Soc. , 132, 16762–16764.

Jiang, D., Zhao, H., Zhang, S., John, R., & Will, G. D. (2003). Photoelectrochemical measurement of phthalic acid adsorption on porous TiO2 film electrodes. J. Photochem. Photobiol. A, 156, 201-206.

Jolley, R. L., Condie, L. W., Johnson, J. D., Katz, S., Minear, A., Mattice, J. S., & Jacobs, V. A. (1990). Water Chlorination: Chemistry, Environmental Impact and Health Effects (6 ed.). Chelsea, MI: Lewis Publishers Inc.

Karunakaran, C., Abiramasundari, G., Gomathisankar, P., Manikandan, G., & Anandi, V. (2010). Cu-doped TiO2 nanoparticles for photocatalytic disinfection of bacteria under visible light. J. Colloid Interface Sci., 352, 68–74.

Kim, D. S., & Kwak, S. Y. (2008). Photocatalytic inactivation of E. coli with a mesoporous TiO2 coated film using the film adhesion method. Environ. Sci. Technol. , 148–151.

Lazarova, V., Savoye, P., Janex, M. L., Blatchley, E. R., & Pommepuy, M. (1999). Advanced wastewater disinfection technologies: state of the art and perspectives. Water Sci. Technol., 40, 203–213.

Leung, T. Y., Chan, C. Y., Hu, C., Yu, J. C., & Wong, P. K. (2008). Photocatalytic disinfection of marine bacteria using fluorescent light. Water Res., 42, 4827–4837.

Li, D., & Qu, J. (2009). The progress of catalytic technologies in water purification: a review. J. Environ. Sci. , 21, 713–719.

Li, L., Liu, S., & Zhu, T. (2010). Application of activated carbon derived from scrap tires for adsorption of Rhodamine B. J. Environ. Sci., 22, 1273-1280.

Li, Y., Wang, J., Yao, H., Dang, L., & Li, Z. (2011). Chemical etching preparation of BiOI/Bi2O3 heterostructures with enhanced photocatalytic activities. Catal. Commun., 12, 660-664.

Ling-Li, W., Hong, M. W., Lian, W. S., Yu, Z., Ke, J. M., Ping, L. R., . . . Ping, H. Y. (2010). The Contrastive Research in the Photocatalytic Activity of BiOBr Synthesized by Different Reactants. J. Nanomater., 1-9.

Maness, P. C., Smolinski, S., Blake, D. M., Huang, Z., Wolfrum, E. J., & Jacob, W. A. (1999). Bactericidal activity of photocatalytic TiO2 reaction: Toward and understanding of its killing mechanism, . Appl. Environ. Microbiol., 65, 4094-4098.

Matsunaga, T., Tomoda, R., Nakajima, T., & Wake, H. (1985). Photoelectrochemical sterilization of microbial cells by semiconductor powders. FEMS Microbiol. Lett. , 29, 211-214.

Schoenen, D. (2002). Role of disinfection in suppressing the spread of pathogens with drinking water: possibilities and limitations. Water Res, 36, 3874-3888.

Shamsun, N., Hasegawa, K., & Kagaya, S. (2006). Photocatalytic degradation of phenol by visible light-responsive iron-doped TiO2 and spontaneous sedimentation of the TiO2 particles. Chemosphere, 65, 1976-1982.

Shang, M., Wang, W., & Zhang, L. (2009). Preparation of BiOBr lamellar structure with high photocatalytic activity by CTAB as Br source and template. J. Hazard. Mater. , 167, 803–809.

Shannon, M. A., Bohn, P. W., Elimelech, M., Georgiadis, J. G., Marinas, B. J., & Mayes, A. M. (2008). Science and technology for water purification in the coming decades. Nature, 452, 301–310.

Shenawi-Khalil, S., Uvarov, V., Kritsman, Y. L., Menes, E., Popov, I., & Sasson, Y. (2011). A New Family of BiO(ClxBr1-X) Visible Light Sensitive Photocatalysts . Catal. Commun., 12, 1136–1141.

Szewzyk, U., Szewzyk, R., Manz, W., & Schleifer, K. H. (2000). Microbiological safety of drinking water. Ann. Rev. Microbiol., 54, 81-127.

Vaara, M. (1992). Agents that increase the permeability of the outer membrane. Microbiol. Rev., 56, 395-411.

Wang, J., Yu, Y., & Zhang, L. (2013). Highly efficient photocatalytic removal of sodium pentachlorophenate with Bi3O4Br under visible light . Appl. Catal. B, 136, 112-121.

Wei, W., Dai, Y., & Huang, B. B. (2009). First-principles characterization of Bi-based photocatalysts: Bi12TiO20, Bi2Ti2O7, and Bi4Ti3O12. J. Phys. Chem. C, 113, 5658-5663.

Wu, T., Liu, G., Zhao, J., Hidaka, H., & Serpone, N. (1998). Photoassisted Degradation of Dye Pollutants. V. Self-Photosensitized Oxidative Transformation of Rhodamine B under Visible Light Irradiation in Aqueous TiO2 Dispersions. J. Phys. Chem. B, 102, 5845-5851.

Xia, J., Yin, S., Li, H., Xu, H., Yan, Y., & Zhang, Q. (2010). Self-assembly and enhanced photocatalytic properties of BiOI hollow microspheres via a reactable ionic liquid. Langmuir , 27, 1200–1206.

Xiao, P., Zhu, L., Zhu, Y., & Qian, Y. (2012). Room Temperature Synthesis of BiOBr Sub-Microflowers and Their Photocatalytic Properties. J. Nanosci. Nanotechnol., 12, 2008-2013.

Xiao, Q., & Ouyang, L. (2010) Photocatalytic photodegradation of xanthate over C, N, S tridoped TiO2 nanotubes under visible light irradiation. J. Phys. Chem. Solids, 72, 39-44.

Yu, J. C., Ho, W. K., Yu, J. G., Yip, H. Y., Wong, P. K., & Zhao, J. C. (2005). Efficient visible-light induced photocatalytic disinfection on sulfur-doped nanocrystalline titania. Environ. Sci. Technol. , 39, 1175–1179.

Yu, J. C., Yu, J. G., Ho, W. K., Jiang, Z. T., & Zhang, L. Z. (2002). Effects of F− doping on the photocatalytic activity and microstructures of nanocrystalline TiO2 powders. Chem. Mater., 14, 3808–3816.

Zhang, D., Wena, M., Jianga, B., Li, G., & Yub, J. (2012). Ionothermal synthesis of hierarchical BiOBr microspheres for water treatment. J. Hazard. Mater., 210, 104-111.

Zhang, J., Shi, F. J., Lin, J., Chen, D. F., Gao, J. M., Huang, Z. X., Tang, C. C. (2008 b). Self- Assembled 3-D architectures of BiOBr as a visible-light-driven photocatalyst. Chem. Mater., 20, 2937–2941.

Zhang, L. S., Wong, K. H., Yip, H. Y., Hu, C., Yu, J. C., Chan, C. Y., & Wong, P. K. (2010). Effective photocatalytic disinfection of E. coli K-12 using AgBr-Ag-Bi2WO6 nanojunction system irradiated by visible light: The role of diffusing hydroxyl radicals. Environ. Sci. Technol., 44, 1392–1398.

Zhang, L., Cao, X. F., Chen, X. T., & Xue, Z. L. (2011). BiOBr hierarchical microspheres: Microwave-assisted solvothermal synthesis, strong adsorption and excellent photocatalytic properties. J. Colloid Interf. Sci. , 354, 630 –636.

Zhang, L., Kanki, T., Sano, N., & Toyoda, A. (2003). Development of TiO2 photocatalyst reaction for water purification. Sep. Purif. Technol. , 31, 105–110.

Zhang, X., Ai, Z., & Jia, F. L. (2008 a). Generalized one-pot synthesis, characterization, and photocatalytic activity of hierarchical BiOX (X = Cl, Br, I) nanoplate microspheres. J. Phys. Chem. C, 112, 747–753.

Zhao, X., Wang, Y., Shi, Z., & Fan, C. (2011). Photocatalytic treatment of MO in water with BiOBr photocatalyst. Materials Science Forum, 694, 554-558.

Zhu, L., He, C., Huang, Y., Chen, Z., Xia, D., Su, M., Shu, D. (2012). Enhanced photocatalytic disinfection of E. coli 8099 using Ag/BiOI composite under visible light irradiation. Sep. Purif. Technol., 91, 59-66.

Chapter 4 – Enhancement of BiOBr Photocatalytic Performance by doping with $PdCl_2$

4.1 Introduction

Textile, paper, leather and paper industries utilize large amount of chemical dyes, of which about 15% is lost in effluents (Behnajady, et al., 2009). These dyes pollute the water by causing unwanted colouring and odours and also release toxic and carcinogenic products that threaten aquatic life (Zhao, et al., 2008; Zhang, et al., 2011; Kansal, et al., 2010). Therefore, treatment of textile effluents is vital prior to their discharge into the water environment (Baiju, et al., 2009; Yang, et al., 2008; Kaur & Gupta, 2009). Traditional processes for removal of dyes from wastewater are inefficient because synthetic dyes are refractory in nature (Behnajady, et al., 2011). Advanced oxidation processes (AOPs) are vital in wastewater treatment because they can transform the pollutants into carbon dioxide, water and mineral acids therefore rendering organic pollutants nontoxic (Behnajady, et al., 2011). The principle of AOPs is the generation of highly reactive radicals which have the ability to effectively treat a variety of pollutants (Gaya & Abdullah, 2007; Tan, et al., 2011). Among the various AOPs, photocatalytic degradation is considered the most effective and convenient method for eliminating organic dyes from wastewater (Parida, et al., 2006; Crini, 2005; Yan & Lee, 2009). Solar photocatalysis is of particular interest for degradation of waste in water due to the employment of solar energy as photon source to activate the catalyst (Suri, et al., 1993; Zhang, et al., 2011).

Bismuth oxyhalides, BiOX (X = Cl, Br, I), have emerged as great photocatalytic materials due to their optical properties and ability to be activated by UV and visible light (Shang, et al., 2009; Wang, et al., 2008). Among these oxyhalides, bismuth oxybromide (BiOBr) has

been investigated to show the highest photocatalytic activity for degradation of rhodamine B (RhB) under the same conditions (An, et al., 2007). The unique electrical, optical and photocatalytic activity of BiOBr is due to its intrinsic crystalline layer and lamellar structure which accelerate separation of electron–hole pairs upon photoexcitation to favor a high photocatalytic efficiency of BiOBr (Zhang, et al., 2008; Liu, et al., 2011). Moreover, it is stable, visible light active and has the ability to degrade a variety of compounds making it an ideal alternative to the commercialized TiO_2 (Zhang, et al., 2008; Zhang, et al., 2008). Many different methods have been developed for the synthesis of BiOBr however there is still a need to further improve its photocatalytic activity for industrial applications (Khalil, et al., 2012; Chang, et al., 2010).

There are a few methods that may be utilized for improvement of photocatalytic activity of a semiconductor. One possible method is construction of a heterostructure whereby an interface is formed between two layers or regions of dissimilar crystalline semiconductors (Khalil, et al., 2012). Heterojunctions of BiOBr have been reported in the literature which include structures using AgBr, BiOI, and BHO (Cao, et al., 2011; Kong, et al., 2012; Khalil, et al., 2012). However, these structures often involve complicated syntheses and show little improvement to photocatalytic activity while in some cases heterostructures even resulted in deactivation of the catalyst (Cao, et al., 2011). Another effective and frequently used method for improving activity of semiconductors is doping, whereby an impurity is added to the catalyst structure to alter equilibrium concentration of electrons to change the electrical and optical properties of the solid (Jiang, et al., 2008; Asahi, et al., 2001). Doping can also extend the optical absorption edge of wide band gap semiconductors (Kong, et al., 2011). Few works about BiOBr doping have been reported which include doping BiOBr

with iodine (I), lead (Pb), titanium (Ti) and silver (Ag) (Wang, et al., 2008; Yu, et al., 2010; Jiang, et al., 2012; Wang, et al., 2011; Yu, et al., 2011). Although doping with these materials showed improvement in photoabsorption and charge separation, there is still need for an effective and efficient dopant that would enhance the activity of BiOBr and would employ a relatively simple doping process.

Platinum group metals (pgm) have widely been used to enhance the photocatalytic performance of semiconductor systems based on titania (Lee & Mills, 2003). Pgms, particularly platinum (Pt) and palladium (Pd), when deposited on the semiconductor surface act as traps for photogenerated electrons and therefore improve charge separation and photocatalytic performance (Jacobs, 1986). It has been shown through many titanium dioxide systems that doping with Pd is always advantageous for the photocatalytic performance (Lee & Mills, 2003; Sakthivel, et al., 2004). It has been reported that of the several metal dopants, Pd had the highest interaction and improved activity of TiO_2 most (Tan, et al., 2011). Several works have been published on the doping of Pd on titania surface and are summarized in reviews by Tan et al. and Lee & Mills (Tan, et al., 2011; Lee & Mills, 2003). However, Pd metal doping has not yet been utilized for BiOBr (or even other bismuth oxyhalide) systems to the best of our knowledge. This study investigates the effect of Pd salt ($PdCl_2$) doping on the photocatalytic performance of BiOBr and consequently introduces the synthesis of a novel $PdCl_2$/BiOBr based photocatalyst. Furthermore, determination of optimal doping and operating parameters was also examined. The stability and reusability of the obtained catalyst was also tested.

4.2 Experimental

4.2.1 Materials

Palladium (II) chloride (purity 99%) and cetyltriethylammnonium bromide (purity >99%) were obtained from Sigma Aldrich and were used as obtained. Laboratory grade bismuth nitrate pentahydrate ($Bi(NO_3)_3 \cdot 5H_2O$), ethylene glycol (EG), Rhodamine B (RhB) and ethanol were obtained from Fisher Scientific and were used without any further purification or alteration. Distilled deionized water, obtained by using a Milli-Q water purification system by Millipore, was utilized throughout the experiment in order to wean out interference from other ions.

4.2.2 Synthesis

BiOBr was synthesized via a simple solvothermal method using $Bi(NO_3)_3 \cdot 5H_2O$ as the Bi source. A common surfactant, cetyltriethylammnonium bromide (CTAB), was used in the synthesis route and it acted as a template as well as a bromide source for the final product. Initially, a calculated amount of CTAB was dissolved in 40 mL of ethylene glycol (EG) solution. Upon complete dissolution of CTAB in EG, an amount of $Bi(NO_3)_3 \cdot 5H_2O$ was added such that the molar ratio between CTAB and $Bi(NO_3)_3 \cdot 5H_2O$ was maintained as 1:1. The resulting solution was stirred magnetically for 20 min at room temperature, and the mixture was transferred to a Teflon lined stainless steel autoclave and heated in an oven at a temperature of 180ºC for 3 hours. Note that these parameters were obtained through optimization performed in our earlier studies. After cooling down to room temperature, the resulting precipitate was filtrated, washed with distilled water and ethanol several times, to remove ionic and organic species and then dried at 60ºC overnight.

The $PdCl_2$ doped BiOBr sample was prepared by an isometric impregnation. In this method, $PdCl_2$ solution of a certain concentration was prepared by dissolution of the salt in distilled deionized water. Then, a calculated amount of the $PdCl_2$ solution was added dropwise to 1 g of BiOBr powdered catalyst in order to obtain different mass percent of Pd (0.5-6 wt%). The suspension was stirred thoroughly using a glass rod to distribute the solution evenly within the powder. The resulting mixture was heated in an oven at 80°C for 2 hours and the final product was obtained in the form of a dry fine powder which was brown in colour, representing the deposition of Pd.

4.2.3 Characterization

The crystal structures and purity of samples were characterized by X-ray powder diffraction (XRD) with a Rigaku Ultima IV Cu-Kα (λ = 0.15418 mm) radiation diffractometer recorded with 2θ scope ranging from 10-80º. Scanning electron microscopy (SEM) was used to take images of the prepared BiOBr samples employing a Tescan VegaII XMU field emission scanning electron microscope with accelerating voltage of 5 or 20 kV. The particles were dispersed onto a gold coated surface using an Anatech Hummer VII sputter coater prior to analysis. The SEM was also equipped with an EDS system. UV-vis diffusion reflectance spectrum of the samples was analyzed with a UV-vis spectrophotometer (Thermo Evolution 300) equipped with an accessory to analyze powder samples.

4.2.4 Measuring Photocatalytic Activity

The photocatalytic activity of each of the prepared samples was evaluated by monitoring the degradation of Rhodamine B (RhB). RhB is an organic textile dye and is commonly used in research as representative for organic dyes in wastewater. For each run, 250 mL of 10 ppm

RhB solution was added to a slurry mode batch reactor and a fixed amount of $PdCl_2$ doped BiOBr was added to the solution. The slurry was magnetically stirred in dark for 40 minutes in order to ensure establishment of adsorption-desorption equilibrium. A 300 Watt tungsten halide lamp was used to mimic sunlight and a cut-off filter was used to filter out any radiation below 410 nm ensuring the photocatalysis was carried out strictly under visible light irradiation. A 2.5 mL sample was taken from the reactor at small time intervals and the sample was centrifuged to separate photocatalyst powder from the solution. Optical density of the supernatant was analyzed by UV-vis spectrophotometer and the concentration of dye at each time interval was determined by using a standard calibration curve of the dye.

4.3 Results and Discussion

4.3.1 Characterization

4.3.1.1 SEM and EDS

The SEM images of $PdCl_2$ doped BiOBr (Figure 1a) reveal that the catalyst particles consist of tiny microspheres of varied diameter, with a mean diameter of 2.15 μm. Upon comparison with non-doped BiOBr (Figure 1b), it can be observed that doped BiOBr particles are generally smaller in size whereby the former diameter was 4.7 μm. This is consistent with literature as it has been observed that Pd doping promotes the production of smaller crystallite TiO_2 and therefore increases the surface area (Tan, et al., 2011; Asilturk, et al., 2009).

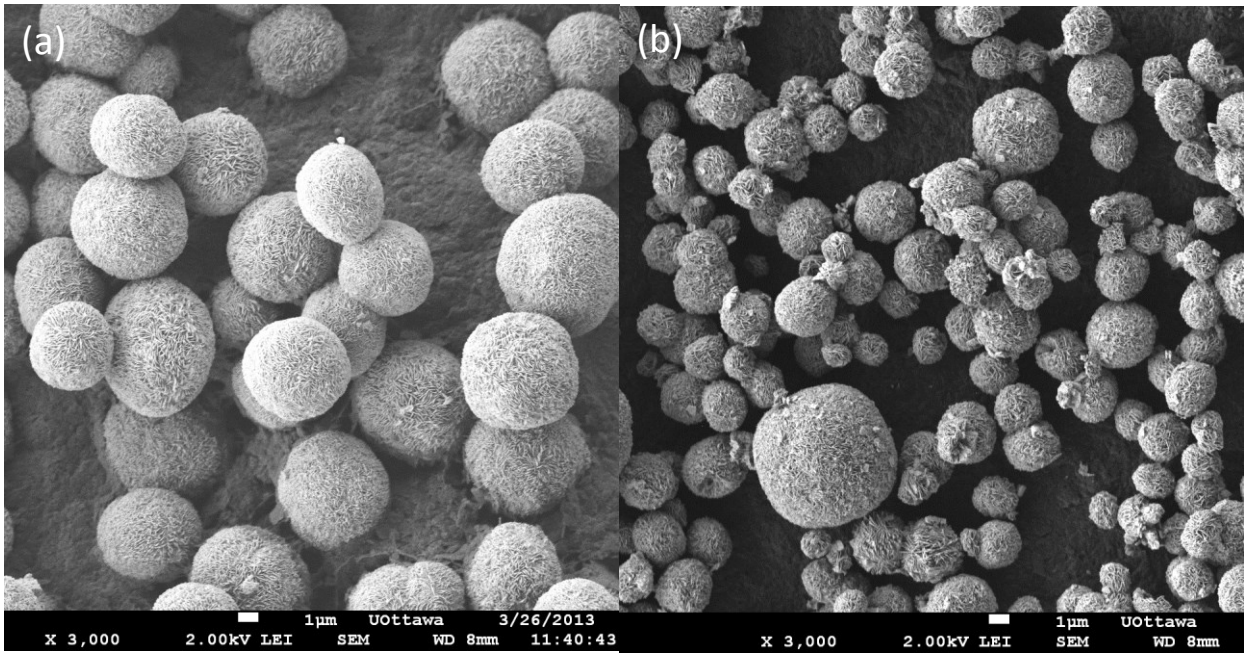

Figure 1 – SEM images (a) $PdCl_2$ doped BiOBr photocatalyst particles (b) non-doped BiOBr photocatalyst particles

In addition to size of crystals, $PdCl_2$ doping also affected the structure and morphology of the crystals, as evident from Figure 2. Non-doped BiOBr particles are spherical with threadlike fibers on the surface (Figure 2b), however the threads do not change the general shape of the crystal. In contrast, $PdCl_2$ doped BiOBr particles consist of well-defined scaly flakes which open up the microspherical crystal structure (Figure 2a), thus making the structures more hollow and crumbled. This increases the surface area to volume ratio of the crystals. At high magnification, the flowerlike morphology of doped catalyst as well as Pd metal particles deposited on the petal like flakes of the doped photocatalyst can be clearly observed (Figure 3). This suggests that the Pd metal becomes a part of the crystal structure of the catalyst and therefore affects its morphology.

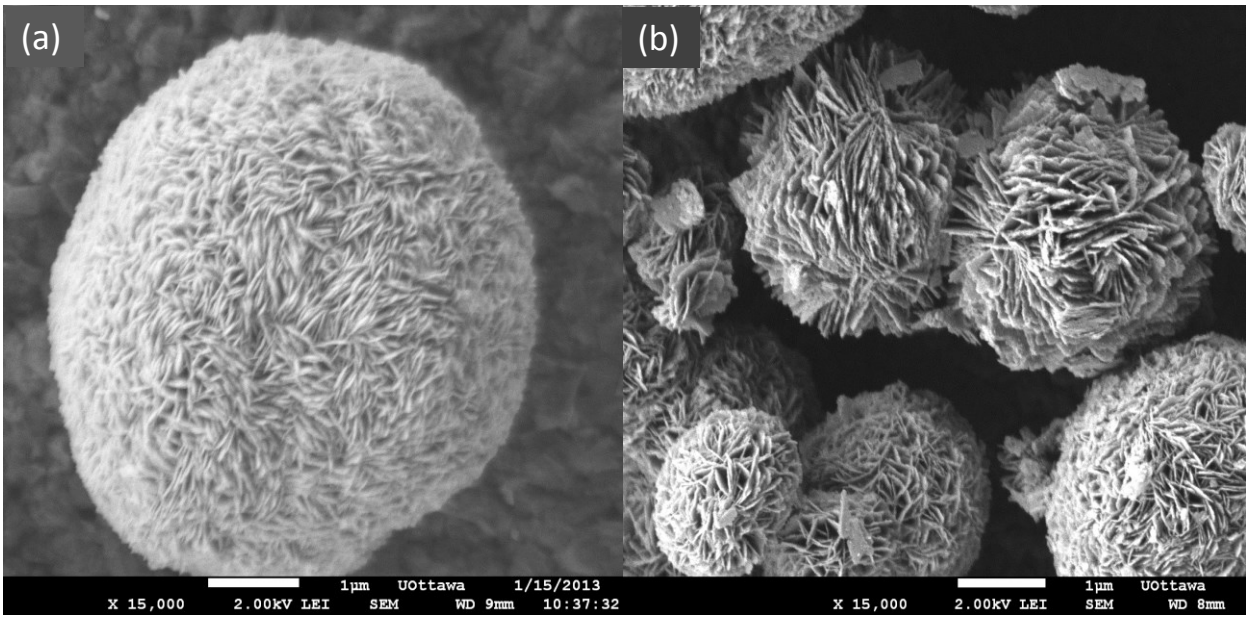

Figure 2- SEM images morphology (a) Non-doped BiOBr Particle (b) $PdCl_2$ doped BiOBr particles

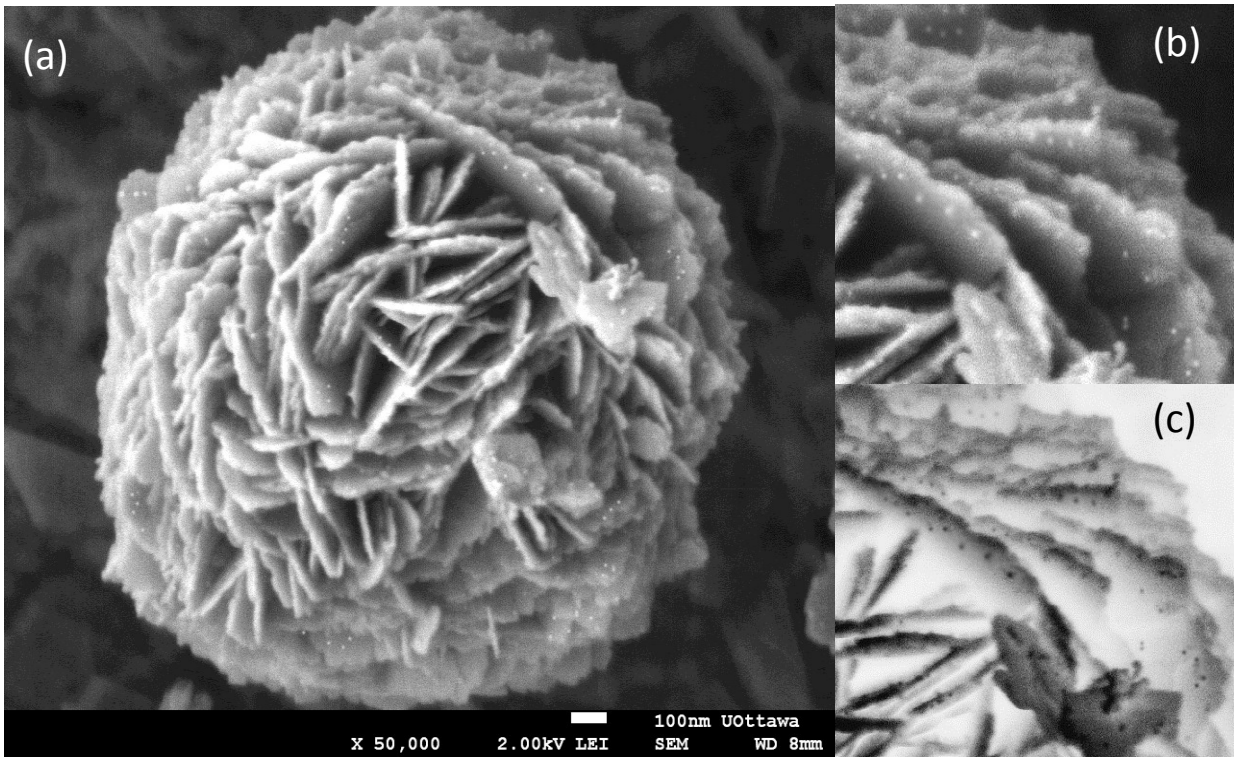

Figure 3 – Enhanced Magnification SEM images of $PdCl_2$ doped BiOBr (a) intact particle (b) magnified flakes (c) inverted colours on magnified flakes to reveal Pd metal particles

Energy dispersion X-ray spectra (EDS) were obtained to characterize the chemical elemental components of the samples (Figure 4). The peaks if Bi, Br and O could easily be found in the spectrum. The EDS results further established the presence of Pd and Cl species within the structure of the catalyst by showing distinctive Pd and Cl peaks, demonstrating successful doping of the $PdCl_2$ on to BiOBr photocatalyst. The C peak in the spectrum can be attributed to CTAB molecule adsorbed by the sample.

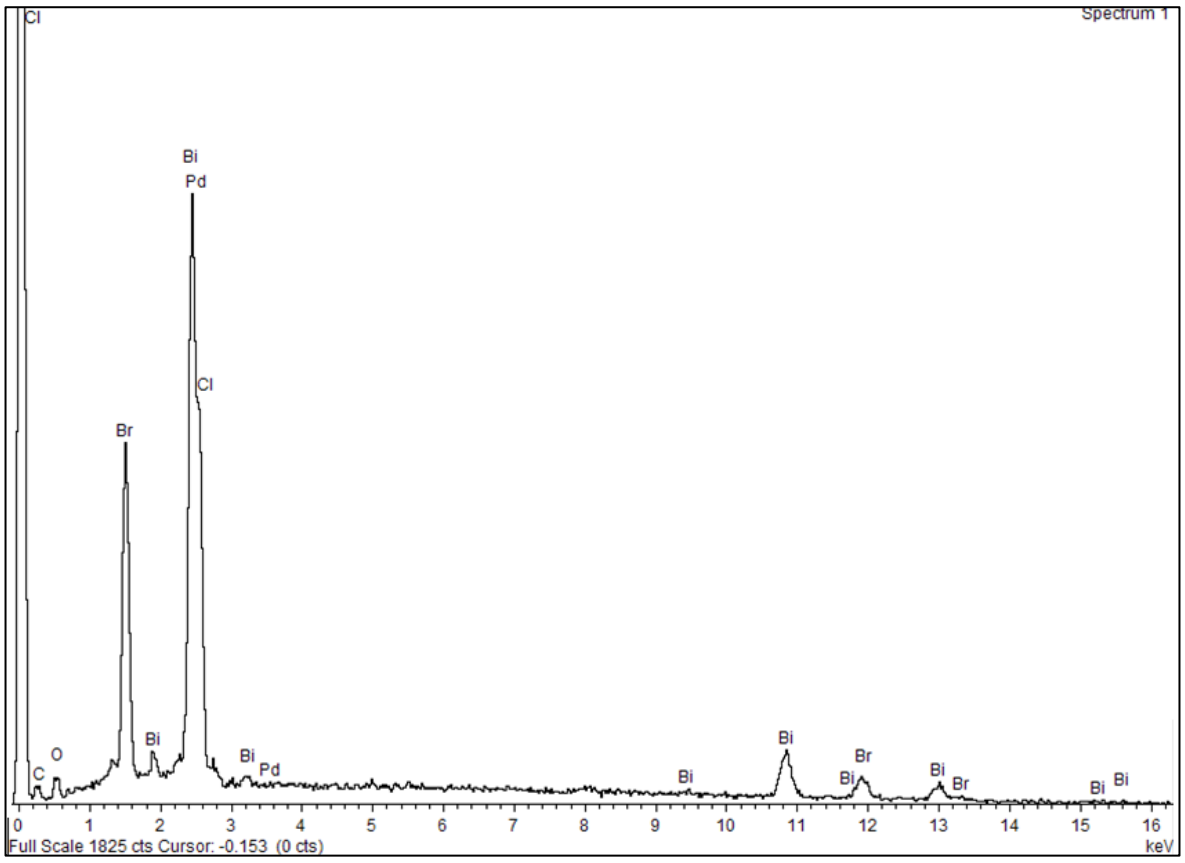

Figure 4 – EDS Spectra of $PdCl_2$ doped BiOBr photocatalyst sample

4.3.1.2 XRD

Photocatalysts require a high crystalline quality since the crystalline quality is inversely proportional to the amount of defects (An, et al., 2007). The defects function as trapping

and recombination centers for photo-generated electrons and holes, resulting in a lower photocatalytic activity. Figure 5 demonstrates the XRD patterns of the sample both before and after doping with $PdCl_2$. For the case of non-doped photocatalyst, it can be observed that there is narrow broadening of peaks, which demonstrates high crystallinity (Chang, et al., 2010). The XRD pattern of $PdCl_2$ doped photocatalyst also demonstrates sharp and well defined peaks, thus implying that the crystallinity and purity of the sample is not reduced due to doping. All of the peaks observed in XRD patterns of non-doped and $PdCl_2$ doped BiOBr can be attributed to the pure tetragonal phase of BiOBr (JCPDS card no. 78-0348) with the exception of the sharp peak occurring at about 13° for the latter case. This sharp peak is established to be due to the presence of Pd metal, and can be attributed to the 001 plane Pd metal (JCPDS card no. 01-072-0710). This further confirms the presence of Pd in the crystal structure of BiOBr for the doped photocatalyst sample. The absence of any peaks related to Cl demonstrates that it does not become a significant part of the crystal structure of the catalyst. These results are further confirmed by XPS analysis. No other peaks were detected besides the indexed ones indicating that no impurity species were formed during the process of synthesis or doping.

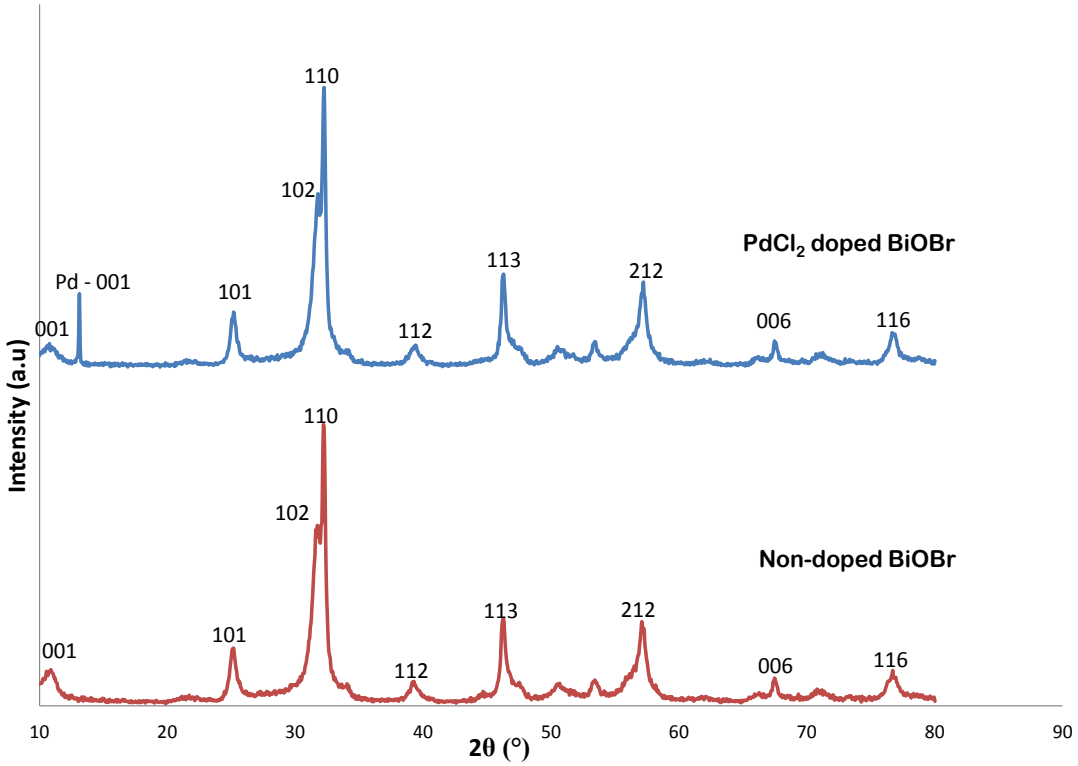

Figure 5- XRD Pattern of $PdCl_2$ doped and non-doped BiOBr photocatalyst samples

4.3.1.3 XPS

X-ray Photoelectron Spectroscopy (XPS) was applied to investigate the surface element composition and chemical states of elements in $PdCl_2$ doped BiOBr photocatalyst (Figures 6-10). The XPS survey revealed that the sample is constituted by elements of Bi, O, Br, Pd, Cl and C.

The carbon peak was attributed to extrinsic elemental carbon on the surface of sample from carbonate species and the atmosphere and was therefore used for calibration purposes only (Feng, et al., 2011). For the XPS of bismuth, it can be observed that two main asymmetrical splitting peaks of Bi 4f are found centered at 158.6 and 163.8 eV which belong to Bi $4f_{7/2}$ and Bi $4f_{5/2}$ respectively (Hwang, et al., 2008; Shi, et al., 2013). These peaks are assigned to the tri-valent state of bismuth, Bi^{3+} as it occurs in BiOBr (Feng, et al., 2011). In addition to these peaks, another less intense peak is also observed at 156.6 eV, which is a Bi $4f_{7/2}$ peak assigned to metallic state of bismuth, Bi^0 suggesting some reduction during sample transfer (Hwang, et al., 2008). The binding energy difference between Bi^0 and Bi^{3+} is 2 eV, which is in agreement with literature (Hwang, et al., 2008). The Br peaks occurring at 68.2 eV are associated with binding energies of Br $3d_{5/2}$ and Br $3d_{3/2}$ (Shi, et al., 2013; Ai, et al., 2011). The XPS spectra of oxygen could be fitted by 2 peaks at binding energies of 530 and 531.75 eV. The dominant peak at 530 eV is characteristic of lattice oxygen, the form bounded to BiOBr (Shi, et al., 2013). The peak at higher binding energy is representative of oxygen present in other components including H_2O, OH etc. adsorbed on the catalyst surface (Ai, et al., 2011).

The XPS spectra for Pd exhibits doublet peaks of Pd 3d occurring at binding energies of 335.8 and 341.1 eV which are associated to Pd $3d_{5/2}$ and Pd $3d_{3/2}$, respectively (Kim, et al., 2006; Suh, et al., 2010). The separation energy for these peaks is 5.3 eV which is in close proximity of values reported in literature (Kim, et al., 2006; Hwang, et al., 2009). The chemical state of Pd deduced from these findings is Pd^{2+}, which is expected due to the state of palladium in $PdCl_2$. The Cl 2p peaks originating at binding energies of 198.5 and 199.7 eV are associated with Cl $2p_{3/2}$ and Cl $2p_{1/2}$, respectively (Drelinkiewicz, et al., 2009; Duan, et al., 2011). This indicates the presence of chlorine in the state of Cl^- in the sample (Duan, et al., 2011). All the obtained results are as expected and indicate effective $PdCl_2$ doping and purity of the BiOBr photocatalyst sample.

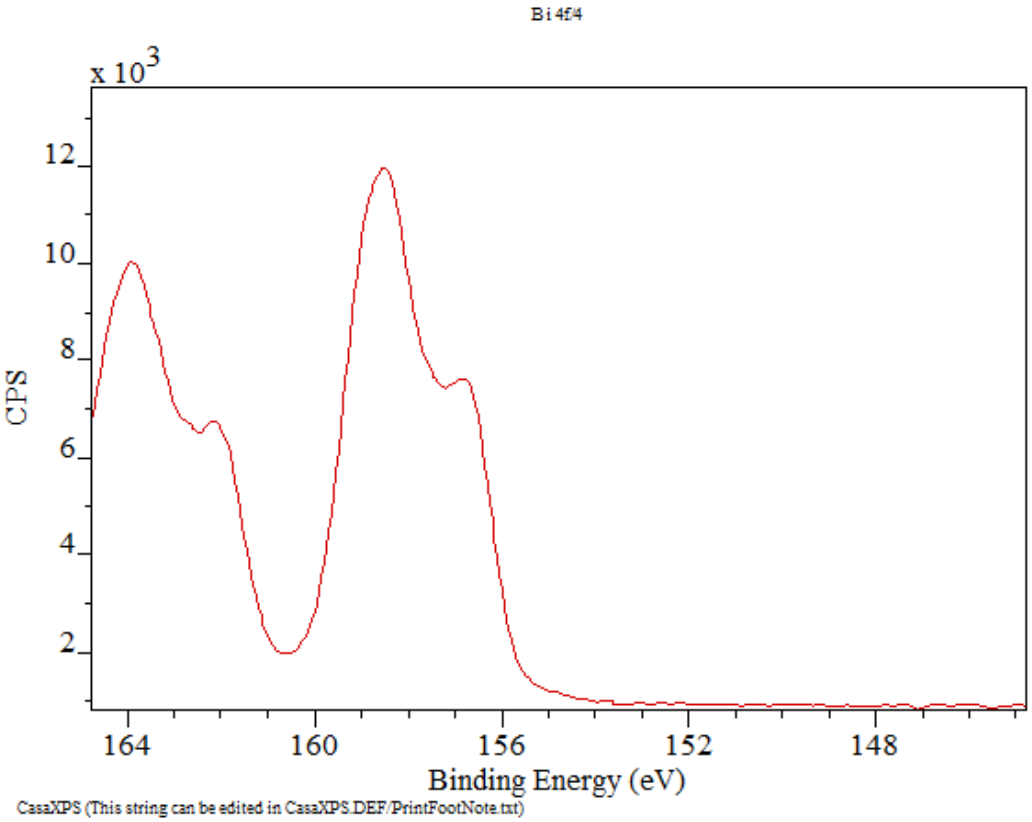

Figure 6 – XPS Spectrum of Bismuth in doped sample

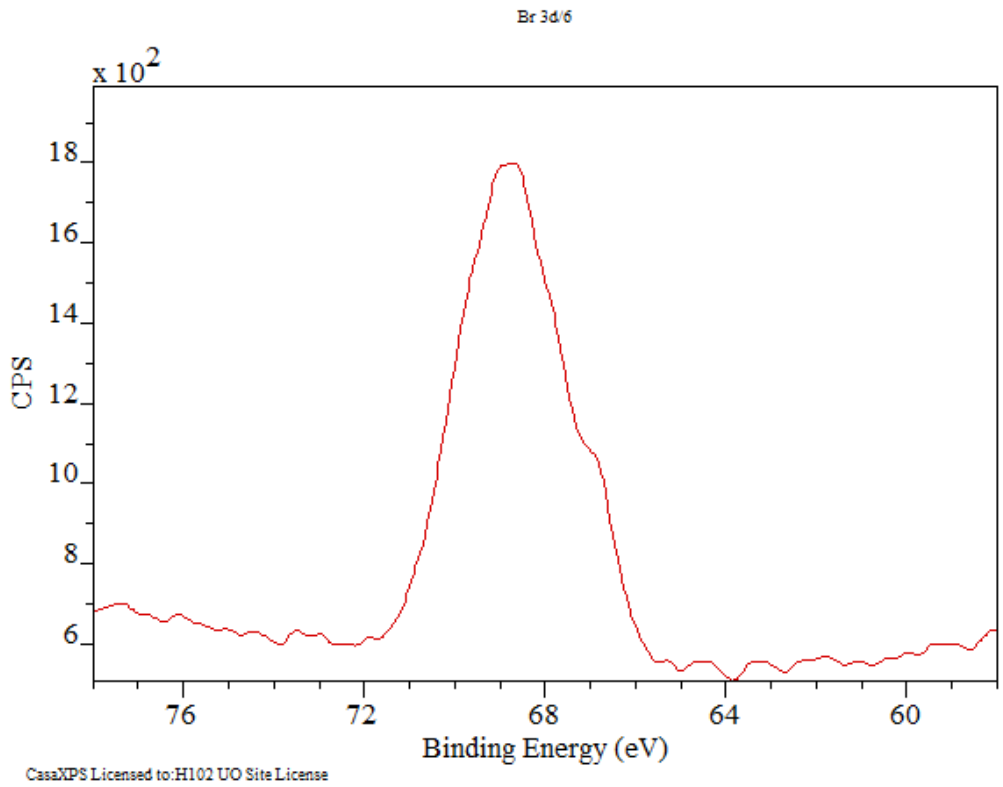

Figure 7 – XPS Spectrum of Bromine in doped sample

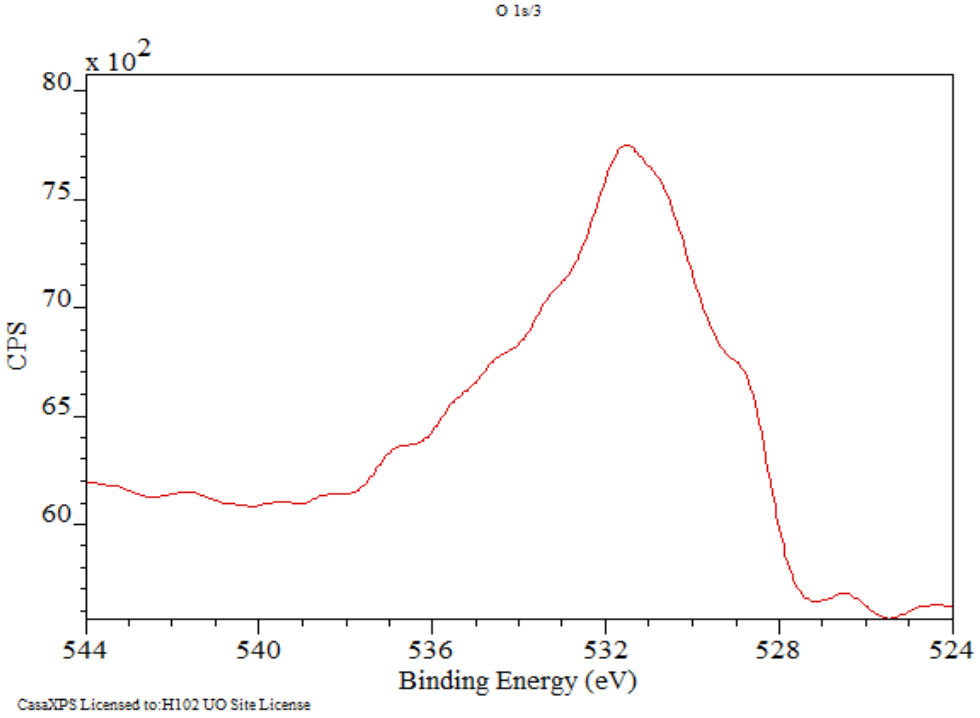

Figure 8 – XPS Spectrum of Oxygen in doped sample

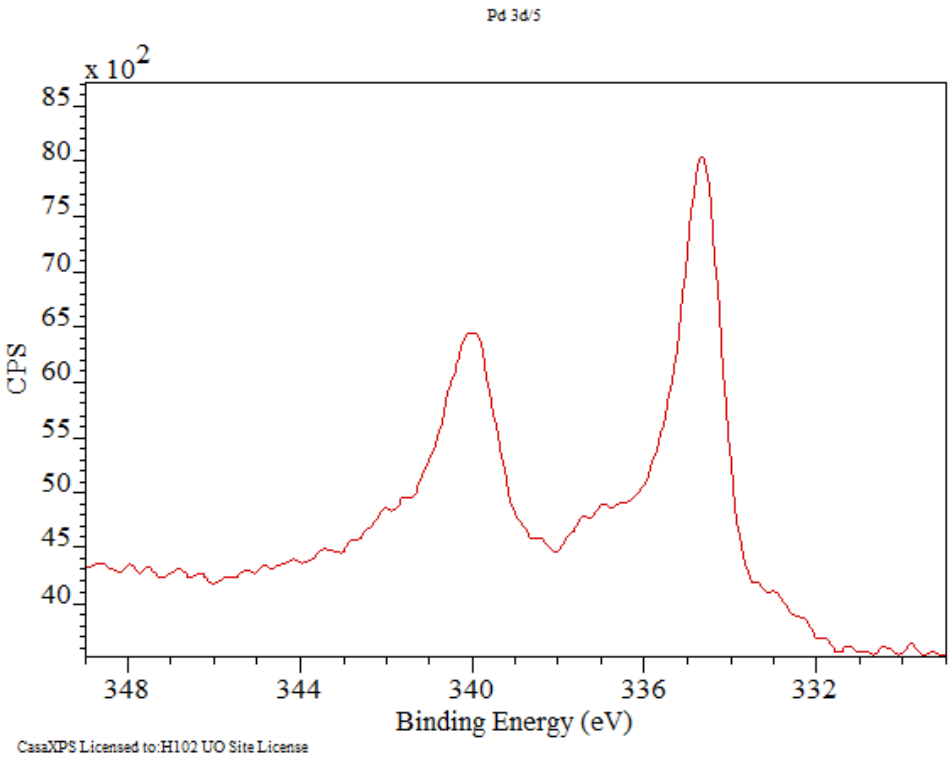

Figure 9 – XPS Spectrum of Palladium in doped sample

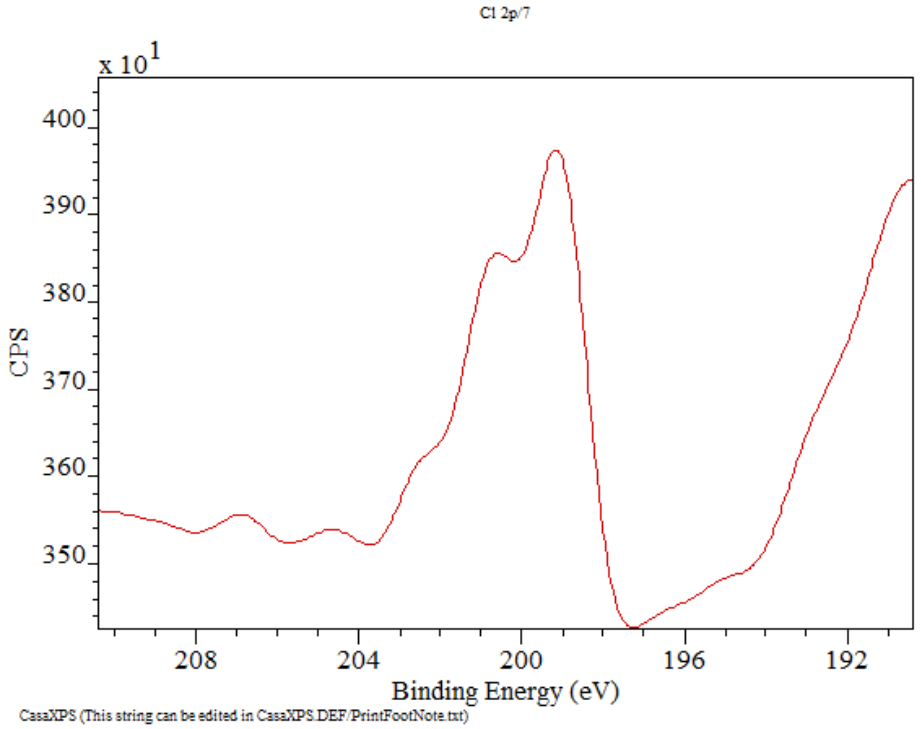

Figure 10 – XPS Spectrum of Chlorine in doped sample

4.3.1.4 UV-Vis Spectroscopy

In order to get insights into the absorption edge and band gap energy of the sample, UV-vis diffuse reflectance spectra of doped samples were investigated and compared to their counterpart, non-doped BiOBr samples. From the UV-vis spectra of $PdCl_2$ doped BiOBr (Figure 11), it can be noted that there is a dip at approximately 420 nm which shows absorption in the visible light region. The steep slope of the spectrum designates that the visible light absorption edge is due to intrinsic transition between the valence and conduction band instead of impurity level transition (Zhang, et al., 2008). $PdCl_2$ loaded BiOBr shows a red shift in the absorption spectrum with respect to non-doped BiOBr exhibiting stronger visible light response. Moreover, doped photocatalyst exhibits a sharp increase in absorption over a larger region, which allows the photocatalyst to utilize more light during photocatalysis and this is known to enhance the photocatalytic performance (Ai, et al., 2011). These results are consistent with the observed light yellow and dark brown colour of the non-doped and doped BiOBr, respectively. The band gap energy (E_g) was calculated from the UV-vis spectra by plots obtained using Kubelka Munk function. The band gap energy of $PdCl_2$ doped BiOBr was found to be 2.63 eV which compares to 2.9 eV for the non-doped catalyst. Although both values are within the range found in literature (Feng, et al., 2011; Jiang, et al., 2010), a decrease in band gap energy is generally indicative of improved light absorption and hence higher photocatalytic activity (Feng, et al., 2011). Therefore, it can be deduced that the visible light absorption properties of the BiOBr catalyst were significantly improved by loading $PdCl_2$.

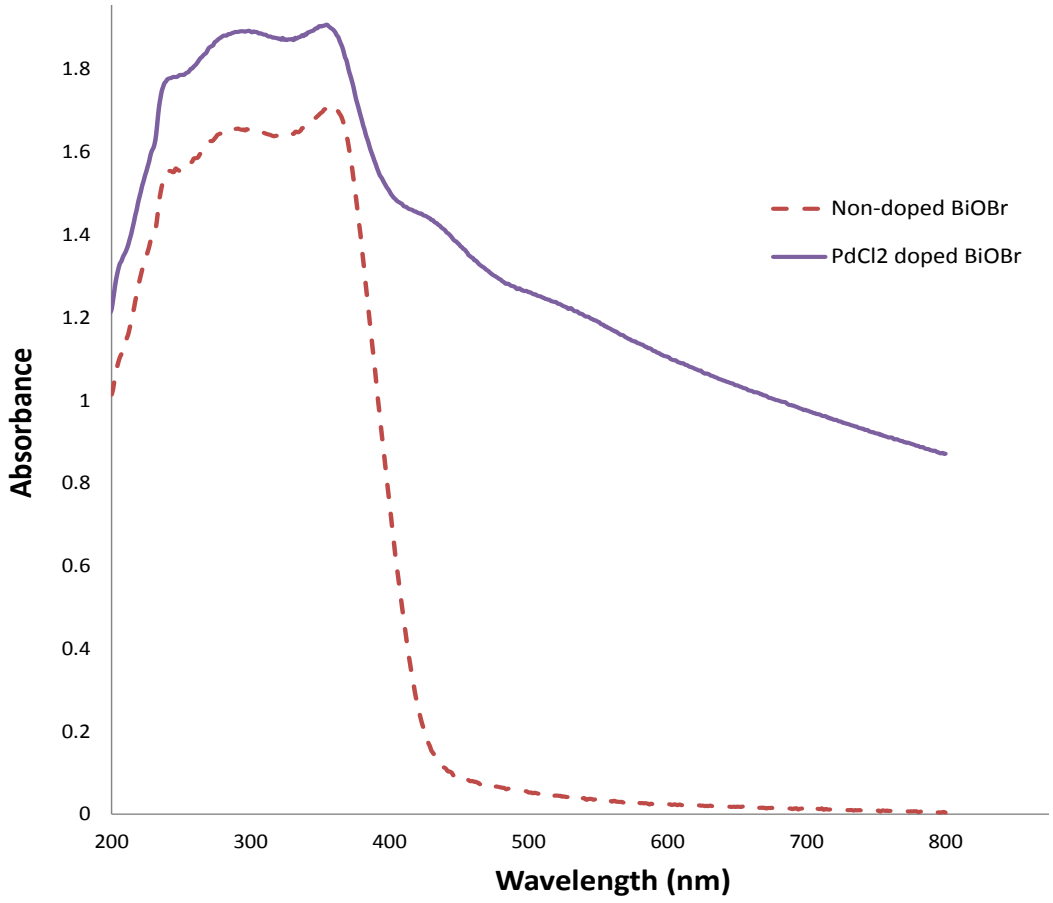

Figure 11 – UV- Vis Diffuse Reflectance Spectra of $PdCl_2$ doped and non-doped BiOBr samples

4.3.2 Effect of $PdCl_2$ Loading

Dopants are generally known to enhance the activity of photocatalysts by enhancing their physicochemical properties. Figure 12 demonstrates the degradation of 10 ppm RhB solution as a function of varying amounts of dopant while the concentration of catalyst was held constant at 0.5 g/L. It can be noted, that doping $PdCl_2$ onto BiOBr significantly improves its photocatalytic activity. These results are expected because it is known that Pd metal can provide electron wells that help separate electron/hole pairs and mediate production of OH^- radicals (Lee & Mills, 2003). Dopants are also known to enhance the physicochemical properties of the photocatalyst, specifically increased crystallinity, higher specific surface area and smaller crystallite sizes (Setiawati & Kawano, 2008; Fan, et al., 2008). Moreover, the smaller crystallite size of the doped catalyst increases the specific

surface area while the flaked exterior enhances its surface to volume ratio. Smaller crystals are also less prone to agglomeration and are more accessible, thus having a higher overall activity (Tan, et al., 2011). All of these factors collectively contribute to the higher photocatalytic activity by $PdCl_2$ doped BiOBr photocatalyst.

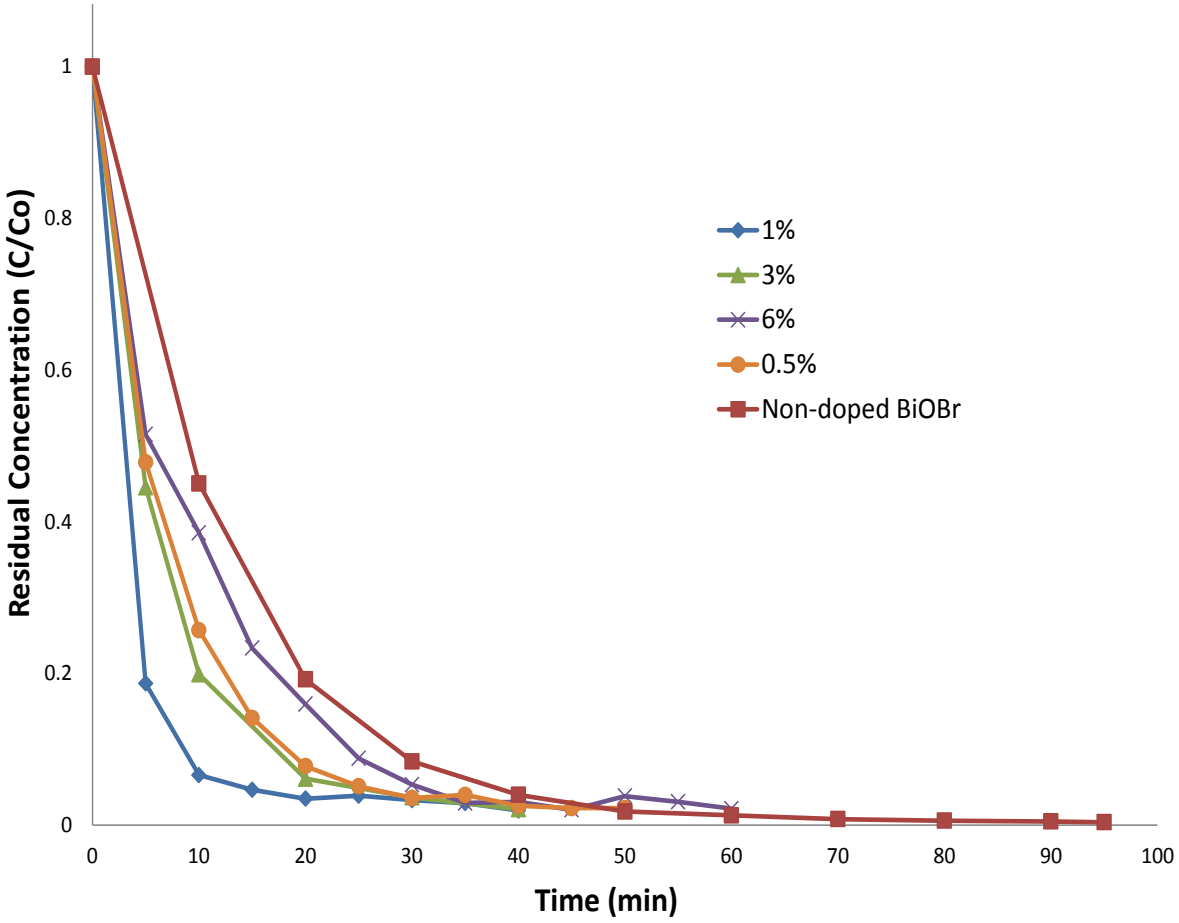

Figure 12 – Degradation of RhB under various amounts of Pd (% w/w) loading on BiOBr photocatalyst

The amount of dopant loaded on the photocatalyst is strongly related to the photocatalytic activity and therefore must be investigated. It was found that initially, as the amount of $PdCl_2$ was increased from 0 to 1% w/w Pd, the photocatalytic activity was directly proportional to the dopant concentration. However, beyond a concentration of 1% w/w Pd, the photocatalytic performance decreased (Figures 12 and 13). An optimum dopant

concentration of 1% w/w for Pd metal is in agreement with values found literature for other semiconductors (Chen, et al., 1999; Tan, et al., 2011). The presence of an optimum concentration can be explained by the phenomenon that as dopant amount is increased, the photonic efficiency of photocatalyst is increased, thus reducing the electron-hole pair recombination (Behnajady, et al., 2011; Lee & Mills, 2003). At higher concentration, Pd provides more electron acceptor centres which increases rate of photocatalysis. However, if the dopant amount is excessively increased, it leads to light shielding and hence lower absorption by the photocatalyst (Behnajady, et al., 2011; Tan, et al., 2011). Also, too much dopant may also block active sites on the catalyst surface, thus reducing photodegradation efficiency (Behnajady, et al., 2011). The optimum dopant concentration of 1% w/w Pd leads to the highest degradation rate constant of 0.13 min^{-1} (Figure 13).

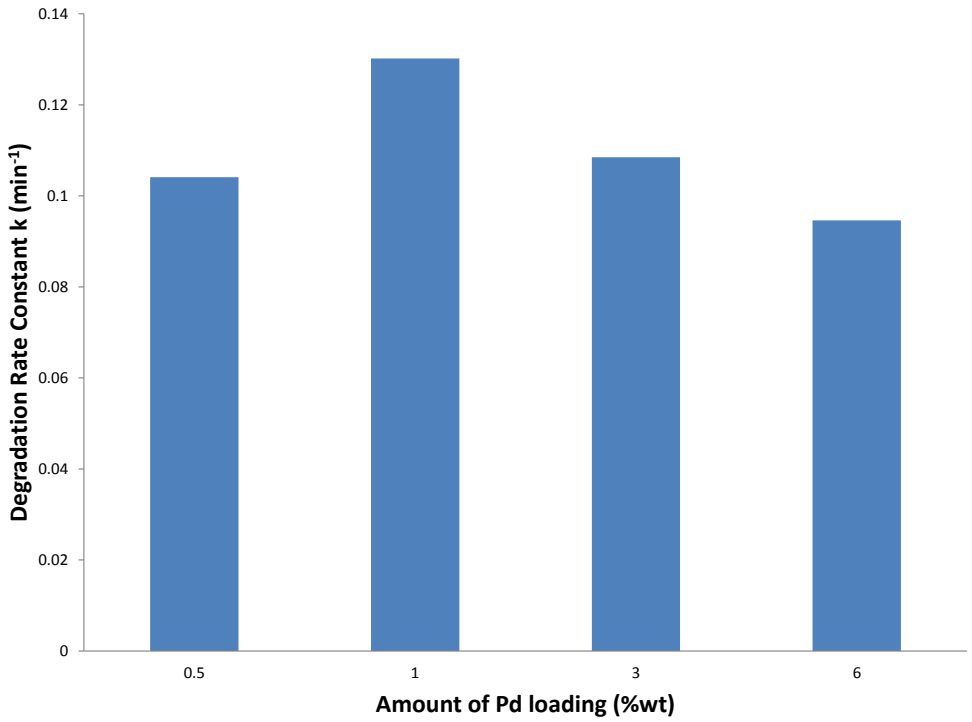

Figure 13 – Degradation rate constants as a function of Pd loading (%w/w) on BiOBr photocatalyst

4.3.3 Effect of Catalyst Concentration

After the ideal $PdCl_2$ loading amount was established, the effect of catalyst dosage on rate of degradation was investigated while maintaining the dopant concentration at its optimum of 1%. Initially, the concentration of pollutant RhB was kept constant (10 ppm) while the catalyst concentration was varied from 0.25 g/L to 1 g/L (Figure 14). It was found that the degradation of RhB significantly increased with an increase in catalyst concentration from 0.25 g/L to 0.5 g/L. However, beyond this concentration, the degradation of RhB decreased with increasing catalyst amount. It is known that at a lower level, increasing catalyst concentration would lead to more active sites for the pollutant molecules to access, resulting in higher degradation (Huang, et al., 2008; Suri, et al., 1993; Behnajady, et al., 2011). However, at excessively high catalyst concentration, although the number of active sites is higher, the opaque catalyst particles may obstruct the light and cause a decrease in light penetration of the solution (Wong & Chu, 2003). The agglomeration of catalyst particles also becomes more likely at higher catalyst concentrations, thus reducing the photocatalytic activity (Huang, et al., 2008). As a result of these competing mechanisms, an optimum was observed at a catalyst concentration of 0.5 g/L at the given concentration of 10 ppm RhB.

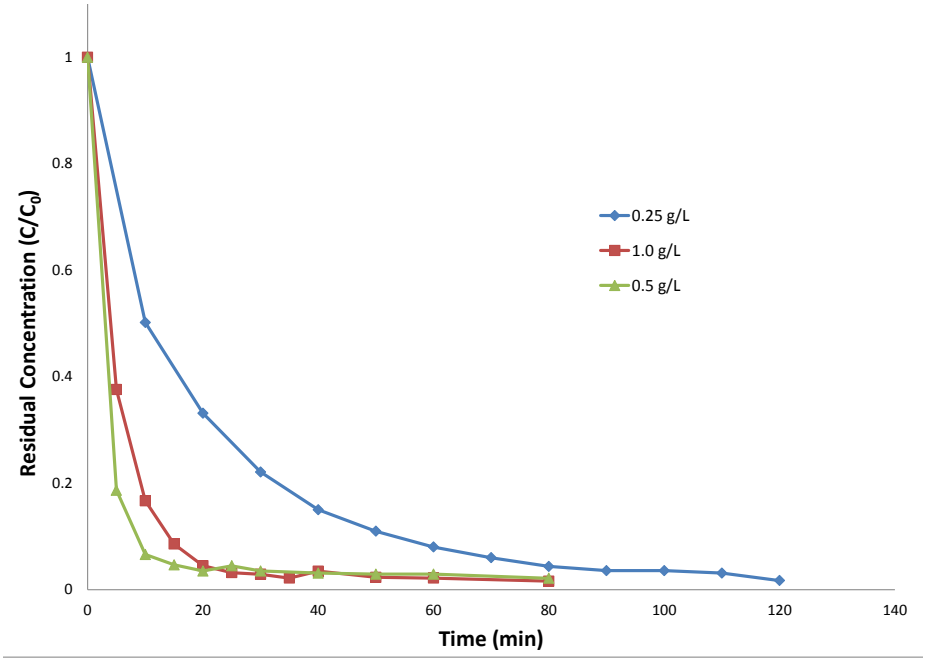

Figure 14 – Effect of $PdCl_2$ doped BiOBr Catalyst Concentration on Degradation of 10 ppm RhB

In order to further investigate the effect of catalyst concentration, and to endorse the abovementioned theories, degradation of a higher RhB concentration (40 ppm) was also investigated as a function of varying catalyst concentrations (Figure 15). It was observed that for 40 ppm RhB, a catalyst concentration of 1 g/L outperforms all other catalyst amounts. Again it can be noted that an optimum exists due to the trade-off between increasing active sites and decreasing light penetration with increased dosage. However, in this case, the optimum has shifted to a higher catalyst concentration. Figure 16 demonstrates the degradation rate constants of various catalyst dosages as a function of the two different pollutant concentrations.

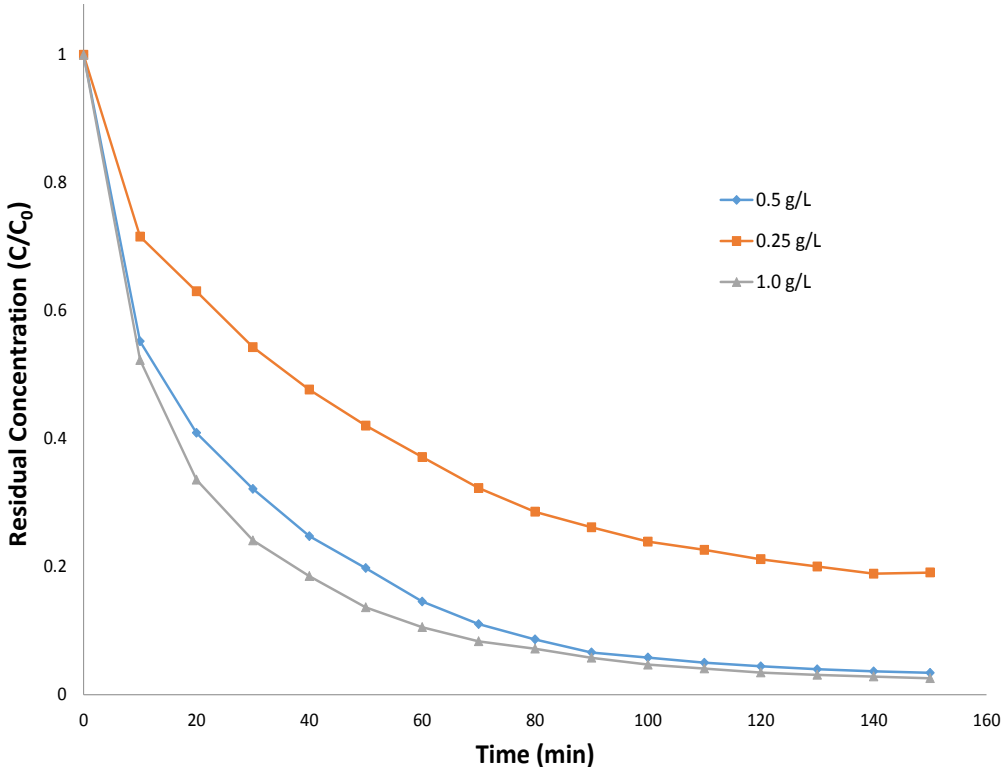

Figure 15 – Effect of $PdCl_2$ doped BiOBr Catalyst Concentration on Degradation of 40 ppm RhB

The obtained results are in accordance with literature and are due to the fact that for a higher pollutant concentration, a larger number of active sites are favoured for faster kinetics (Suri, et al., 1993). On the other hand, for lower pollutant concentrations, the presence of a higher number of active sites is less critical due to a lower number of pollutant molecules and therefore lower catalyst concentration is given preference because it allows better light penetration. These results suggest that different catalyst amounts may be suitable depending on the concentration of pollutants in the wastewater, however a lower pollutant concentration of 10 ppm is more realistic while 40 ppm was selected merely for experimental purposes to test photocatalytic behaviour at higher concentrations.

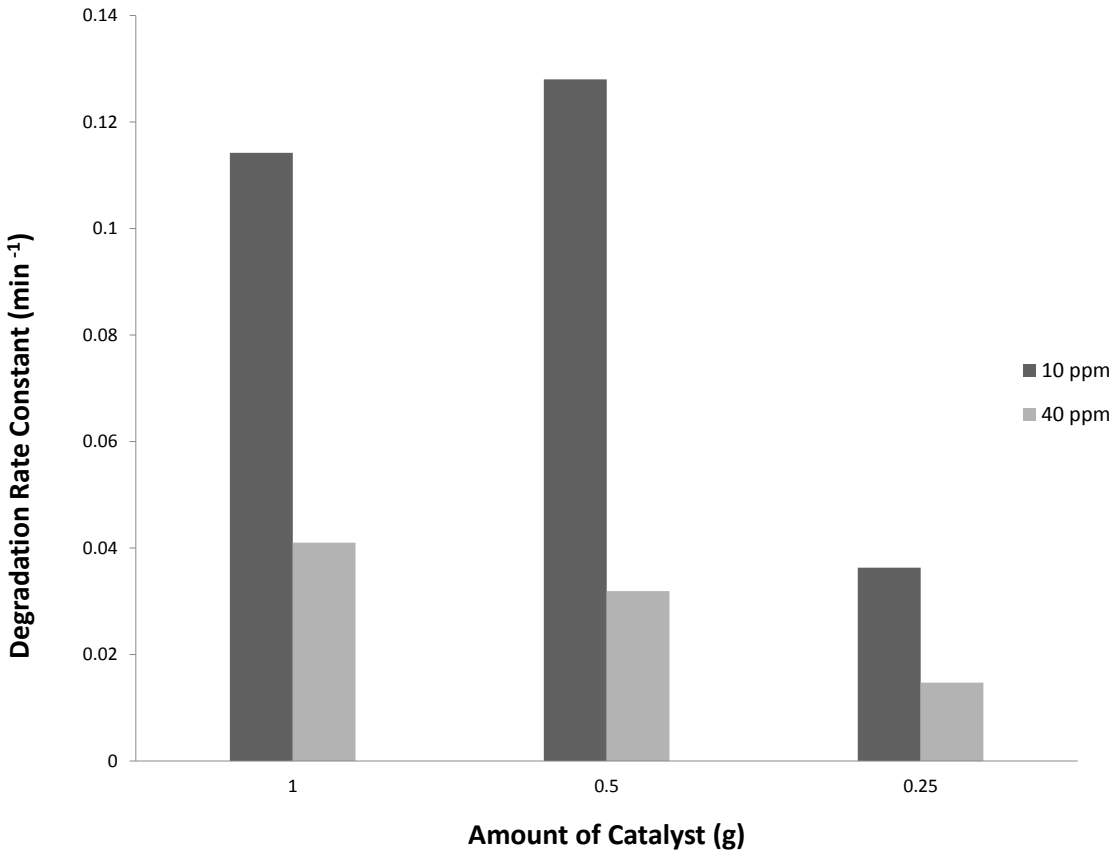

Figure 16 – Degradation Rate Constant at Various Catalyst and Dye Concentrations

4.3.4 Effect of Initial Pollutant Concentration

From an application point of view, it is important to study the influence of initial reactant concentration on photocatalytic degradation. In order to establish the dependence of removal efficiency on the initial pollutant concentration, solutions of different initial concentration of RhB were degraded using the same dopant concentration and amount of photocatalyst, 1% wt Pd and 0.5 g/L respectively. The results of this study shown in Figure 17, indicate that the activity of the photocatalyst decreases with increasing the initial reactant concentration, which is in agreement with literature (Tan, et al., 2011). The relationship between initial pollutant concentration and photocatalytic activity is associated with the adsorption of reactant on the surface of photocatalyst (Tan, et al., 2011). Therefore, increasing the initial pollutant concentration decreases activity due to the limitation of the number of active sites available for pollutant molecules on the photocatalyst surface (Andronic, et al., 2009). Also with increasing initial pollutant concentration, more and more organic intermediates compete with hydroxyl ions for adsorption at the active sites of $PdCl_2$ doped BiOBr photocatalyst, thus reducing the generation of hydroxyl radicals (Jamalluddin & Abdullah, 2011; Behnajady, et al., 2011). Another reason for decrease in photodegradation of RhB with increasing concentrations is the light screening effect due to more dye molecules which inhibits penetration of light (Verma, et al., 2006; Venkatachalam, et al., 2007; Jamalluddin & Abdullah, 2011). Studying the kinetic curves and degradation rate constants for this study demonstrates that all reaction rates obey the pseudo first order kinetic equation and that the rate constants decrease accordingly with increasing RhB concentrations (Figure 18) as established by other studies (Matthews, 1988; Chen & Jeng, 1998).

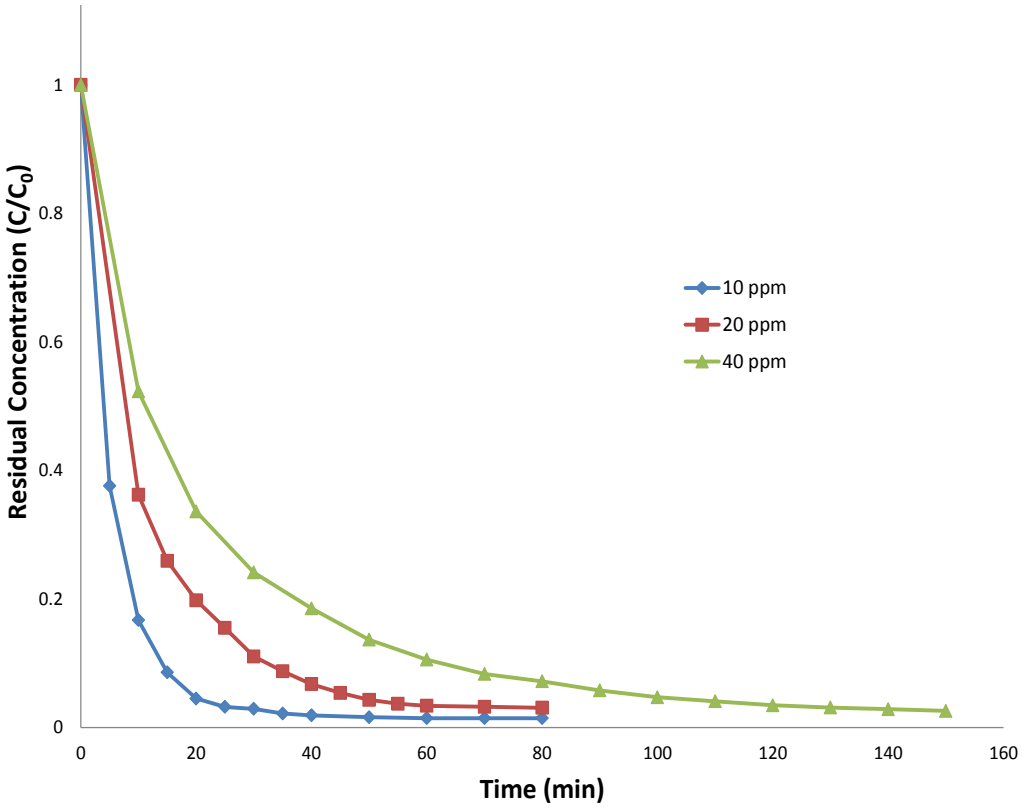

Figure 17 – Effect of Initial Pollutant Concentration on Degradation of RhB by $PdCl_2$ doped BiOBr

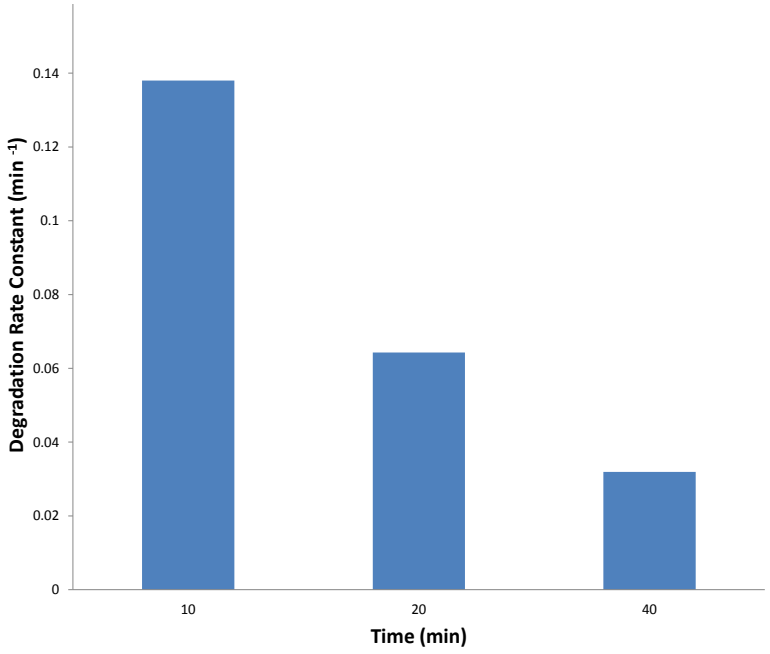

Figure 18 – Degradation Rate Constants of $PdCl_2$ doped BiOBr at various Dye Concentrations

4.3.5 Effect of Photocatalyst Stability

The stability and reusability of photocatalyst is very important for practical applications of any photocatalyst. Recyclability of $PdCl_2$ loaded BiOBr was tested in manner similar to the photocatalytic activity tests except for this case, the catalyst was recovered at the end of the run. The catalyst was filtered, washed and then dried to regenerate it in powder form. Subsequent runs were then carried out with this catalyst sample. Figure 19 demonstrates the results obtained from recyclability experiments. It can be noted that the efficacy of catalyst is not significantly affected by recycling and even after the 5^{th} run, degradation efficiency is only reduced by 2%. This demonstrates that $PdCl_2$ doped BiOBr catalyst is stable and may be reused over many runs, which is an important prerequisite for any photocatalyst.

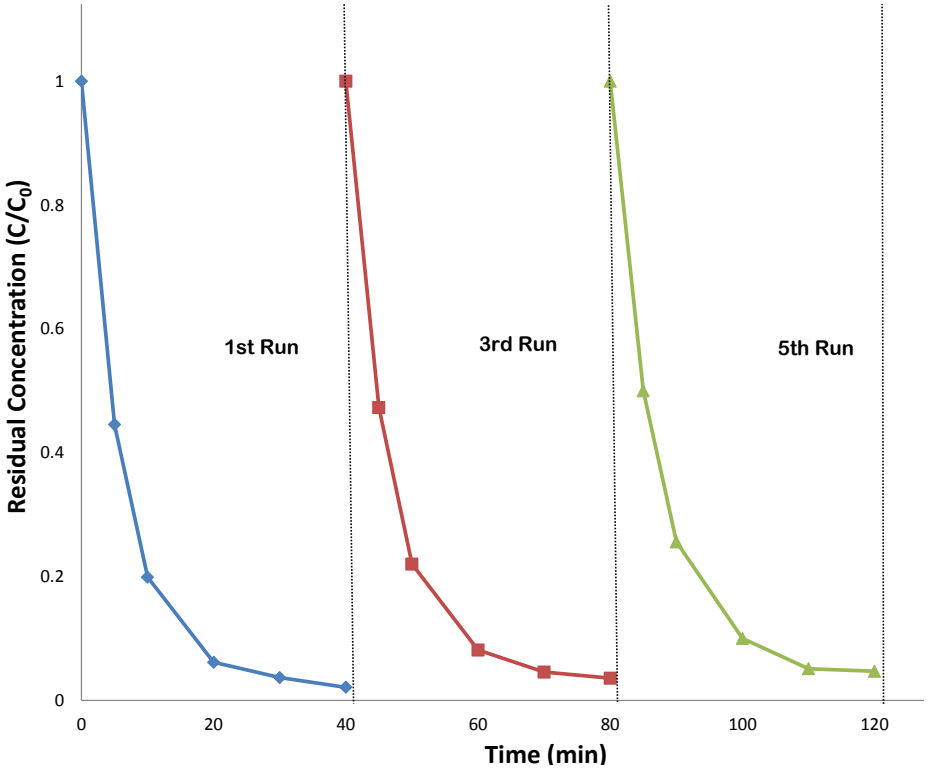

Figure 19 – Recyclability Tests for $PdCl_2$ doped BiOBr Photocatalyst

4.4 Conclusion

In this study, $PdCl_2$ was doped on the surface of solvothermally synthesized BiOBr photocatalyst. The photocatalytic activity of the prepared samples was evaluated under a series of different experimental and operating conditions. It was discovered that doping $PdCl_2$ on BiOBr significantly improves its photocatalytic performance and the highest activity is obtained with a loading amount of 1% w/w Pd. The optimum amount of catalyst for a 10 ppm RhB solution was 0.5 g/L and at those conditions, more than 95 % of dye could be degraded within the first 15 minutes under visible light irradiation. The photocatalyst prepared using the described synthesis method is also found to be stable and reusable. In summary, it was demonstrated that BiOBr photocatalytic activity was enhanced using $PdCl_2$ doping and the results are promising for applying this novel photocatalyst for wastewater treatment. This also opens new avenues in bismuth oxyhalide photocatalyst research as such a dopant had previously not been investigated for BiOBr. Further research can be conducted in doping other transition metal salts as well as reduced metals on BiOBr and evaluating their effects on its performance.

Author Information:

Ayla Ahmad – University of Ottawa (Canada)
Zisheng Zhang* – University of Ottawa (Canada)
Susana Lordano Luiz - Universidade Federal de Alfenas (Brazil)
*Corresponding author

References

Ai, Z., Ho, W., & Lee, S. (2011). Efficient Visible Light Photocatalytic Removal of NO with BiOBr-Graphene Nanocomposites. J. Phys. Chem. C, 115, 25330-25337.

An, H., Du, Y., Wang, T., Hao, W., & Zhang, J. (2007). Photocatalytic Properties of BiOX (X= Cl, Br, and I). Rare Met., 27, 243-251.

Andronic, L., Enesca, A., Vladuta, C., & Duta, A. (2009). Photocatalytic activity of cadmium doped TiO2 films for photocatalytic degradation of dyes. Chem. Eng. J., 152, 64-71.

Asahi, R., Morikawa, T., Ohwaki, T., Aoki, K., & Taga, Y. (2001). Visible-Light Photocatalysis in Nitrogen-Doped Titanium Oxides. Science, 293, 269-271.

Asilturk, M., Sayilkan, F., & Arpac, E. (2009). Effect of Fe3+ ion doping to TiO2 on the photocatalytic degradation of Malachite Green dye under UV and vis-irradiation. J. Photocem. Photobiol., 203, 64-71.

Baiju, K. V., Shukla, S., Biju, S., Reddy, M. L., & Warrier, K. G. (2009). Hydrothermal processing of dye-adsorbing one-dimensional hydrogen titanate. Mater. Lett., 63, 923-926.

Behnajady, M. A., Alizade, B., & Modirshahla, N. (2011). Synthesis of Mg-Doped TiO2 nanoparticles under different conditions and its photocatalytic activity. Photochem. Photobiol., 87, 1308-1314.

Behnajady, M. A., Vahid, B., Mordirshahla, N., & Shokri, M. (2009). Evaluation of electrical energy per order (EEO) with kinetic modeling on the removal of Malachite Green by US/ UV/ H2O2 process. Desalination, 249, 99-103.

Cao, J., Xu, B., Lin, H., Luo, B., & Chen, S. (2011). Chemical etching preparation of BiOI/BiOBr heterostructures with enhanced photocatalytic properties for organic dye removal. Chem. Eng. J., 185, 91-99.

Chang, X. F., Yu, G., Huang, J., Li, Z., Zhu, S. F., Yu, P. F., . . . Ji, G. B. (2010). Enhancement of photocatalytic activity over NaBiO3/BiOCl composite prepared by an in situ formation strategy. Catal. Today, 153, 193-199.

Chang, X., Huang, J., Cheng, C., Sui, Q., Sha, W., Ji, G., . . . Yu, G. (2010). BiOX (X = Cl, Br, I) photocatalysts prepared using NaBiO3 as the Bi source: Characterization and catalytic performance. Catal. Commun., 11, 460-464.

Chen, J., Ollis, D. F., Rulkens, W. H., & Bruning, H. (1999). Photocatalyzed oxidation of alcohols and organochlorides in the presence of native TiO2 and metallized TiO2 suspensions. Part (I): photocatalytic activity and pH influence. Water Res. , 33, 661-668.

Chen, P. H., & Jeng, C. H. (1998). Kinetics of photocatalytic oxidation of trace organic compounds over titanium dioxid. Environ. Int., 24, 871-879.

Crini, G. (2005). Recent developments in polysaccharide-based materials. Prog. Polym. Sci., 30, 38-70.

Drelinkiewicz, A., Sobczak, J., Sobczak, E., Krawczyk, M., Zieba, A., & Waksmundzka-Gora, A. (2009). Physicochemical and catalytic properties of Pt-poly(4-vinylpyridine) composites. Mater. Chem. Phys., 114, 763-773.

Duan, F., Zheng, Y., & Chen, M. (2011). Flowerlike PtCl4/Bi2WO6 composite photocatalyst with enhanced visible-light-induced photocatalytic activity. Applied Surface Science , 257, 1972-1978.

Fan, X., Chen, X., & Zhu, S. (2008). The structural, physical and photocatalytic properties of the mesoporous Cr-doped TiO2. J. Mol. Catal. A, 284, 155-160.

Feng, Y., Li, L., Li, J., & Wang, J. (2011). Synthesis of mesoporous BiOBr 3D microspheres and their photodecomposition for toluene. J. Hazar. Mater., 192, 538-544.

Gaya, U. M., & Abdullah, A. H. (2007). Heterogeneous photocatalytic degradation of organic contaminants over titanium dioxide: a review of fundamentals progress and problems. J. Photochem. Photobiol., 9, 1-12.

Huang, M., Xu, C., Wu, Z., Huang, Y., Lin, J., & Wu, J. (2008). Photocatalytic discolorization of methyl orange solution by Pt modified TiO2 loaded on natural zeolite. Dyes Pigm., 77, 327-334.

Hwang, G. H., Han, W. K., Park, J. S., & Kang, S. G. (2008). An electrochemical sensor based on the reduction of screen-printed bismuth oxide for the determination of trace lead and cadmium. Sens. Actuators, B, 135, 309-316.

Hwang, S. M., Lim, J. H., Lee, C. M., Park, E. C., Choi, J. H., Joo, J., Jung, S. B. (2009). Fabrication of two-layer flexible copper clad laminate by electroless-Cu plating on surface modified polyimide. Trans. Nonferrous Met. Soc. China, 19, 970-974.

Jacobs, J. W. (1986). Photochemical nucleation and growth of palladium on titanium dioxide films studied with electron microscopy and quantitative analytical techniques. J. Phys. Chem, 90, 6507-6517.

Jamalluddin, N. A., & Abdullah, A. Z. (2011). Reactive dye degradation by combined Fe(III)/TiO2 catalyst and ultrasonic irradiation: effect of Fe(III) loading and calcination temperature. Ultrason. Sonochem., 18, 669-678.

Jiang, G., Wang, R., Wang, X., Xi, X., Hu, R., Zhou, Y., Chen, W. (2012). Novel Highly Active Visible-Light-Induced Photocatalysts Based on BiOBr with Ti Doping and Ag Decorating. Appl. Mater. Interfaces, 4, 4440-4444.

Jiang, Z., Yang, F., Luo, N., Chu, B. T., Sun, D., Shi, H., Edwards, P. P. (2008). Solvothermal synthesis of N-doped TiO2 nanotubes for visible-light-responsive photocatalysis. Chem. Commun., 9, 6372-6374.

Jiang, Z., Yang, F., Yang, G., Kong, L., Jones, M. O., Xiao, T., & Edwards, P. P. (2010). The hydrothermal synthesis of BiOBr flakes for visible-light-responsive photocatalytic degradation of methyl orange. . J. Photochem. Photobiol. A, 212, 8-13.

Kansal, S. K., Ali, A. H., & Kapoor, S. (2010). Photocatalytic decolorization of biebrich scarlet dye in aquesous phase using different nanophotocatalysts. Desalination, 259, 147-155.

Kaur, A., & Gupta, U. (2009). A review on applications of nanoparticles for the preconcentration of environmental pollutants. J. Mater. Chem., 19, 8279-8289.

Khalil, S. S., Uvarov, V., Fronton, S., Popov, I., & Sasson, Y. (2012). A Novel Heterojunction BiOBr/Bismuth Oxyhydrate Photocatalyst with Highly Enhanced Visible Light Photocatalytic Properties. J. Phys. Chem., 116, 11004-11012.

Kim, Y. S., Shin, J., Cho, J. H., Eyck, G. T., Liu, D. L., Pimanpang, S., Shin, H. S. (2006). Surface characterization of copper electroless deposition on atomic layer deposited palladium on iridium and tungsten. Surf. Coat. Technol., 200, 5760-5766.

Kong, L., Jiang, Z., Lai, H. H., Nicholls, R. J., Xiao, T., Jones, M. O., & Edwards, P. P. (2012). Unusual reactivity of visible-light-responsive AgBr–BiOBr heterojunction photocatalysts. J. Catal., 293, 116-125.

Kong, L., Jiang, Z., Xiao, T., Lu, L., Jones, M. O., & Edwards, P. P. (2011). Exceptional visible-light-driven photocatalytic activity over. Chem. Commun. , 47, 5512-5514.

Lee, S. K., & Mills, A. (2003). Platinum and Palladium in Semiconductor Photocatalytic Systems . Plat. Met. Rev., 47, 61-72.

Liu, Y., Son, W. J., Lu, J., Huang, B., Dai, Y., & Whangho, M. H. (2011). Composition Dependence of the Photocatalytic Activities of BiOCl1-xBrx Solid Solutions under Visible Light. Chem. Eur. J., 17, 9342-9349.

Matthews, R. W. (1988). Kinetics of photocatalytic oxidation of organic solutes over titanium dioxide. J. Catal., 111, 264-272.

Parida, S. K., Dash, S., Patel, S., & Mishra, B. M. (2006). Removal of organic molecules on silica surface. Adv. Colloid Interface Sci., 121, 77-110.

Sakthivel, S., Shankar, M. V., Palanichamy, M., Arabindoo, B., Bahnemann, W., & Murugesan, V. (2004). Enhancement of photocatalytic activity by metal deposition: characterisation and photonic efficiency of Pt, Au and Pd deposited on TiO2 catalyst. Water Res., 38, 3001-3008.

Setiawati, E., & Kawano, K. (2008). Stabilization of anatase phase in the rare earth; Eu and Sm ion doped nanoparticle TiO2. J. Alloys Compd., 451, 293-296.

Shang, M., Wang, W., & Zhang, L. (2009). Prepearation of BiOB lamellar structure with high photocatalytic activity by CTAB as Br source and template. J. Hazard. Mater., 167, 803-809.

Shi, X., Chen, X., Chen, X., Zhou, S., Lou, S., Wang, Y., & Yuan, L. (2013). PVP assisted hydrothermal synthesis of BiOBr hierarchical nanostructures and high photocatalytic capacity. Chem. Eng. J., 222, 120-127.

Suh, S., Kim, J., Kim, S., & Park, B. (2010). Effect of PI film surface on printing of Pd(Ⅱ)catalytic ink for electroless copper plating in the printed electronics. J. Ind. Eng. Chem., 18, 209-294.

Suri, R., Liu, J., Hand, D. W., Crittenden, J. C., Perram, D. L., & Mullins, M. E. (n.d.).

Suri, R., Liu, J., Hand, D. W., Crittenden, J. C., Perram, D. L., & Mullins, M. E. (1993). Heterogeneous photocatalytic oxidation of hazardous organic contaminants in water. Water Environ. Res., 65, 665-673.

Tan, Y. N., Wong, C. L., & Mohamed, A. R. (2011). An Overview on the Photocatalytic activity of nano-doped TiO2 in the Degradation of Organic Pollutants. ISRN Materials Science, 2011, 1-18.

Tan, Y. N., Wong, C. L., & Mohamed, A. R. (2011). An Overview on the Photocatalytic Activity of Nano-Doped-TiO2 in the Degradation of Organic Pollutants. ISRS Materials Science, 1-18.

Venkatachalam, N., Palanichamy, M., Arabindoo, B., & Murugesan, V. (2007). Enhanced photocatalytic degradation of 4-chlorophenol by Zr4+ doped nano TiO2. J. Molec. Catal. A, 266, 158-165.

Verma, A., Bakhshi, A. K., & Agnihotry, S. A. (2006). Effect of different precursor sols on the properties of CeO2-TiO2 films for electrochromic window applications. Electrochim. Acta, 51, 4639–4648.

Wang, R., Jiang, G., Wang, X., Hu, R., Xi, X., Bao, S., Chen, W. (2011). Efficient visible-light-induced photocatalytic activity over the novel Ti-doped BiOBr microspheres. Powder Technology, 228, 258-263.

Wang, W., Huang, F., Lin, X., & Yang, J. (2008). Visible-light-responsive photocatalysts xBiOBr-(1-x) BiOI. Catal. Commun., 9, 8-12.

Wong, C. C., & Chu, W. (2003). The direct photolysis and photocatalytic degradation of alachlor at different TiO2 and UV sources. Chemosphere, 50, 981-987.

Yan, C. Y., & Lee, J. (2009). Crystallographic alignment of ZnO nanorod arrays on Zn2GeO4 nanocrystals: promising lattice-matched substrates. J. Phys. Chem C, 114, 263-268.

Yang, D. J., Zheng, Z. F., Zhu, H. Y., Liu, H. W., & Gao, X. P. (2008). Titanate nanofibers as intelligent absorbents for the removal of radioactive ions from water. Adv. Mater., 20, 2777-2781.

Yu, C., Fan, C., Meng, X., Yang, K., Cao, F., & Li, X. (2011). A novel Ag/BiOBr nanoplate catalyst with high photocatalytic activity in the decomposition of dyes. Reac. Kinet. Mech. Cat., 103, 141-151.

Yu, C., Yu, J. C., Fan, C., Wen, H., & Hu, S. (2010). Synthesis and characterization of Pt/BiOI nanoplate catalyst with enhanced activity under visible light irradiation. Sci. Eng. B., 166, 213-219.

Zhang, J., Shi, F. J., Lin, J., Chem, D. F., Gao, J. M., Huang, Z. X., Tang, C. C. (2008). Self- Assembled 3-D architectures of BiOBr as a visible-light-driven photocatalyst. Chem. Mater., 20, 2937-2941.

Zhang, L., Cao, X. F., Chen, X. T., & Xue, Z. L. (2011). BiOBr hierarchical microspheres: Microwave-assisted solvothermal synthesis, strong adsorption and excellent photocatalytic properties. J. Colloid Interf. Sci., 354, 630-636.

Zhang, X., Ai, Z., Jia, F., & Zhang, L. (2008). Generalized One-Pot Synthesis, Characterization, and Photocatalytic Activity of Hierarchical BiOX (X = Cl, Br, I) Nanoplate Microspheres. J. Phys. Chem. C, 112, 747-753.

Zhao, M. F., Tang, Z. B., & Liu, P. (2008). Removal of Methylene Blue from Aquesous Solution with Silica Nano-sheets Derived from Vermiculite. J. Hazard. Mater., 158, 43-51.

Chapter 5 - Summary and Conclusions

Based on the series of experiments performed in this study, it can be inferred that BiOBr shows promising results for applications in solar-activated wastewater and drinking water treatments. BiOBr was effectively synthesized by both solvothermal and hydrothermal methods under a series of different conditions and it was established that during synthesis processes, parameters of time and temperature play a key role in the performance of photocatalyst. The synthesized BiOBr samples were characterized by using technologies of XRD, SEM, EDS and UV-vis diffraction in order to get insights into the crystallinity, morphology, structure, absorption edge and band gap energy of the photocatalyst. The versatility of the photocatalyst was also tested by application to organic textile dye Rhodamine B and colourless aromatic phenol and by altering pollutant and catalyst concentrations. The performance of BiOBr under various pH conditions was also carried out since pH is an important operational parameter in water treatment processes. Bactericidal activity of BiOBr under visible light irradiation was studied using *E. coli* as model microorganism in order to examine its applications in disinfection of water. Finally, a novel photocatalyst using $PdCl_2$/BiOBr was developed which is a chemical variant of BiOBr. This photocatalyst demonstrated excellent photocatalytic performance under visible light irradiation. Recyclability tests were performed for each sample in order to ensure the stability and reusability of the photocatalysts.

The main conclusions drawn from this study can be briefly summarized as follows

- It was found that solvothermal method is superior to the hydrothermal method due to formation of 3-D microspheres in the former rather than nanoplates which are formed through the latter method. At higher temperature of thermal treatment, crystals formed are smaller in diameter and thus offer a higher surface area. Shorter thermal treatment times bring about defined formation of rough fibers on surface which contribute to a higher surface-to-volume ratio and become deteriorated if time of treatment is prolonged. Consequently, optimal temperature and time of 180ºC and 3 h, respectively, were proposed.

- The effect of pH on activity of BiOBr was also evaluated and it was construed that a pH value that is too high or too low is detrimental to the photocatalytic performance of BiOBr. A marginally alkaline pH of 8 was found to be optimal for high activity.

- The bacterial inactivation studies suggested strong potential of BiOBr in photocatalysis-induced disinfection systems. It was determined that over 95% of bacteria could be inactivated within 60 minutes while using only 1 g/L of photocatalyst and almost the entire population of 10^6 CFU/mL was inactivated by the end of the 2 hour study.

- Phenol degradation studies revealed that BiOBr can degrade organic pollutants in water, although activity in visible light irradiation for phenol was lower.

- The highlight of this study was the successful synthesis of a novel $PdCl_2$/BiOBr photocatalyst as a variant of BiOBr by $PdCl_2$ doping on BiOBr. This variation was found to significantly improve photocatalytic performance of solvothermal BiOBr and demonstrated further development prospects in the area of BiOBr research. It was found that the highest activity is obtained at a loading amount of 1% w/w Pd.

- The optimum amount of catalyst concentration (for a 10 ppm RhB solution) was found to be 1 g/L and 0.5 g/L for the BiOBr and $PdCl_2$ doped BiOBr photocatalysts, respectively. The photocatalysts prepared using the described synthesis methods are also found to be stable and reusable even after several subsequent runs.

Overall, it was demonstrated that solvothermally synthesized BiOBr photocatalyst seems promising for applications in wastewater and drinking water treatments since it can degrade a range of pollutants in varying conditions and has disinfection properties in visible light. The production of novel $PdCl_2$/BiOBr composite photocatalyst also opens up new possibilities of utilizing platinum group metal doping in bismuth oxyhalides photocatalysis.

Chapter 6 - Recommendations

Over the course of this study, a myriad of problem statements and possible approaches were encountered, all of which could not be fit into the scope of the current project. However, they offer a prospective for further research and development to promote commercialization of photocatalysis based wastewater treatment systems. A few recommendations for future work in the area of photocatalysis described in this thesis are listed as follows.

- In the current study, solely solvothermal and hydrothermal methods of synthesis for BiOBr were focused on since they are the most efficient methods reported in literature thus far. However, additional methods of synthesis, such as synthesis by method of ionic liquids, are gaining interest. These methods, although complex, may also be tested for production of BiOBr and their applicability evaluated extensively. An experimental optimization of synthesis parameters other than temperature and time such as pH, agitation, calcination etc., would also provide a more holistic list of optimized synthesis conditions.

- As in majority of photocatalytic disinfection studies performed to date, this study also used laboratory-cultured microorganism suspended in distilled deionized water and saline solutions. However, some researchers have recently started to investigate more practical situations whereby the test water is sourced from environmental origins such as secondary effluents from wastewater treatment plants, reservoirs and ponds. Although these investigations show slower kinetics and are more difficult to integrate into quantitative experiments, they may provide a more accurate perspective on the suitability of photocatalysts for wastewater and drinking water treatment. Such studies may be coupled with BiOBr in order to deliver a more accurate measure of its expediency in real-world problems. In addition, the use of natural sunlight instead of artificial visible light irradiation would also prove useful in endorsing the practical applications of BiOBr in wastewater treatment.

- A detailed study of photocatalytic degradation of other compounds and metallic ions with varying characteristics under different conditions would further the adaptability of applications.

- Loading platinum group metal salt, $PdCl_2$, on BiOBr was proven to be useful in this study. This finding can be advanced by loading other pgms on this photocatalyst. In some studies, reduced forms of metal dopants have also proven useful. Consequently, doping studies using Pd metal, pgms and other noble metals such as Pt, Au, and Ru may also offer promising results.

- Once the BiOBr photocatalysis process is established, modeling studies may also be performed in order to describe the kinetics of degradation more accurately. Studies of reaction intermediates, although available for a few pollutants, may also prove useful for commercial applications.

- In the case of BiOBr photocatalysis, research is in earlier phases and therefore its commercialization is not foreseen in the near future. However, as research is progressing, more promising results are being obtained. In view of that, integration of the photocatalyst with pilot scale photocatalytic generators and solar cells for large scale photocatalytic systems also seems pertinent.

Implementation of abovementioned studies would provide insights into the practical applications and industrialization potentials of BiOBr based photocatalysts, thus furthering the vision of solar-photocatalysis based wastewater treatment systems in the coming future.

Appendix A – Reaction Kinetic Model

The degradation reaction taking place in photocatalysis is designated as a heterogeneous catalytic reaction. The kinetics of a heterogeneous catalytic reaction system can be described by the Langmuir-Hinshelwood (LH) model which is numerically described as

$$r = -\frac{dC}{dt} = \frac{k_r KC}{1+KC} \qquad (1)$$

where, r = the rate of reaction (mg/L·min)

K = the equilibrium constant (L/mg)

k_r = the limiting constant of reaction at the maximum coverage (mg/ L·min)

This model is based on the assumption that both involved molecules adsorb and the adsorbed molecules undergo a bimolecular reaction. The model assumes the reaction steps to be the adsorption of reactants, surface reaction, and desorption of products. The expression can be integrated and rearranged as follows:

$$\ln\left(\frac{C_0}{C}\right) + K(C_0 - C) = k_r Kt \qquad (2)$$

At dilute concentrations ($C_0 < 10^{-3}$ mol/L), the term $K(C_0-C) \ll 1$ and it can be assumed that the reaction follows first order kinetics. In this study, very low solute concentrations have been used ($\sim 10^{-5}$ mol/L) and hence it can be assumed that the KC terms are negligible and reaction follows a pseudo-first order reaction with the following reduced model:

$$\ln\left(\frac{C_0}{C}\right) = k_r Kt = k_{app} t \qquad (3)$$

where, k_{app}=kr·K, and is the pseudo-first order rate constant also called the apparent rate constant.

The above model has been used for kinetics of photocatalytic degradation throughout this study and the degradation rate constants reported in the body of the thesis are calculated based on graphical method using pseudo-first order kinetics. It can be noted from Equation (3) that when ln (C_0/C) is plotted as a function of time, the degradation constant can be calculated from the slope of resulting linear equation. Following is a figure showing rate constant equations plotted for three different samples of BiOBr. For clarity, only the highest activity samples in each class are reported in the figure.

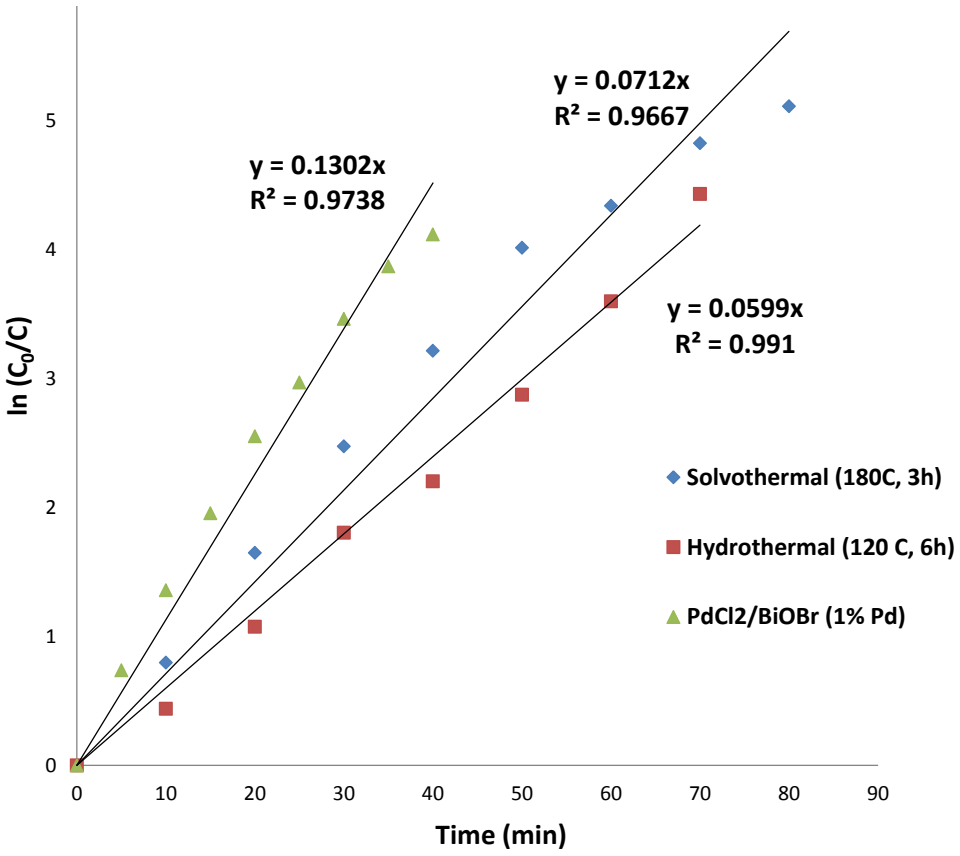

Figure A1 – Pseudo-First Order Rate Equation Model Fit to Three Types of BiOBr Samples

References

Chen, R. G., Bi, J. H., Wu, L., Li, Z. H., Fu, X. Z. (2009) Orthorhombic Bi2GeO5 Nanobelts: Synthesis, Characterization, and Photocatalytic Properties. Cryst. Growth, 9, 1775-1779.

Herrmann, J. M. (1999) Heterogeneous photocatalysis: fundamentals and applications to the removal of various types of aqueous pollutants. Catal. Today, 53, 115-129.

Herrmann, J. M, Tahiri, H, Ait-Ichou, A, Lassaletta, G, González-Elipe, A. R., Fernandez, A (1997) Characterization and photocatalytic activity in aqueous medium of TiO2 and Ag-TiO2 coatings on quartz. Appl. Catal. B., 13, 219–228.

Appendix B – Kubelka Munk Function for Band Gap Energy Determination

The optical absorption of BiOBr is an important aspect of study since the UV-vis absorption edge is pertinent to band gap energy, which in turn affects photocatalytic performance of a semiconductor. In this study, diffuse reflectance data were collected experimentally by analyzing the BiOBr photocatalyst powders and the absorption coefficient was calculated using the Kubelka Munk (KM) function. This function is numerically defined as follows

$$F(R_\infty) = \frac{\propto}{S} = \frac{(1-R_\infty)^2}{R_\infty} \quad (1)$$

where, α = absorption coefficient
S = Scattering coefficient
$F(R_\infty)$ = KM function

For semiconductors, it has been established that the optical absorption near the band edge follows the formula described below

$$\propto \cdot E = C(E - E_g)^n \quad (2)$$

where, α = absorption coefficient
E = incident photon energy
E_g = optical absorption edge energy
C = a constant

In Equation 2, the exponent "n" depends on optical transition and is assigned a value of ½ for direct allowed transition, which is the case for BiOBr. For diffuse reflectance spectra, KM function can be used instead of α and the band gap energy, E_g, can be calculated by the intercept on abscissa of the line obtained by plotting $(F(R_\infty)E)^{1/2}$ versus photoenergy. Following are the plots obtained through the Kubelka Munk function for BiOBr samples and as it can be interpreted from the figures, the band gaps for solvothermal BiOBr and $PdCl_2$/BiOBr samples are 2.9 and 2.63 eV, respectively.

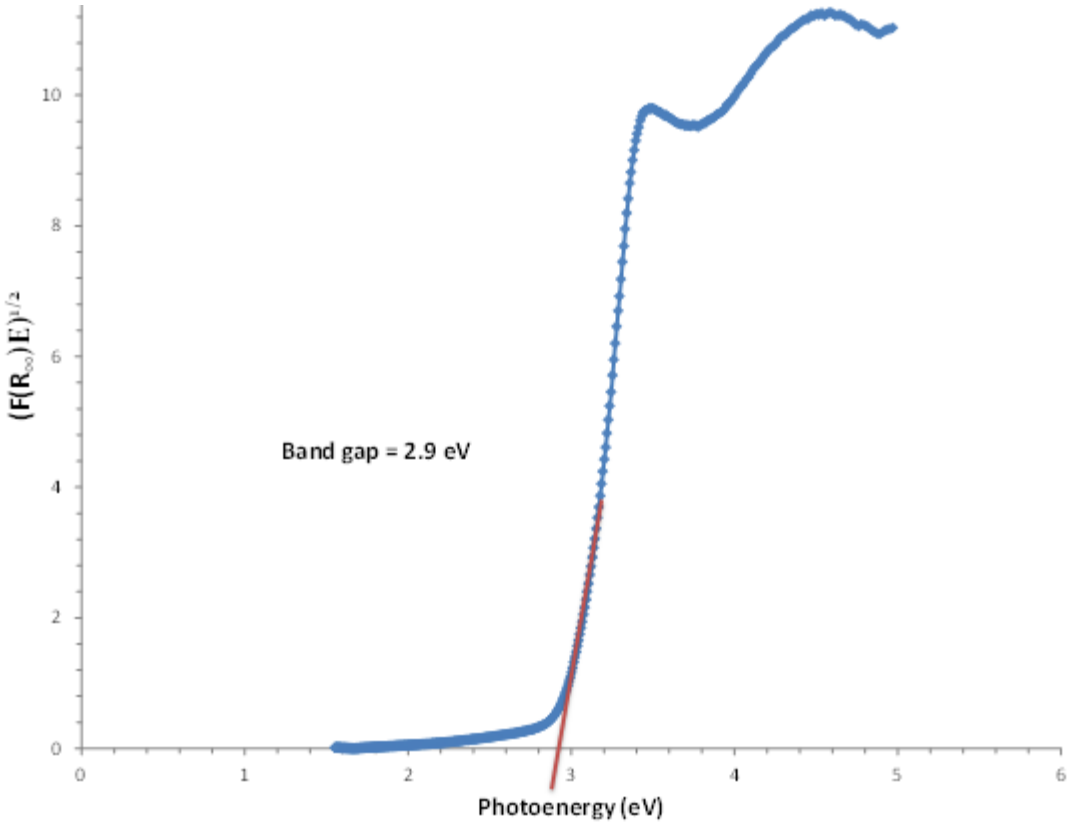

Figure B1 – Plot of $(F(R_\infty)E)^{1/2}$ versus photoenergy for estimating band gap energy of Solvothermal BiOBr

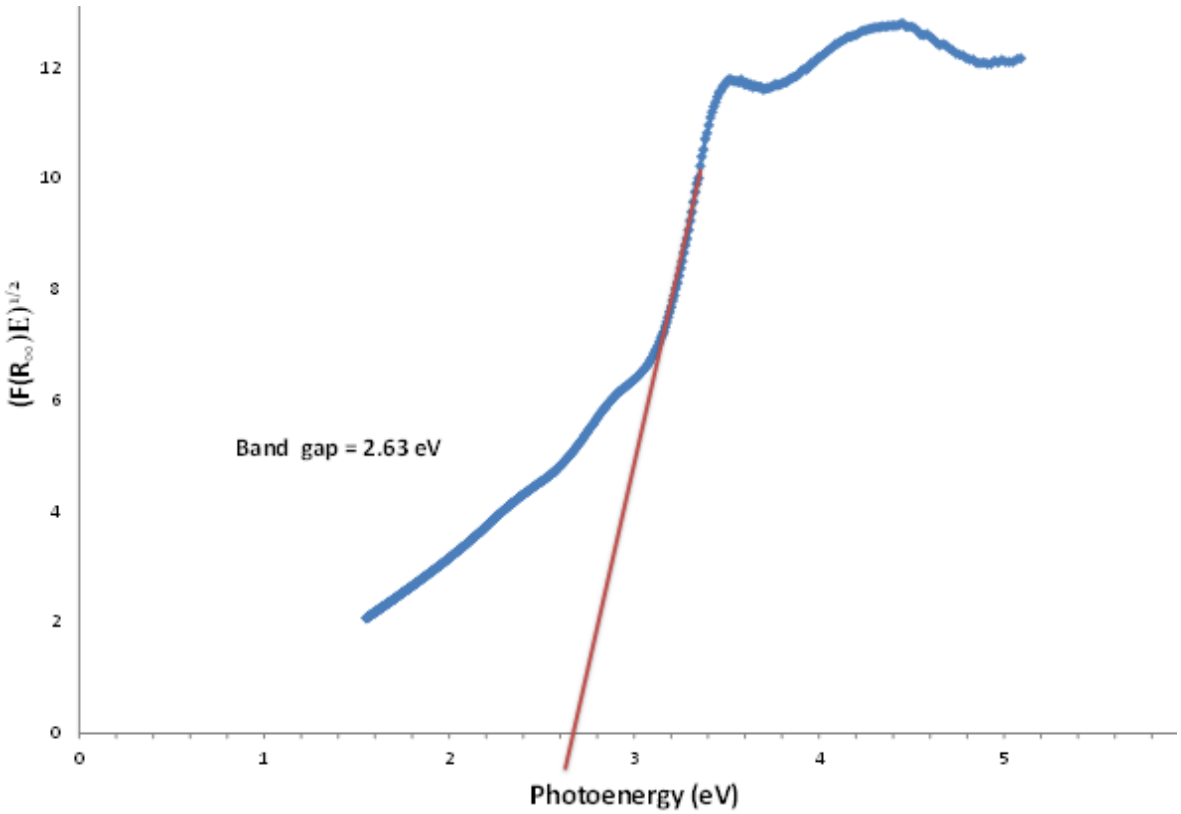

Figure B2 – Plot of $(F(R_\infty)E)^{1/2}$ versus photoenergy for estimating band gap energy of $PdCl_2$ doped BiOBr

References

Yang, L., Kruse, B. (2004) Revised Kubelka–Munk theory. I. Theory and application. J. Opt. Soc. Am. A 21, 1933-1941

Zhang, L., Cao, X. F., Chen, X. T. & Xue, Z. L., 2011. BiOBr hierarchical microspheres: Microwave-assisted solvothermal synthesis, strong adsorption and excellent photocatalytic properties. J. Colloid Interf. Sci., 354, 630-636.

Appendix C – Standard and Calibration Curves

The standard absorbance and calibration curves used in this study are presented in this section.

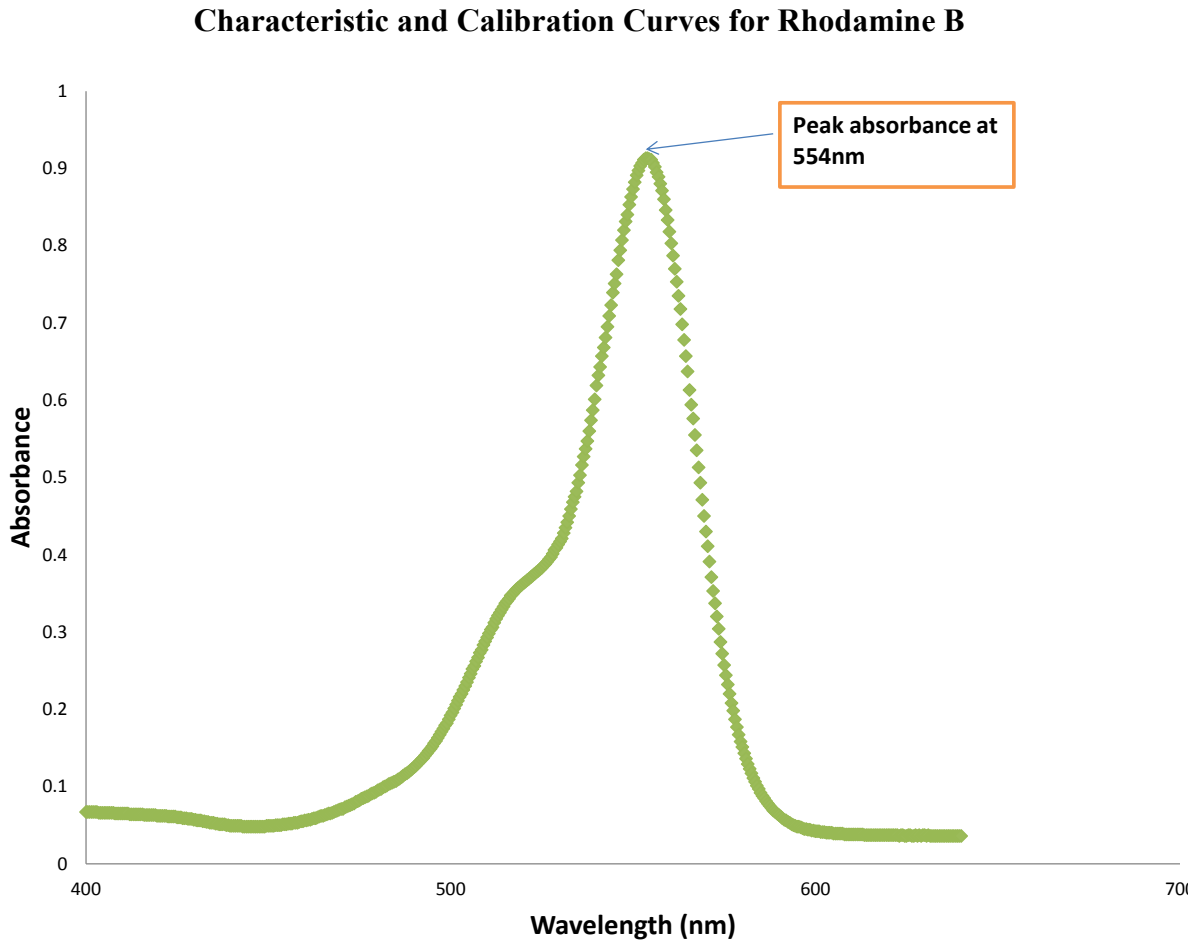

Figure C1 – Absorbance peak determination for RhB

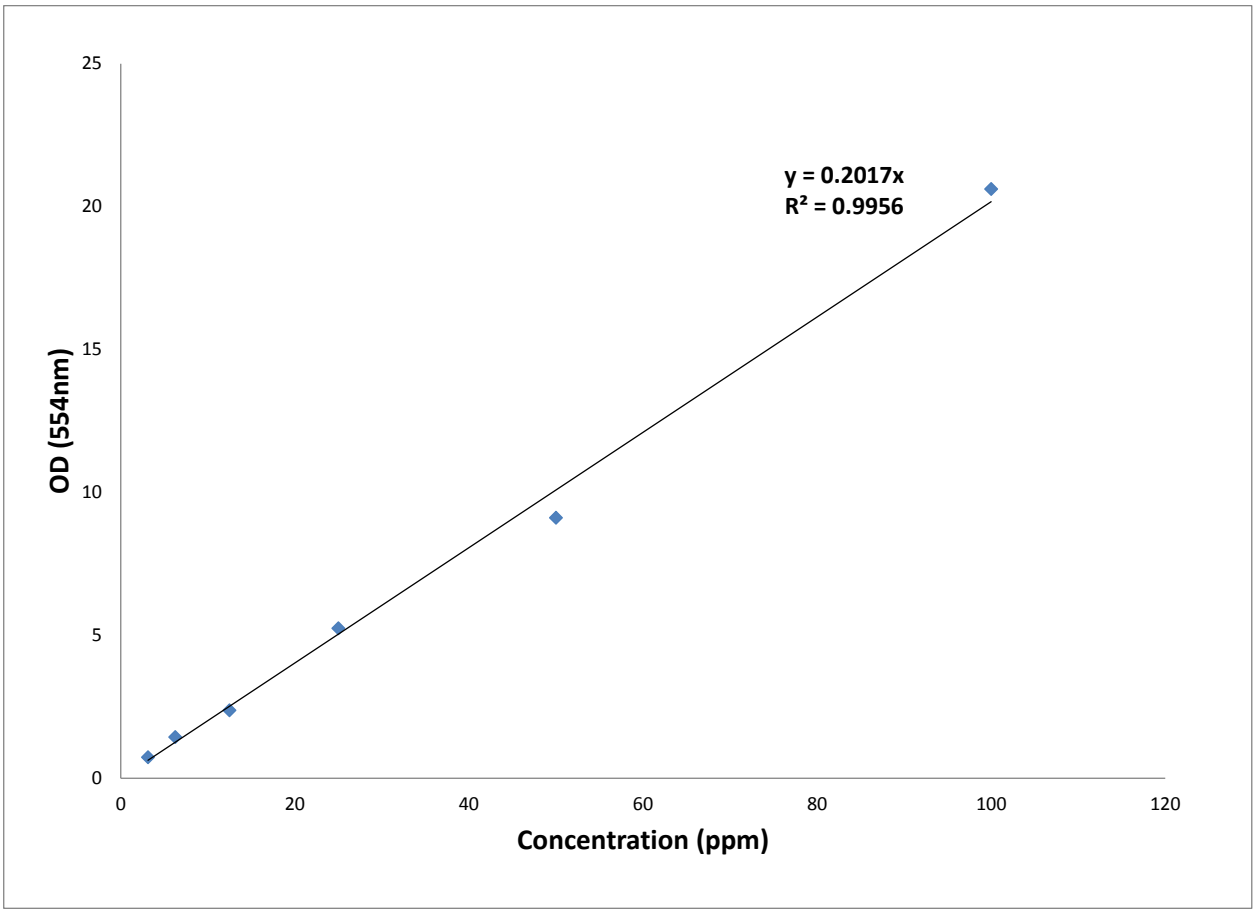

Figure C2 – Standard Calibration Curve for RhB prepared at Absorbance of 554nm

Characteristic and Calibration Curves for Phenol

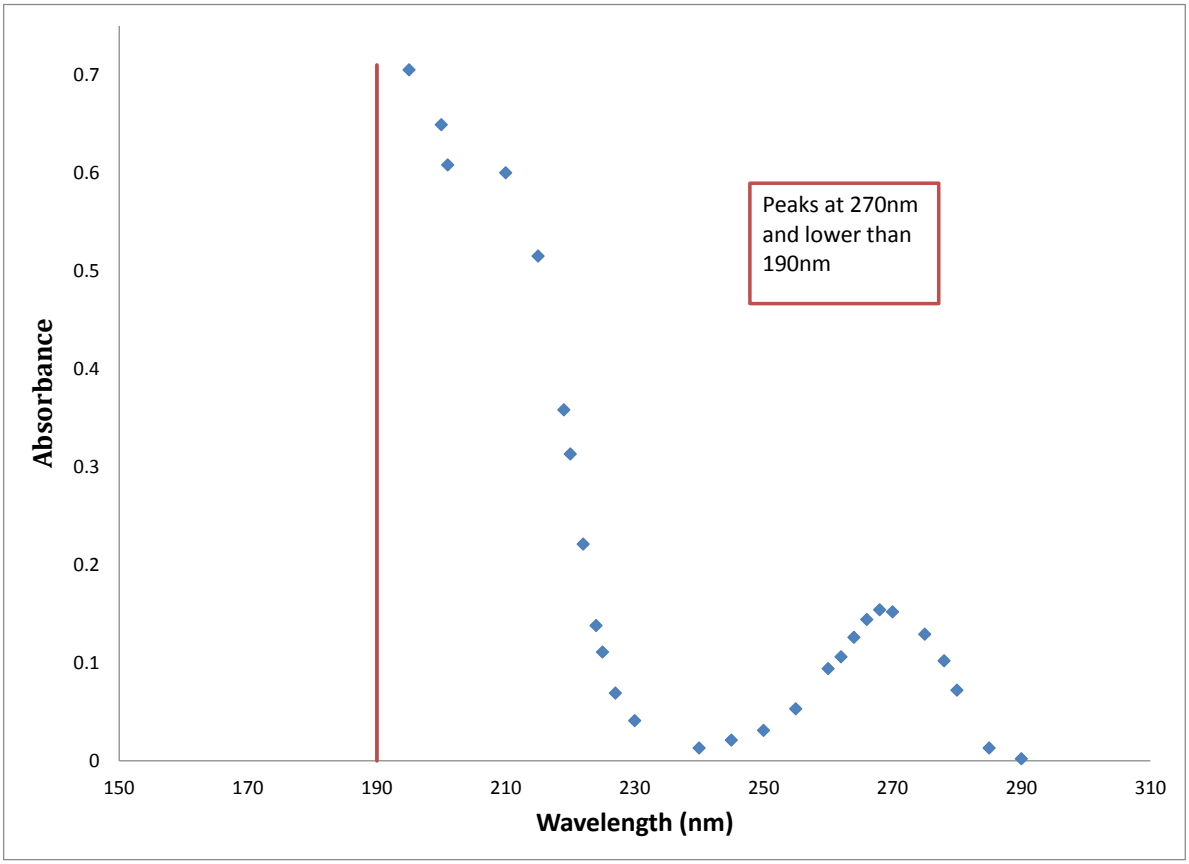

Figure C3 – Absorbance peak determination for Phenol

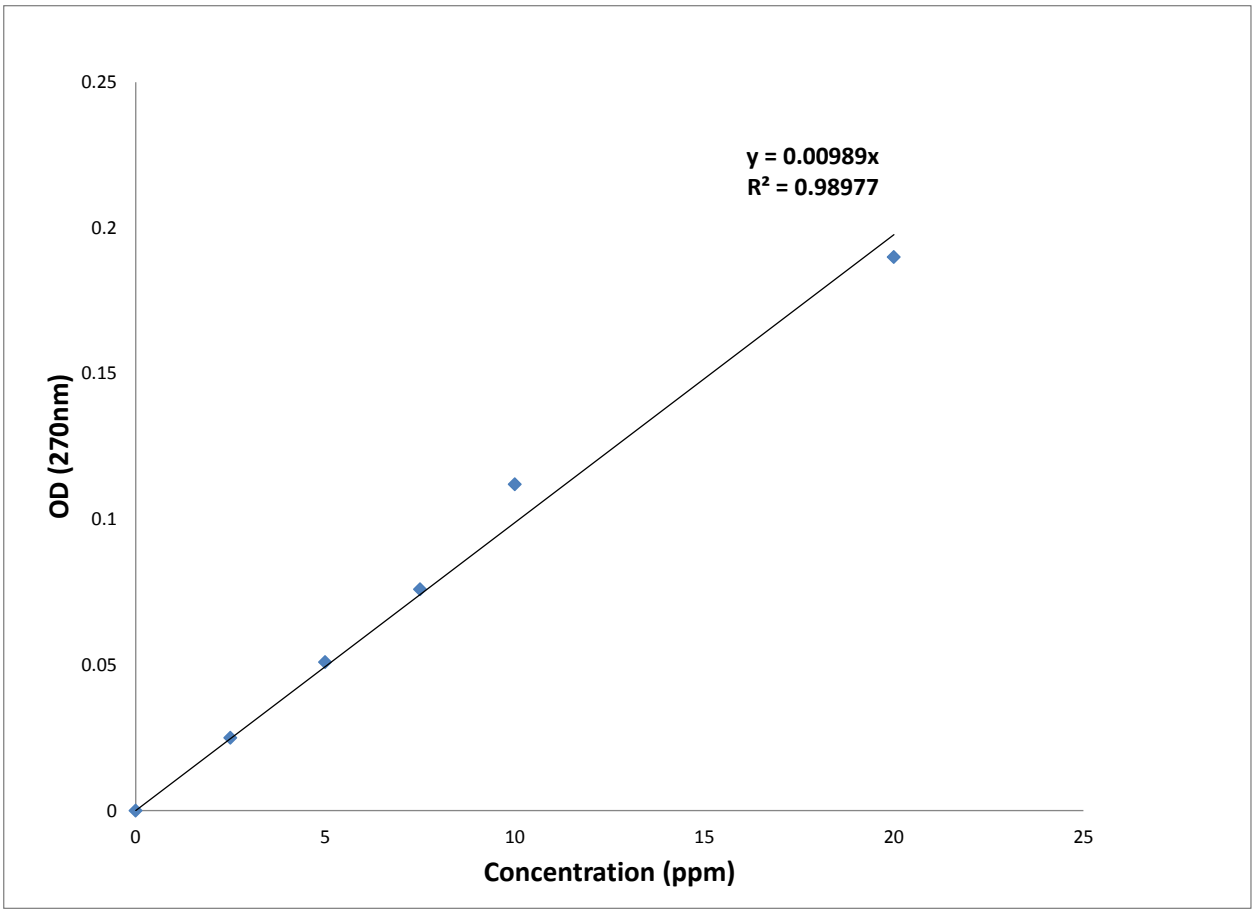

Figure C2 – Standard Calibration Curve for Phenol prepared at Absorbance of 270nm

Appendix D – Tungsten Halide Illumination

Following figure demonstrates the relative spectral distributions of metal halide illumination and confers it with regular terrestrial solar spectrum.

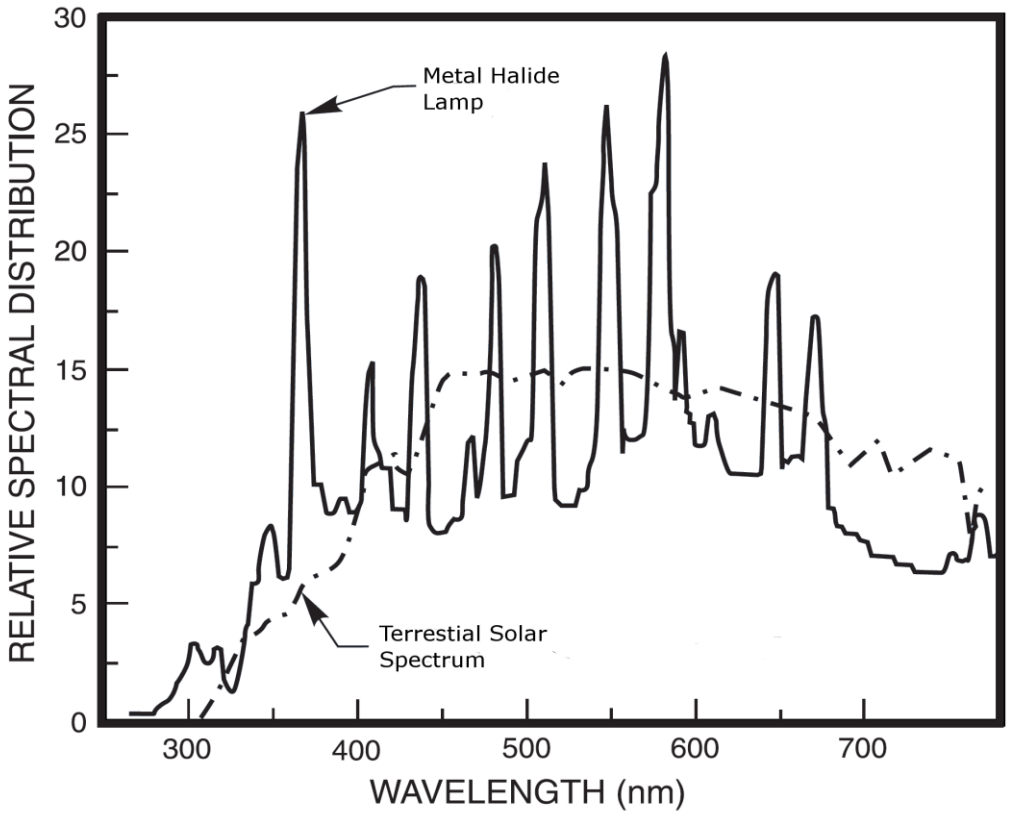

Figure D1 - Emission spectrum of metal halide and terrestrial radiation (Newport, 2001)

Appendix E – Mass Recovery Ratios

During the recyclability experiments, mass recovery per cycle is also another important parameter though it is often exchanged for photocatalytic efficiency in reports. Herein, the results of mass recovery for solvothermal photocatalyst over four runs are shown.

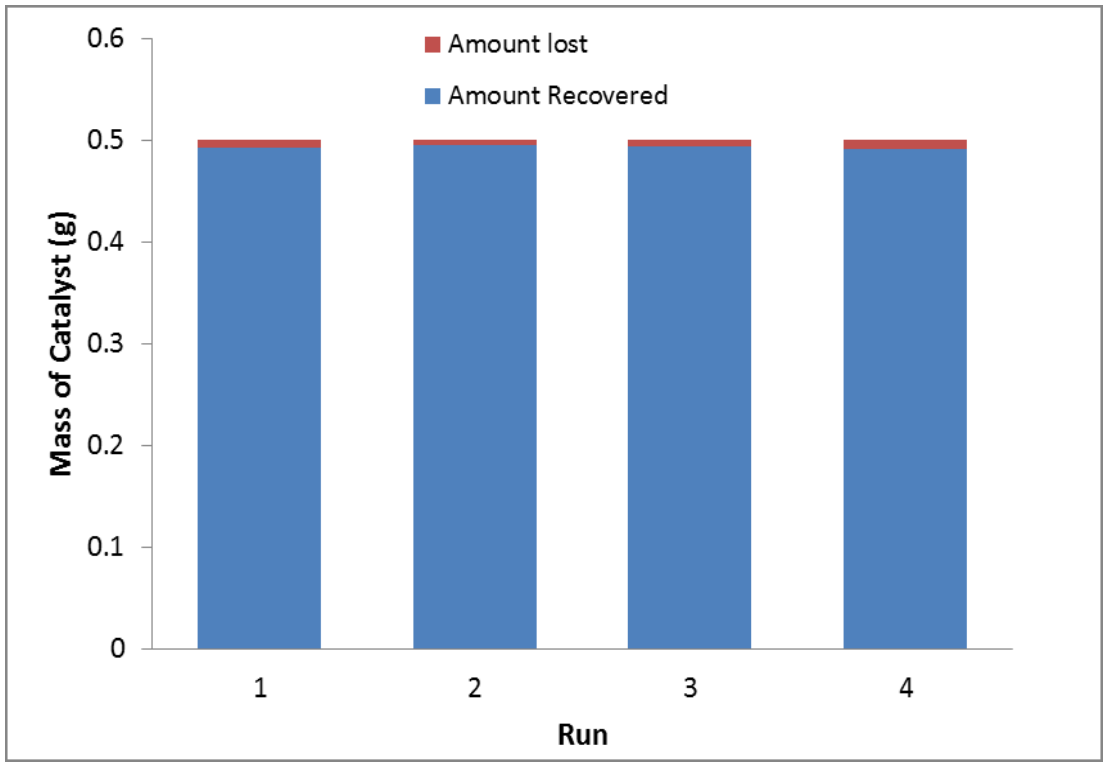

Figure E1 – Mass recovered and lost per cycle

Despite most of the catalyst being removed by filtration, as demonstrated in Figure E1, there is still a small amount of it remaining in the solution. In order to address the concern of residual catalyst in the water, a preliminary report is presented in this section. The toxicology data for BiOBr is not available, however that of its derivatives and close in structure compound BiOCl is listed below.

Table E1 – Lethal doses of possible materials left over in water

Material	LD50 (mg/kg)	Reference
BiOCl	22000	[1]
Bi	5000	[2]
Br	7000	[3]
Cl	< 1.0	[4]

Hazardous short term degradation products are not likely for BiOBr [5]. Moreover, according to the Canadian Drinking water guidelines [6], chlorine is "not required to be regulated" and is allowed at concentrations as high as 2 mg/L in drinking water. Noting that chlorine LD_{50} is much lower than any of BiOBr related products, one can hypothesize that a small quantity of this photocatalyst (within ppm level) would not be very problematic. However, further studies and toxicology experiments must be conducted to establish safety of residual BiOBr in water.

References

[1] Organometallics in Environment and Toxicology (pg 504) edited by Astrid Sigel, Helmut Sigel, Roland K. O. Sigel

[2] MSDS (https://www.fishersci.ca/viewmsds.do?catNo=AC195851000)

[3] Groff F, Tripod J, Meyer R (1955) Zur pharmakologischen karakterisierung des Schlafmittels Doriden. *Schweizerische Medizinische Wochenschrift*, 85:305.

[4] MSDS (http://www.mathesongas.com/pdfs/msds/MATH0027.pdf)

[5] Chemical Properties of Bismuth (http://www.lenntech.com/periodic/elements/bi.htm#ixzz2jzJXjmt3)

[6] Canadian Drinking Water Guidelines (http://www.hc-sc.gc.ca/ewh-semt/pubs/water-eau

Appendix F – Experimental Setup

The activity measurement was carried out using a photoreactor and the following setup (Figure F1). A slurry mode batch reactor, where all the components are kept in well mixed state by magnetic stirring, was used for the photoreaction. The reactor was also equipped with a cooling jacket in order to ensure that the temperature stays within room temperature range. A 300 watt tungsten halide lamp was used to mimic sunlight and a cut-off filter was used to filter out any radiation below 410 nm ensuring the photocatalysis was carried out strictly under visible light irradiation. A 2.5 ml sample was taken from the reactor at small time intervals and photocatalyst was separated from the solution by centrifugation. The entire setup was placed in a reflective housing in order to prevent external light from entering the system as well as keep the light generated by the lamp within the setup.

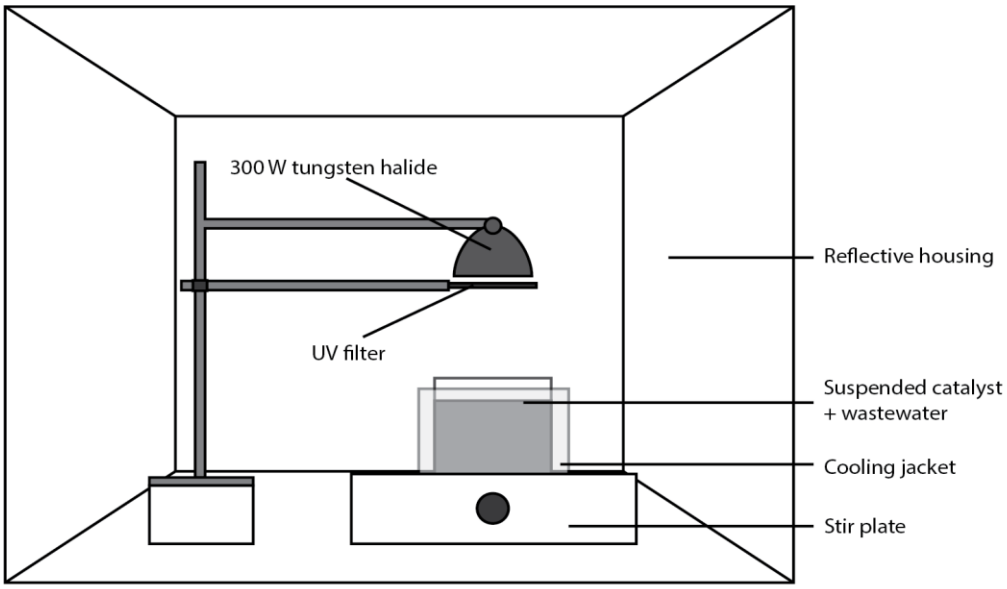

Figure F1 – Experimental setup of photocatalytic reactor